Geopolitical Barriers to Globalization

Tianyu Fan
Yale University

Mai Wo
Yale University

Wei Xiang
University of Michigan

March 25, 2026

(Click here for the most recent version)

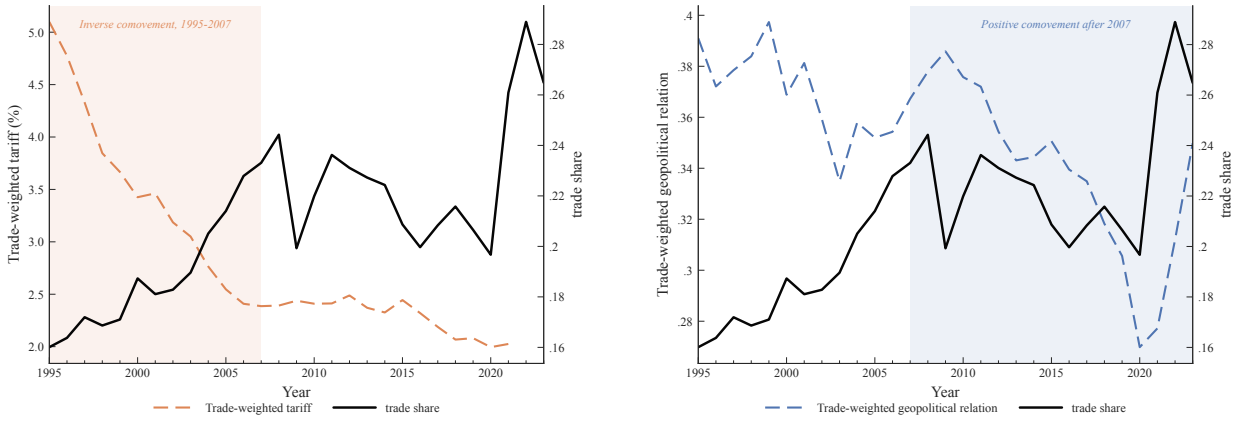
We show that, since the mid-1990s, the trade-promoting effects of tariff liberalization have been increasingly offset by deteriorating geopolitical relations, stalling trade globalization after 2007. To quantify this barrier, we compile a database of 833,485 geopolitical events across 193 countries from 1950 to 2024 using large language models and construct a bilateral geopolitical alignment index. Local projections estimate that a one-standard-deviation permanent improvement in alignment raises bilateral trade by 20 percent in the long run. From 1995 to 2021, tariff reductions added 9.5 percentage points to trade growth, while geopolitical deterioration subtracted 6.8 percentage points and produced more uneven welfare effects.

JEL Classification: F14, F15, F51, C55
Keywords: geopolitical alignment, international trade, fragmentation, gravity model, large language models

Tianyu Fan: tianyu.fan@yale.edu. Mai Wo: mai.wo@yale.edu. Wei Xiang: xwe@umich.edu. We especially thank Stephen Terry for his constructive feedback. We thank Costas Arkolakis, Rüdiger Bachmann, Chris Clayton, Javier Cravino, Sam Kortum, John Leahy, Fernando Leibovici, Andrei Levchenko, Ana Maria Santacreu, Matthew Schwartzman, Sebastian Sotelo, Linda Tesar, and Erik Voeten for their comments. We thank Imryoung Jeong for her research assistance.

1. Introduction

From the mid-1990s to 2007, trade as a share of GDP rose as tariff rates fell. After 2007, this relationship weakened. Applied tariff rates remained low by historical standards, regional trade agreements continued to accumulate, and the WTO, though weakened, persisted. Yet trade integration stalled. This paper shows that a second force increasingly shaped trade globalization: the deterioration of bilateral geopolitical relations. Trade liberalization continued to promote trade, but its effects were substantially offset by geopolitical fragmentation (Figure 1).



A. Tariffs and trade share

B. Geopolitical relations and trade share

FIGURE 1. Aggregate Trade Shares, Tariffs, and Geopolitical Relations

Notes: The black line in both panels plots global trade as a share of world GDP. Panel A plots the trade-weighted average bilateral tariff, and Panel B plots the trade-weighted average bilateral geopolitical alignment measure constructed in the paper. The orange shaded region in Panel A, 1995–2007, highlights the period in which trade shares moved inversely with tariffs. The blue shaded region in Panel B, 2007–2023, highlights the period in which trade shares moved positively with geopolitical alignment.

We develop this argument in three steps. First, using large language models, we build a new database of bilateral geopolitical events and from it construct a new event-based measure of geopolitical alignment covering all 193 UN member states from 1950 to 2024. Second, we estimate the effect of geopolitical alignment on trade using local projections within a gravity framework. Third, we embed the estimated elasticities in a quantitative general equilibrium model to assess the aggregate and distributional consequences of geopolitical change.

We begin by constructing a bilateral measure of geopolitical alignment for all 193 UN member states from 1950 to 2024. Building on Fan (2025), who cover 24 major economies, we extend the data to all $193 \times 192/2$ country pairs. Using a large language model (LLM), Gemini 2.5 Pro, with web search capability, we compile a database of 833,485 major bilateral political events. For each country pair and year, we identify salient political interactions, classify them using the Conflict and Mediation Event Observations (CAMEO) framework (Schrodt and Yilmaz 2012), map them into Goldstein scores from −10 to +10 (Goldstein 1992), and aggregate them into a dynamic bilateral index ranging from −1 to +1. Relative to standard proxies such as UN voting similarity, the measure offers

broader coverage, captures bilateral political relations directly rather than multilateral positioning, and delivers substantial within-pair variation for panel gravity estimation. Section 2 validates the measure through case studies, comparisons with existing proxies, and robustness checks across alternative model runs.

Before turning to estimating the effects of geopolitical alignment on trade, we document three patterns in the data. First, case studies of major-power dyads and regional rivals show that periods of stronger geopolitical alignment coincide with stronger bilateral trade, while periods of deterioration coincide with weaker trade. Second, this relationship also appears more broadly across dyads: among major economies, residualized trade and residualized geopolitical alignment are positively correlated in both the Cold War and post-1991 periods. Third, a similar positive association is visible in regional aggregate time-series data. Together, these patterns show that the relationship between geopolitics and trade is systematic rather than confined to a few prominent cases.

We next show that geopolitical alignment is an important bilateral correlate of trade in a standard gravity framework. In cross-sectional gravity regressions with origin-year and destination-year fixed effects, the coefficient on geopolitical alignment is positive and precisely estimated even after controlling for distance, contiguity, and linguistic distance. In the sample of 32 major economies, a one-standard-deviation increase in alignment (0.26 units) is associated with 11.9 log points higher bilateral trade. In the full sample, the association is larger still. Geopolitical alignment is therefore quantitatively comparable to standard bilateral gravity variables such as linguistic distance and the border effect, and captures a dimension of bilateral trade costs not reflected in conventional proxies.

We then estimate the dynamic effect of geopolitical alignment on bilateral trade using local projections with country-pair, origin-year, and destination-year fixed effects, so identification comes from within-pair changes in relations. In the benchmark sample of 32 major economies, a unit improvement in geopolitical alignment raises bilateral trade by about 28 log points at its peak. Decomposing the response into transitory and permanent components shows that even temporary diplomatic improvements generate trade gains that persist for five to seven years, while a one-standard-deviation permanent realignment raises trade by roughly 20 percent (about 18 log points) in the long run.[1]

These results are robust across samples, periods, and alternative measures. The positive effect of geopolitical alignment holds when we extend the sample beyond major-economy pairs, split the sample into pre- and post-1995 subsamples, vary the construction of the alignment measure, and distinguish between positive and negative shocks as well as economic and non-economic events. The effect is stronger for country pairs with greater executive discretion and lower institutional quality, but weaker within formal alliances. At the sectoral level, the effects are broad-based and especially pronounced in manufacturing.

We also study the mechanisms linking geopolitics to trade. Deteriorating geopolitical alignment

[1] One standard deviation is 0.23 units, close to the deterioration in U.S.–China bilateral alignment around the 2018 trade war shown in Figure 2.

increases the use of sanctions and other restrictive trade measures, while having little systematic effect on tariffs. Sanctions, however, account for roughly 18 percent of the trade response, implying that formal policy instruments explain only part of the effect. We also provide suggestive evidence that geopolitical alignment affects trade through uncertainty and social attitudes: country pairs with stronger alignment exhibit more favorable bilateral attitudes, and these attitudes are positively associated with trade.

Finally, we integrate the reduced-form estimates into a quantitative model of international trade. Using an Armington model with perfect competition, we decompose the evolution of global trade from 1995 to 2021 into geopolitical change, tariff liberalization, and residual trade barriers. Global trade rises by 27.4 percent in the baseline. Relative to this benchmark, tariff liberalization contributes 9.5 percentage points, while geopolitical deterioration subtracts 6.8 percentage points. Tariff liberalization therefore continued to support integration, but a substantial share of those gains was offset by worsening geopolitical relations.

These aggregate effects mask substantial heterogeneity in welfare consequences. Tariff liberalization generates modest average gains that are broadly shared across countries, although part of the gain is offset by lower tariff revenue. By contrast, geopolitical realignment produces more dispersed welfare effects: the mean effect is negative, the dispersion is much larger, and most countries lose from geopolitical deterioration. Geopolitical change therefore emerges as a quantitatively important and highly uneven determinant of economic welfare.

Literature Our paper contributes to three strands of literature: the measurement of geopolitical alignment, the empirical analysis of how geopolitics shapes trade, and the estimation of trade barriers in gravity frameworks.

Measuring Global Geopolitical Alignment. We build on the Event-CAMEO-Goldstein framework of Fan (2025) and extend it to universal coverage of UN member states from 1950 to 2024. Most prior work relies on UN General Assembly voting similarity (Signorino and Ritter 1999; Bailey, Strezhnev, and Voeten 2017; Qiu, Xia, and Yetman 2024). However, UN voting primarily captures multilateral positioning rather than bilateral relations, exhibits limited within-dyad time variation (Broner et al. 2025a), and may not preserve a stable meaning across countries and periods (Airaudo et al. 2025). Other approaches also face limitations in studying the geopolitics-trade nexus. Discrete measures capture only particular relationship types, such as strategic rivalry (Thompson 2001; Aghion et al. 2019), alliances (Gibler 2008), sanctions (Felbermayr et al. 2020, 2021), or treaties (Broner et al. 2025b), and therefore miss the broader spectrum of bilateral interaction. Aggregate measures of geopolitical risk or fragmentation (Caldara and Iacoviello 2022; Fernández-Villaverde, Mineyama, and Song 2024) are useful for macro analysis but do not provide the bilateral variation needed for trade. Our event-based measure addresses these limitations by constructing a continuous bilateral score from -1 to $+1$ that captures both the timing and intensity of geopolitical relations.

We also contribute to the literature on machine-learning-based measurement. Whereas standard text-based approaches typically infer political risk from keyword frequencies (Baker, Bloom, and Davis 2016; Caldara and Iacoviello 2022; Hassan et al. 2019), we use an LLM to identify, classify,

and score major bilateral geopolitical events using contextual information (Clayton et al. 2025; Dell 2025; Fang, Li, and Lu 2025). Our approach uses LLMs not to summarize text, but to construct a structured measure of bilateral geopolitical relations.

Geopolitics and Trade. We engage with the growing literature on how geopolitics shapes trade patterns. Early work dates back to Hirschman (1945). Recent theoretical work has advanced rapidly (Alesina, Spolaore, and Wacziarg 2000; Couttenier et al. 2024; Becko and O'Connor 2024; Clayton et al. 2025; Clayton, Maggiori, and Schreger 2025; Mayer, Mejean, and Thoenig 2025), and Mohr and Trebesch (2025) provides a recent review. Empirical progress, however, has been constrained by measurement challenges (Aiyar and Ohnsorge 2024), though notable exceptions include Federle et al. (2026) on the economic impact of war. Our paper provides systematic evidence on how geopolitical changes translate into trade reallocation and welfare effects.

The closest related empirical paper is Gopinath et al. (2025), which studies trade flows within and across geopolitical blocs defined using UN voting similarity and documents recent evidence of fragmentation. While their bloc-based analysis uncovers important aggregate patterns, our bilateral event-based measure allows us to estimate dynamic trade elasticities, trace adjustment paths, and quantify aggregate and distributional welfare effects in general equilibrium. Our paper also relates to recent quantitative work on fragmentation, which has measured rising trade barriers through bilateral trade-cost changes for specific country pairs (Chen, Hsieh, and Song 2022; Bonadio et al. 2025; Cai, Xiang, and Zhao 2025) and country image (Chang, Fujii, and Jin 2022). Our measure differs by providing continuous bilateral coverage of all country pairs over seven decades, which allows us to estimate the dynamic causal effect of geopolitical alignment on trade rather than inferring fragmentation from observed trade-cost shifts.

More broadly, our paper connects to a literature on international politics and trade (Grossman and Helpman 1994; Morrow, Siverson, and Tabares 1998; Mansfield, Milner, and Rosendorff 2000; Martin, Mayer, and Thoenig 2008), to studies of the channels linking geopolitics to trade (Korovkin and Makarin 2023; Kleinman, Liu, and Redding 2024; Liu and Yang 2025), and to work on how geopolitical tensions shape innovation (Alfaro et al. 2025; Flynn et al. 2025), asset allocation (Pellegrino, Spolaore, and Wacziarg 2025), and growth (Fan 2025). Goldberg and Ruta (2025) reviews how geopolitical shifts are reshaping trade and development.

Gravity Estimation and Trade Barriers. Finally, we contribute to the literature on gravity models and trade barriers (Anderson and Van Wincoop 2003, 2004; Head and Mayer 2014). Our use of local projections within a gravity framework is closest to Boehm, Levchenko, and Pandalai-Nayar (2023). Whereas traditional gravity estimates focus on observable trade costs such as tariffs (Baier and Bergstrand 2007; Caliendo and Parro 2015), distance (Disdier and Head 2008), language (Melitz 2008), and regulatory barriers (Looi Kee, Nicita, and Olarreaga 2009), we show that geopolitical alignment is an important and often omitted component of bilateral trade frictions.

Roadmap The remainder of the paper is organized as follows. Section 2 introduces our measure of global geopolitical alignment. Section 3 presents descriptive evidence linking geopolitical alignment to trade patterns through case studies, cross-dyad correlations, and aggregate time-series evidence.

Section 4 estimates dynamic trade elasticities using local projections within a gravity framework. Section 5 examines heterogeneity and mechanisms. Section 6 embeds the estimated elasticities in a quantitative general equilibrium model to decompose trade evolution and quantify welfare effects. Section 7 concludes.

2. Measuring Global Geopolitical Alignment

We construct a bilateral measure of geopolitical alignment for all 193 UN member states from 1950 to 2024. Geopolitical alignment refers to the state of the strategic and diplomatic relationship between two countries, as reflected in the degree to which their bilateral interactions are cooperative rather than conflictual. Our approach extends Fan (2025), which focuses on 24 countries, to universal country coverage. The resulting measure combines broad historical span with substantial bilateral variation, making it well suited to the panel trade analysis that follows.

For exposition, we describe the construction in three steps. First, we construct a global database of major bilateral political events. Second, we classify each event and map it into a numerical score. Third, we aggregate event-level scores into an annual country-pair measure of geopolitical alignment.[2]

2.1. Step 1: Event Database Construction

We use Gemini 2.5 Pro, a large language model with web search capability, to construct a database of major bilateral political events for all undirected country-pair-year observations from 1950 to 2024.[3] For each country-pair-year observation, the model verifies the relevant political entities, accounting for state succession when necessary, and identifies the major political events involving the two countries in that year. Appendix B.7 reports the full prompt and implementation details. The prompt prioritizes four types of sources: official government materials, international organizations, major news archives, and academic or diplomatic archives. The resulting database contains 833,485 political events.

Our approach differs from existing global event databases such as GDELT (Leetaru and Schrodt 2013) and ICEWS (Boschee et al. 2015) in two respects. First, we focus on major bilateral political events that are most likely to affect the underlying relationship between two countries, rather than attempting to capture the full universe of international interactions. This narrower scope reduces noise from routine or low-salience events and yields a cleaner record of meaningful bilateral political developments. Second, our data span 1950–2024, extending historical coverage well beyond GDELT and ICEWS and aligning more closely with the trade panel used in the empirical analysis.

[2] In implementation, the prompt performs the first two tasks jointly: it identifies relevant bilateral political events, classifies them using the CAMEO framework, and assigns Goldstein scores within a single workflow.

[3] Web search augments the model's pretraining knowledge but is not essential for well-documented dyad-years, especially among prominent countries whose major bilateral events are extensively covered in news archives, government documents, and scholarly sources.

Table 1 illustrates the database using U.S.–China interactions in 2024. The seven events include diplomatic exchanges, military dialogue, tariffs, sanctions, export controls, and security tensions. Together they capture the mix of crisis-management diplomacy and strategic rivalry that characterized the bilateral relationship in that year.

TABLE 1. Major U.S.-China Bilateral Events in 2024: LLM Analysis Results

Event Name	**Event Description**	**CAMEO Class.**	**Econ. Type**	**Goldstein Score**
US-China Defense Chiefs Meet in Singapore	Defense Secretary Austin and Minister Dong Jun met at the Shangri-La Dialogue, agreeing to resume military communications and crisis-management discussions	Verbal Cooperation (04-044)	Not econ.	+4.5
Resumption of US-China MMCA Talks	U.S. and Chinese defense officials resumed Military Maritime Consultative Agreement (MMCA) talks in Honolulu after a two-year suspension, reopening a channel to manage military incidents	Verbal Cooperation (04-040)	Not econ.	+4.0
Blinken Visit to China	Secretary Blinken visited Shanghai and Beijing in April, meeting senior Chinese officials to discuss Russia, trade frictions, and regional security	Verbal Cooperation (04-042)	Not econ.	+3.0
US Tariff Increases on Chinese Goods	The Biden administration raised tariffs on $18 billion of Chinese imports, including electric vehicles, solar cells, semiconductors, and medical products	Material Conflict (16-163)	Tariff	−6.5
US Sanctions Chinese Companies Supporting Russia	The U.S. sanctioned Chinese and Hong Kong firms supplying inputs to Russia's military-industrial base, linking bilateral tensions to the Ukraine war	Material Conflict (17-172)	Sanction	−7.0
US Adds Chinese Firms to Entity List	The Commerce Department added 42 Chinese companies to the Entity List for supporting Russia's defense industrial base, intensifying technological pressure	Material Conflict (17-172)	Sanction	−7.0
Mainland China Military Drills Around Taiwan	Mainland China conducted large-scale PLA exercises around Taiwan in May, raising cross-Strait tensions and bilateral tensions with the United States	Material Conflict (15-150)	Not econ.	−8.0

2.2. Step 2: Mapping Events into Scores

Although event identification and scoring are implemented jointly, it is useful to separate the scoring logic conceptually. We classify each event using the Conflict and Mediation Event Observations (CAMEO) framework (Schrodt and Yilmaz 2012) and map each CAMEO category to a Goldstein score (Goldstein 1992). CAMEO provides a standardized classification of political interactions along two dimensions: cooperation versus conflict, and verbal versus material action. The Goldstein scale then assigns each event type a numerical weight from −10 to +10, with more negative values indicating more conflictual behavior and more positive values indicating more cooperative behavior.

We use the standard CAMEO-to-Goldstein mapping as the benchmark and allow the model to make limited contextual adjustments based on event severity and historical setting.[4] This preserves comparability with existing event datasets while allowing the scoring to reflect the context of particular bilateral episodes.

Table 2 reports summary statistics by era. The Cold War has the highest conflict share, the lowest mean Goldstein score, and the greatest dispersion. The globalization period is more cooperative on average, while the fragmentation period partly reverses that shift, with more conflict and a lower mean score. Event counts rise after 2010 despite the shorter time span, indicating that recent decades feature more recorded bilateral interactions but less cooperative average relations.

TABLE 2. Summary of Bilateral Geopolitical Events by Era, 1950–2024

	Event Counts				Goldstein Score	
Period	Cooperation	Conflict	Total	Conflict (%)	Mean	SD
Cold War (1950–1990)	206,857	58,770	265,627	22.1	2.33	5.04
Globalization (1991–2009)	220,840	37,958	258,798	14.7	3.92	4.11
Fragmentation (2010–2024)	251,060	58,000	309,060	18.8	3.70	3.68
Full Period	678,757	154,728	833,485	18.6	3.38	4.33

Notes: This table summarizes 833,485 bilateral geopolitical events classified using our event-based methodology across three eras. Events are categorized as cooperation or conflict. Goldstein scores range from −10 (maximum conflict) to +10 (maximum cooperation).

Appendix B.3 shows that the measure is robust to model choice and highly replicable across repeated runs. Cross-model correlations on randomly selected dyad-years yield a pooled $\rho = 0.88$, and within-model reruns achieve $\rho = 0.93$.

2.3. Step 3: Aggregating Events into Bilateral Relationship Scores

We now aggregate event-level scores into an annual country-pair measure of geopolitical alignment. Two features of the data motivate our procedure. First, bilateral relations are persistent, so current events should be interpreted in light of past interactions. Second, the number of events varies substantially across country pairs and years, so annual averages are measured with different precision. Following Fan (2025), we address both features with a recursively updated score that combines current events with lagged relationship history and assigns more weight to years with richer event information.

Construction of Geopolitical Scores. For each country pair (o, d) and year t, let $\{s^n_{od,t}\}_{n=1}^{\tilde{N}_{od,t}}$ denote the Goldstein scores of the $\tilde{N}_{od,t}$ recorded bilateral events. We first define the annual event score

[4] Appendix B.7 reports the scoring guidelines. While the implementation allows limited contextual adjustment, it remains anchored to the standard CAMEO-to-Goldstein mapping used in established event-data projects.

as the average Goldstein score, normalized to the interval $[-1, 1]$:

$$\tilde{S}_{od,t} = \frac{1}{\tilde{N}_{od,t}} \sum_{n=1}^{\tilde{N}_{od,t}} s^{n}_{od,t}/10. \tag{1}$$

We then define the geopolitical alignment score recursively as

$$\begin{aligned} S_{od,t} &= (1 - \phi_{od,t}) S_{od,t-1} + \phi_{od,t} \tilde{S}_{od,t}, \\ \phi_{od,t} &= \tilde{N}_{od,t}/N_{od,t}, \qquad N_{od,t} = (1 - \lambda) N_{od,t-1} + \tilde{N}_{od,t}, \end{aligned} \tag{2}$$

where $N_{od,t}$ is the effective cumulative event count and $\phi_{od,t}$ is the updating weight. The score changes gradually when event flow is sparse and responds more strongly when many events are recorded in a given year. We set $\lambda = 0.3$, which implies persistence over several years while placing declining weight on older events.[5] By construction, $S_{od,t} \in [-1, 1]$. Because the measure is bilateral rather than directional, it is symmetric: $S_{od,t} = S_{do,t}$. Higher values indicate stronger geopolitical alignment.

TABLE 3. Summary Statistics of Bilateral Geopolitical Scores

	All Countries		Major-Major Pairs		Dynamics (All)	
Period	Mean	Std Dev	Mean	Std Dev	% Decline	% Improve
Cold War (1950–1990)	0.092	0.229	0.241	0.287	17.8	13.2
Globalization (1991–2009)	0.146	0.231	0.301	0.257	18.5	15.1
Fragmentation (2010–2024)	0.201	0.232	0.323	0.255	22.1	16.9
Variance Decomposition (All Countries):						
Between-dyad: 28.8%				Within-dyad: 71.2%		

Notes: Summary statistics for bilateral geopolitical alignment scores covering 18,528 country pairs from 1950 to 2024. Scores range from −1 to +1 and are constructed using equation (2) with $\lambda = 0.3$. The Dynamics columns report the share of dyad-years with annual score changes below −0.05 and above +0.05, respectively.

Table 3 reports summary statistics. Mean alignment rises over time, from 0.092 in the Cold War to 0.146 during globalization and 0.201 in the fragmentation period, while the cross-sectional standard deviation remains close to 0.23. Both tails become more active after 2010: the share of deteriorating dyad-years rises from 17.8 percent to 22.1 percent, and the share of improving dyad-years rises from 13.2 percent to 16.9 percent. Major-economy pairs have higher mean alignment throughout, although the gap narrows over time. Most important for the empirical analysis, 71.2 percent of total variation is within pair rather than between pairs, leaving substantial within-pair

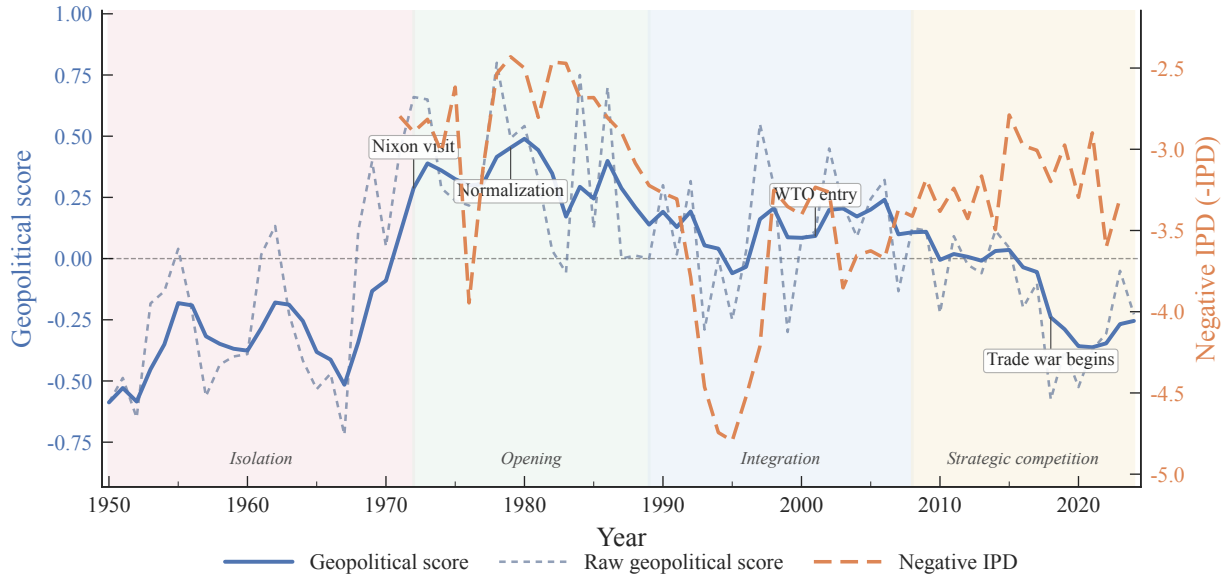
[5] Section 4.3 shows that our results are robust to the choice of λ. Unsmoothed annual event scores exhibit rapid mean reversion and generate smaller immediate trade effects, but the cumulative long-run impact of permanent changes in event flows converges to our baseline estimates. Since the local projection controls for lags of alignment, the identifying variation comes from innovations rather than the accumulated stock, making the estimates close after accounting for the persistence of each measure.

variation for gravity estimation.

2.4. Case Study: United States and China

Figure 2 illustrates the measure using the United States and China. The dynamic score captures the sharp diplomatic opening initiated by Nixon's 1972 visit and consolidated by normalization in 1979, the more cooperative environment associated with commercial integration through the 1990s and China's WTO entry in 2001, and the renewed deterioration after 2018 amid the trade war and Taiwan tensions. Appendix B.4 provides additional evidence for other dyads.

FIGURE 2. Geopolitical Scores Between the United States and China, 1950–2024



Notes: The solid blue line reports the dynamic geopolitical score. The light blue dashed line reports the raw annual event score. The orange dashed line reports negative Ideal Point Distance (IPD) from United Nations General Assembly (UNGA) voting data. Shaded regions denote major phases of U.S.–China relations.

The figure also plots negative IPD from UNGA voting data (Bailey, Strezhnev, and Voeten 2017). The event-based series tracks major bilateral turning points closely, rising after 1972, stabilizing during the integration era, and declining after 2018. Negative IPD exhibits less variation over the same period, consistent with the view that it captures multilateral positioning rather than bilateral relations. In the U.S.–China case, the two measures are correlated, since China's distance from U.S.-led positions on multilateral issues partly reflects bilateral tensions. But IPD misses the bilateral inflection points most relevant for trade, particularly the sharp deterioration around 2018.

2.5. Bilateral and Multilateral Dimensions of Geopolitical Alignment

Moving beyond the U.S.–China case, we now examine systematically whether UNGA voting and our event-based measure capture different dimensions of geopolitical relations.

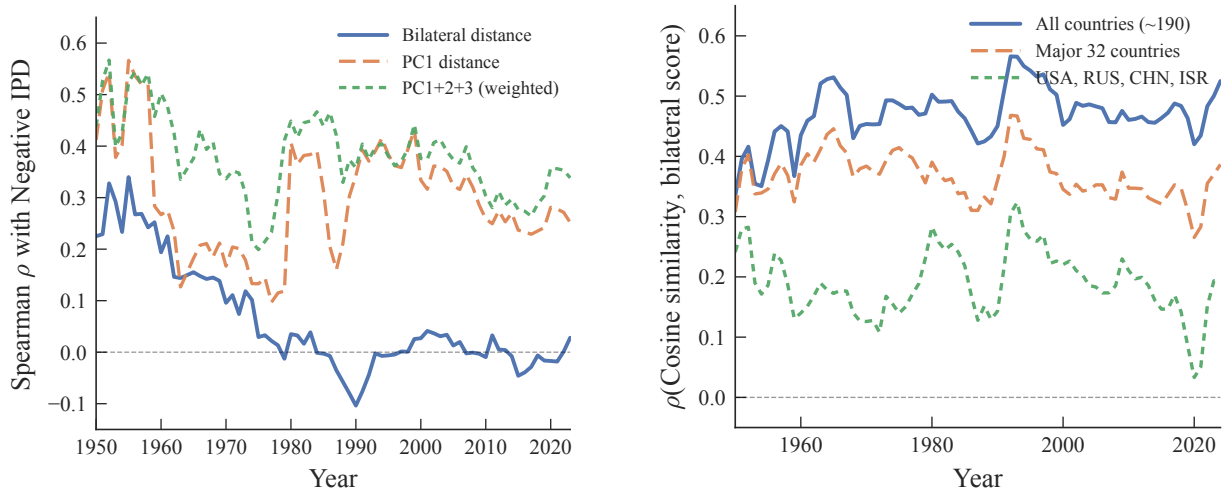
2.5.1. UNGA Voting and Multilateral Positioning

Figure 3A compares the two measures across all country pairs. The year-by-year cross-sectional Spearman correlation between the raw bilateral score and UNGA voting similarity (negative IPD) is low after the 1960s, averaging only 0.06. While the U.S.–China case shows partial correlation between the two measures, the near-zero average correlation across all dyads indicates that UNGA voting primarily reflects multilateral positioning rather than bilateral relations (Voeten 2026).

To sharpen this comparison, we extract principal components from the annual bilateral score matrix.[6] Principal component distances correlate more strongly with negative IPD than the raw bilateral score does: the mean correlation rises to 0.30 using the first principal component and to 0.38 using a variance-weighted distance based on the first three components. This pattern indicates that UNGA voting captures the broad multilateral structure embedded in bilateral relations, while most of the dyad-specific variation in our measure is orthogonal to voting behavior.

Appendix Figure A3 reinforces this distinction at the aggregate level. UNGA voting similarity continued to improve after 2007, even as trade globalization stagnated. Our event-based measure, by contrast, records bilateral deterioration over the same period (Figure 1b). The two measures thus track different dimensions of the international system: one tied to multilateral positioning, the other to bilateral political relations.

FIGURE 3. Bilateral and Multilateral Dimensions of Geopolitical Alignment



A. Bilateral alignment vs. UNGA voting similarity

B. Multilateral position vs. bilateral score

Notes: Panel A reports the annual Spearman correlation between UNGA voting similarity (negative IPD) and three bilateral distance measures based on our data. Panel B reports the annual Spearman correlation between cosine similarity of third-country stance vectors and the bilateral score under alternative reference sets.

[6] For each year t, we construct the symmetric $N_t \times N_t$ matrix of bilateral scores $\mathbf{S}_t = [S_{ij,t}]$ and extract principal components. Let $p_{ik,t}$ denote the PCk score for country i and $\sigma^2_{k,t}$ the share of total variance explained by the k-th component. The PCk distance for dyad (i, j) is $|p_{ik,t} - p_{jk,t}|$. The variance-weighted PC1+2+3 distance is $d^{w3}_{ij,t} = \sum_{k=1}^{3} \omega_{k,t} |p_{ik,t} - p_{jk,t}|$, where $\omega_{k,t} = \sigma^2_{k,t} / \sum_{\ell=1}^{3} \sigma^2_{\ell,t}$.

2.5.2. Irreducibly Bilateral Variation

A related approach in the literature summarizes bilateral alignment using countries' relations with a small number of reference powers (Bonadio et al. 2025; Gopinath et al. 2025; Liu and Yang 2025). To assess how much bilateral variation this approach recovers, we compute cosine similarity in countries' third-country stance vectors and compare it with the direct bilateral score $S_{od,t}$. Figure 3B reports the year-by-year cross-sectional correlation under alternative reference sets.

Even using the full set of countries as references, the correlation stabilizes at only 0.45 to 0.55, implying an R^2 of roughly 0.25. Most bilateral variation is therefore not recoverable from countries' broader geopolitical orientation. Reducing the reference set to four geopolitical poles weakens the correlation to 0.10–0.30, accounting for a much smaller fraction of bilateral geopolitical alignment. Bilateral relations cannot be summarized well by countries' positions relative to a few hegemons.

These results point to two distinct dimensions of the international system: a multilateral dimension, which UNGA voting and low-dimensional projections partially capture, and a bilateral dimension, shaped by dyad-specific diplomatic, security, and economic interactions. For trade, where frictions operate through country-pair channels, this bilateral dimension is essential.

3. Geopolitical Alignment and Trade Patterns

Before estimating the effects of geopolitical alignment on trade, we document a positive association between geopolitical alignment and trade. We begin with bilateral case studies, then turn to cross-dyad correlations among major economies, and finally examine aggregate regional time series.

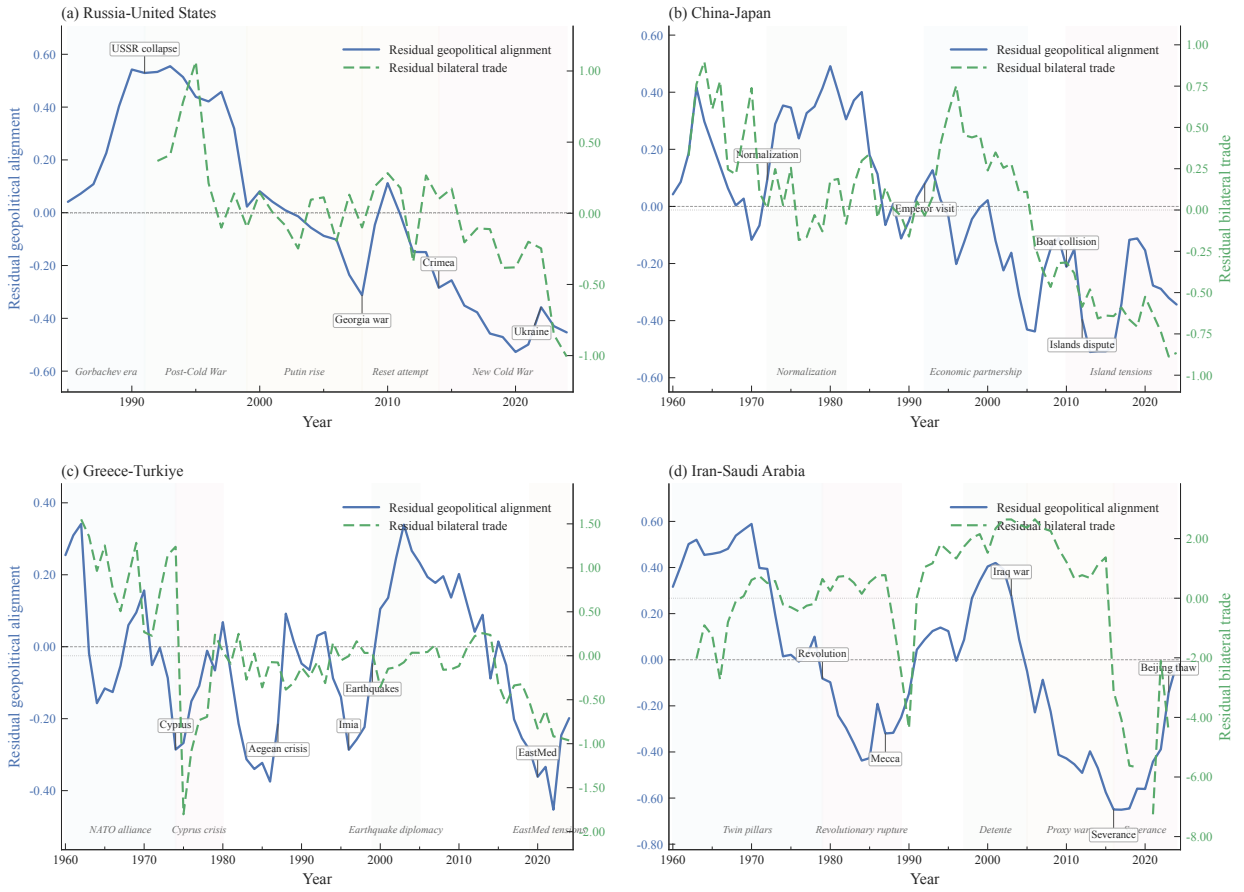
3.1. Case Studies: Geopolitics and Trade Dynamics

We begin with bilateral case studies that illustrate how geopolitical alignment and trade comove across different political settings. Figure 4 plots residualized geopolitical alignment against residualized bilateral trade for four dyads spanning major-power relations and regional rivalries. In each case, periods of stronger geopolitical alignment are associated with stronger bilateral trade, while periods of deterioration coincide with weaker trade. Both series are residualized to isolate bilateral variation from global and country-specific trends: geopolitical scores are residualized on two country-year and dyad fixed effects, and trade flows (log COMTRADE values) on origin-year, destination-year, and origin-destination fixed effects.

Panels (a) and (b) examine major-power dyads. The Russia–U.S. relationship shows a post-Soviet improvement in alignment coinciding with stronger trade, followed by renewed deterioration beginning in the late 1990s and intensifying after 2014, which coincides with sharply weaker bilateral trade. The China–Japan relationship displays a similar pattern: the improvement in relations during the 1990s is associated with stronger trade, while the deterioration after 2010 amid territorial disputes coincides with declining trade residuals.

Panels (c) and (d) extend the analysis to regional rivalries outside the major-power sample. In the Greece–Türkiye dyad, episodes of political conflict coincide with weaker trade, while periods

FIGURE 4. Geopolitics and Trade: Selected Bilateral Relationships



Notes: Each panel plots residualized geopolitical alignment (blue, left axis) against residualized bilateral trade (red, right axis). Geopolitical scores are residualized on two country-year fixed effects and dyad fixed effects. Trade flows (log values from COMTRADE) are residualized on origin-year, destination-year, and origin-destination fixed effects. Shaded regions indicate major diplomatic periods.

of diplomatic improvement coincide with stronger trade. In the Iran–Saudi Arabia dyad, the improvement in relations around the late 1990s is associated with stronger bilateral trade, while renewed deterioration after the mid-2000s and especially after 2016 coincides with sharply weaker trade.

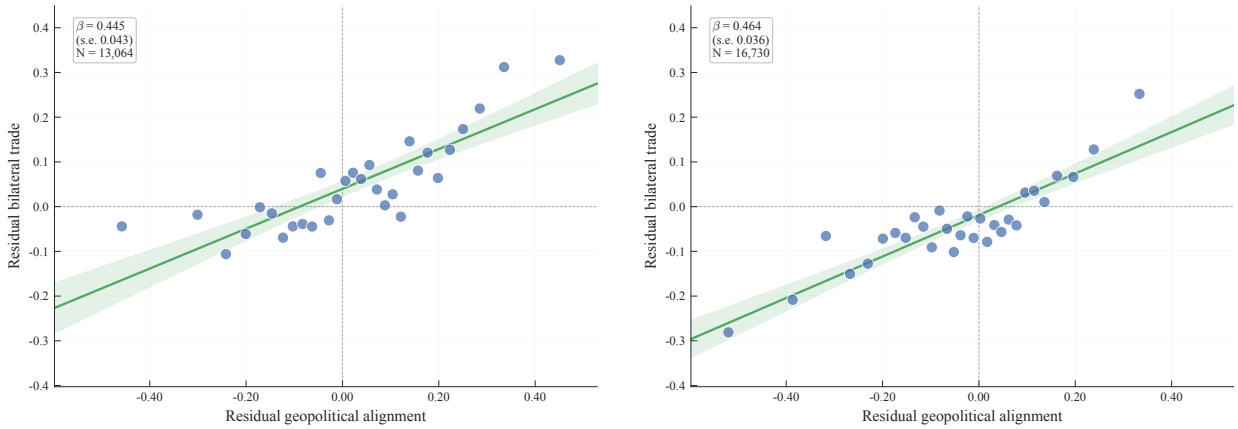
These cases are illustrative rather than exhaustive. Appendices A.2 and A.3 present additional dyads and show similar patterns across a broader set of bilateral relationships.

3.2. Cross-Dyad Correlation

We next move from case studies to the full set of major-economy dyads. Figure 5 plots residualized bilateral trade against residualized geopolitical alignment separately for the Cold War and post-1991 periods. The relationship is positive in both subsamples. A one-unit increase in residual geopolitical alignment is associated with a 45 log point increase in residual trade in the Cold War era ($\beta = 0.445$,

s.e. = 0.043, N = 13,064) and a 46 log point increase in the post-1991 period (β = 0.464, s.e. = 0.036, N = 16,730). The positive association is therefore stable across markedly different international regimes.

FIGURE 5. Geopolitical Alignment and Trade Intensity: Major-Economy Dyads



A. Cold War Era (Pre-1991)

B. Post-Cold War (1991–2024)

Notes: Binscatter plots of residualized log trade flows against residualized geopolitical alignment for dyads among 32 major economies. Each point represents the mean within 30 quantile-based bins. Fitted lines from bivariate regressions are shown with 95% confidence intervals. Trade and geopolitical scores are residualized as in Figure 4. Major economies are defined as countries that appeared among the top 20 in global GDP at any point since 1960.

Appendix A.5 reports a variance decomposition of bilateral trade flows. Geographic distance explains the largest share of the variation, but geopolitical alignment accounts for 3.4 percent across all countries, comparable to linguistic distance (2.6 percent) and larger than the border effect (1.1 percent). Time-varying political relations are therefore quantitatively relevant even relative to standard gravity variables.

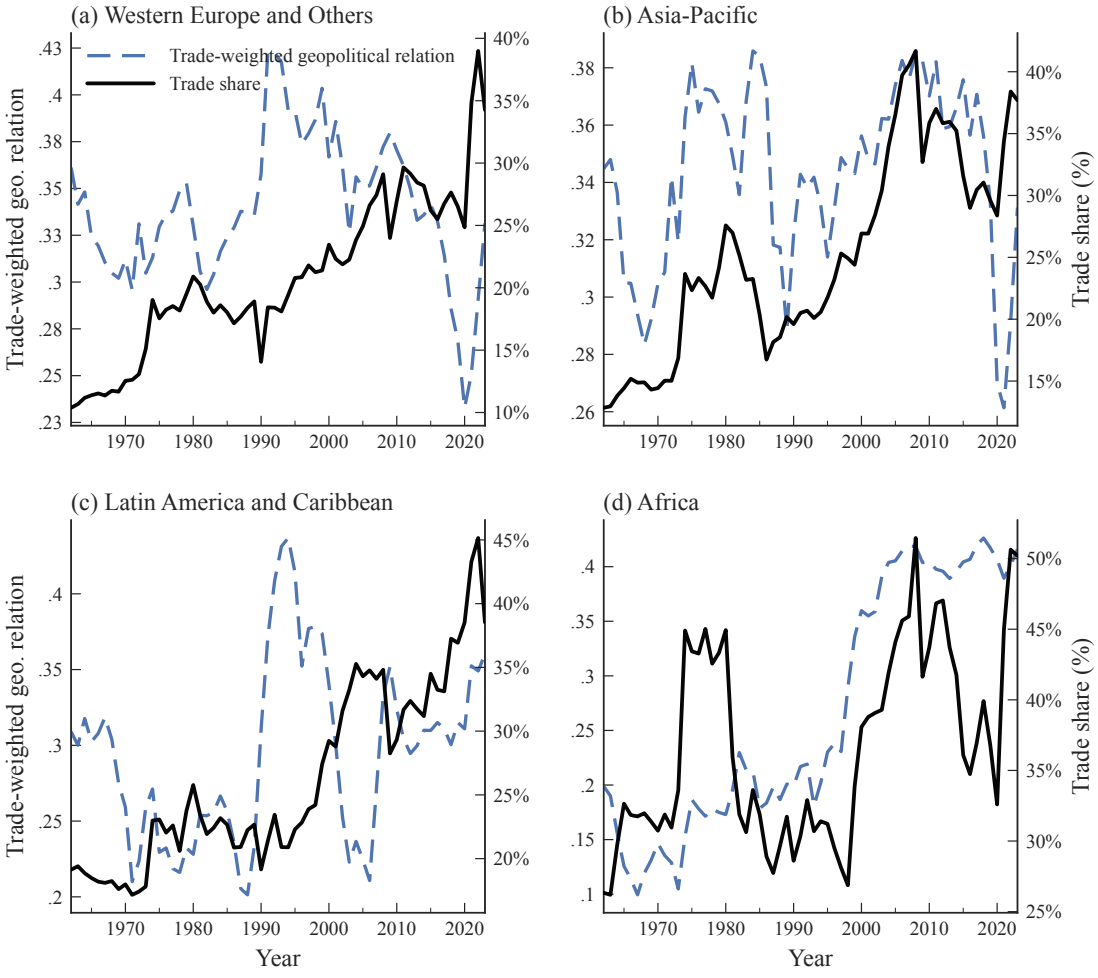
3.3. Aggregate Time-Series Correlation

Finally, we examine whether these bilateral patterns also appear in regional aggregate time series. Figure 6 plots average geopolitical alignment against trade shares for four regional groupings: Western Europe and Others, Asia-Pacific, Latin America and the Caribbean, and Africa.

The figure reveals substantial regional heterogeneity but a common positive association between geopolitical alignment and trade shares. In Western Europe and Others, trade shares rise steadily from the 1970s through the 2000s, while average geopolitical alignment improves over much of the same period before weakening after the late 2000s. In Asia-Pacific, the comovement is especially pronounced during the globalization era: stronger alignment coincides with rapid trade integration through the 1990s and 2000s, while weaker alignment after the late 2000s is associated with slower trade growth.

Latin America and the Caribbean and Africa display noisier patterns, but the same broad

FIGURE 6. Geopolitics and Trade over Time across Regions



Notes: Each panel plots trade-flow-weighted geopolitical alignment (left axis) against region-related trade shares (right axis). For each region-year, trade share is total bilateral trade involving at least one country from the region divided by aggregate regional GDP. Geopolitical alignment is the trade-flow-weighted mean of bilateral dynamic geopolitical scores over the same set of dyads.

relationship remains visible. In both regions, periods of stronger alignment tend to coincide with higher trade shares, while periods of deterioration are associated with weaker trade integration. The timing and magnitude differ across regions, reflecting differences in exposure to global markets, regional institutions, and geopolitical shocks.

These aggregate correlations confirm that the positive relationship between geopolitical alignment and trade is visible not only in bilateral data but also in aggregate regional time series. Together with the case studies and cross-dyad evidence, the descriptive analysis points to a consistent pattern: stronger geopolitical alignment is associated with stronger trade. Section 4 moves beyond these descriptive patterns by exploiting within-dyad variation to estimate the dynamic effects of geopolitical alignment on trade.

4. Trade Elasticities to Geopolitical Alignment

We now estimate the effect of geopolitical alignment on trade. Cross-sectional gravity estimates quantify the geopolitical barrier to bilateral trade. Local projections then trace how changes in bilateral alignment propagate to trade over time, providing the reduced-form elasticities that underpin the quantitative analysis in Section 6.

4.1. Cross-Country Gravity Estimates

We begin by estimating a standard gravity equation:

$$\ln X_{od,t} = \alpha S_{od,t} + \boldsymbol{\beta}' \mathbf{Z}_{od} + \delta_{ot} + \delta_{dt} + \varepsilon_{od,t}, \tag{3}$$

where $X_{od,t}$ denotes bilateral trade from origin o to destination d in year t, $S_{od,t}$ is our measure of geopolitical alignment, and $\mathbf{Z}_{od}$ includes standard time-invariant gravity controls: geographic distance, contiguity, and linguistic distance. Origin-year and destination-year fixed effects absorb all country-specific time-varying determinants of trade, including GDP, multilateral resistance, and unilateral trade policies, so that identification relies on cross-sectional variation in bilateral relationships. We omit country-pair fixed effects in the baseline specification to compare geopolitical alignment directly with standard gravity variables. Appendix Table A3 reports results with country-pair fixed effects included.

We estimate this specification on two samples. The benchmark sample consists of 32 major economies, defined as countries that appeared among the top 20 in global GDP at any point since 1960. Trade among these economies accounts for 59–71% of world trade over our sample period (Figure A1), despite representing fewer than 3% of potential country pairs. Because bilateral trade flows within this group are almost always strictly positive, the log-linear specification raises limited concerns about selection from zero flows. The full sample includes all country pairs.

Table 4 reports the baseline estimates. The coefficient on geopolitical alignment is positive and precisely estimated in all specifications. In the major-economy sample (columns 1–2), a one-standard-deviation increase in alignment (0.26 units, comparable in magnitude to the U.S.–China deterioration around the 2018 trade war) is associated with 11.9 ($= 0.26 \times 0.458$) log points higher bilateral trade after controlling for geography and language. Without gravity controls (column 1), the bivariate association is 19.0 log points.

Table A1 reports a variance decomposition that quantifies the share of bilateral trade variation explained by different gravity variables. Geopolitical alignment is comparable in magnitude to standard trade barriers such as language: among major countries, geopolitical alignment explains 2.2% of the variation in bilateral trade, compared with 2.8% for linguistic distance.

The estimated effect is larger in the full sample (columns 4–5): a one-standard-deviation increase in alignment is associated with 26.8 log points higher bilateral trade after controlling for gravity variables. The larger coefficient partly reflects the wider dispersion in alignment scores among

TABLE 4. Geopolitical Barriers to Bilateral Trade: Gravity Estimates

	Major Countries			All Countries		
Dependent Variable: log Trade Value	(1)	(2)	(3)	(4)	(5)	(6)
Geopolitical Score	0.729	0.458		2.571	1.096	
	(0.121)	(0.106)		(0.043)	(0.027)	
UNGA Voting Similarity:			-0.342			-0.084
Negative Ideal Point Distance			(0.045)			(0.013)
Geographic Distance		-0.813	-0.947		-1.448	-1.562
		(0.052)	(0.051)		(0.016)	(0.017)
1[neighbor]		0.226	0.257		0.843	0.765
		(0.171)	(0.157)		(0.079)	(0.083)
Linguistic Distance		-1.099	-1.705		-1.701	-1.905
		(0.330)	(0.301)		(0.075)	(0.078)
Mean Dep. Var.	12.52	12.52	12.72	7.23	7.23	7.26
Observations	58,948	58,948	50,946	1,087,543	1,087,543	974,780
Origin × Year FE	Yes	Yes	Yes	Yes	Yes	Yes
Destination × Year FE	Yes	Yes	Yes	Yes	Yes	Yes

Notes: The unit of observation is an origin-destination country pair in a year. Columns 1–3 report results for country pairs among 32 major countries, while columns 4–6 include all country pairs. Standard errors are clustered at the country-pair level.

smaller-economy pairs. Appendix Table A2 confirms robustness to Poisson pseudo-maximum likelihood (PPML) and inverse hyperbolic sine (IHS) specifications that account for zero trade flows.

To benchmark our measure against the standard approach in the literature, columns 3 and 6 replace geopolitical alignment with UNGA voting similarity (negative Ideal Point Distance). The coefficient is negative, implying that countries with more similar voting patterns tend to trade *less*. This counterintuitive sign is consistent with the evidence in Section 2.5 that UNGA voting captures multilateral positioning rather than bilateral relations. India–Pakistan and Greece–Türkiye illustrate the disconnect: both dyads exhibit high voting similarity despite persistent bilateral tensions.

Robustness The results are robust along several dimensions. First, adding country-pair fixed effects preserves the main finding. Table A3 shows that the coefficient on geopolitical alignment remains positive and precisely estimated, though it attenuates in the full sample, suggesting that for non-major economies alignment is more strongly correlated with persistent bilateral characteristics absorbed by pair fixed effects. The coefficient on UNGA voting similarity switches sign in these specifications, becoming positive. Second, Table A4 shows that the results are unchanged when we use BACI or IMF trade data in place of UN Comtrade. Third, Table A5 reports similar coefficients using alternative geopolitical alignment measures such as raw scores, alternative discount factors λ, and moving-average measures. Fourth, Figure A4 reports repeated cross-sectional gravity estimates by year. The coefficient is large during the Cold War, declines in the post–Cold War period, and rises again after 2018, indicating that the relationship between geopolitics and trade varies across international regimes while remaining economically important throughout.

4.2. Dynamic Effects of Geopolitical Alignment on Trade

To identify the dynamic response of trade to geopolitical shocks, we estimate local projections (Jordà 2005; Jordà and Taylor 2025), following the empirical strategy of Boehm, Levchenko, and Pandalai-Nayar (2023). This approach traces both the contemporaneous impact and the adjustment path of trade following changes in alignment, and accommodates the autocorrelation structure of both geopolitical alignment and trade flows.[7]

4.2.1. Empirical Specification

Our specification traces the full impulse response function:

$$\ln X_{od,t+h} = \beta_h S_{od,t} + \sum_{\ell=1}^{L} \gamma_{h,\ell} \ln X_{od,t-\ell} + \sum_{\ell=1}^{L} \beta_{h,\ell} S_{od,t-\ell} + \delta_{od} + \delta_{ot} + \delta_{dt} + \varepsilon_{od,t+h} \tag{4}$$

for horizons $h \in \{-8, -7, \ldots, 19, 20\}$. The coefficient β_h captures the response of bilateral trade at horizon h to a unit change in geopolitical alignment at time t, controlling for the autocorrelation in both variables through $L = 3$ lags.[8]

Our identification strategy exploits within-dyad temporal variation through a triple fixed effects structure. Country-pair fixed effects (δ_{od}) absorb all time-invariant bilateral determinants: geographic distance, colonial history, common language, and other standard gravity variables. Origin-year (δ_{ot}) and destination-year (δ_{dt}) fixed effects control for all country-specific time-varying factors, including GDP, multilateral resistance terms, unilateral trade policies, and global value chain participation. Identification therefore derives exclusively from differential changes in bilateral geopolitical alignment, isolating the relationship-specific component from both global trends and country-level shocks.

Discussion of Identification The key identifying assumption is that, conditional on the fixed effects and lagged controls, current geopolitical alignment is uncorrelated with future innovations in bilateral trade:

$$\mathbb{E}\left[\varepsilon_{od,t+h} \mid S_{od,t}, \mathbf{X}_{od,t}, \delta_{od}, \delta_{ot}, \delta_{dt}\right] = 0, \tag{5}$$

where $\mathbf{X}_{od,t} \equiv \{\ln X_{od,t-\ell}, S_{od,t-\ell}\}_{\ell=1}^{L}$. Two threats to this assumption are reverse causality and omitted time-varying bilateral confounders.

A potential concern is reverse causality, whereby bilateral trade affects geopolitical alignment. This concern is primarily relevant at $h = 0$, where trade shocks may directly influence alignment.

[7] Local projections offer three key advantages over VAR methods (Jordà 2005; Montiel Olea and Plagborg-Møller 2021; Plagborg-Møller and Wolf 2021). First, they remain robust to mis-specification of the underlying dynamic process. Second, they naturally accommodate our high-dimensional fixed effects structure. Third, estimating pre-treatment responses for $h < 0$ provides a direct test for reverse causality and anticipation.

[8] Appendix Figure A5 demonstrates robustness to alternative lag specifications. Using $L = 5$ yields virtually identical impulse responses, confirming that three lags adequately capture the relevant dynamics.

For horizons $h > 0$, reverse causality would require future trade shocks to affect past geopolitical alignment, which is unlikely. For $h < 0$, the estimates provide a pre-trend test. If trade influences alignment, then past trade shocks should predict current geopolitical alignment. In that case, we would expect to observe significant coefficients at negative horizons. The absence of such pre-trends mitigates concerns about reverse causality. We further assess this issue directly in Section 4.3.5, where we instrument bilateral trade using predicted trade flows from a gravity model with time-varying transportation costs. The results show that exogenous trade shocks do not affect subsequent geopolitical alignment.

A second threat comes from omitted bilateral shocks. The triple fixed effects absorb any confounder $Z_{od,t}$ that decomposes as $Z_{od,t} = a_{od} + b_{ot} + c_{dt}$. The remaining concern is a genuinely bilateral time-varying shock correlated with both the innovation on geopolitical alignment and trade. Two candidates illustrate the scope of this concern. First, bilateral unobservable factors such as investment commitments, lending arrangements, or infrastructure projects from o to d can raise trade directly and improve political relations through diplomatic engagement. To the extent that such factors involve observable political acts—loan signings, project announcements, or state visits—they enter $S_{od,t}$; the residual concern is the trade effect of these activities themselves, which unfolds gradually and is at least partly absorbed by the dyad fixed effect and lagged controls. Second, events involving a third country k may affect both alignment and trade between o and d. Our construction of $S_{od,t}$ addresses much of this concern: multilateral events are translated into bilateral scores for all relevant pairs, and country-year fixed effects absorb changes in each country's overall external posture. The remaining concern is limited to pair-specific third-country factors not reflected in the event data and not absorbed by the fixed effects.

More generally, any remaining omitted variable must not be captured by $S_{od,t}$, must not be absorbed by the fixed effects, and must still be correlated with future bilateral trade. This is a narrow class of confounders, which limits the scope for omitted-variable bias, though it cannot be ruled out entirely. We address this concern by showing in Section 4.3 that the dynamic relationship between geopolitical alignment and future trade is universal across country pairs, operates for both improvements and deteriorations in alignment, and holds across six decades spanning Cold War bipolarity and post–Cold War globalization. A bilateral confounder that could generate these patterns would need to be present across all these dimensions simultaneously.

4.2.2. Main Results

Our analysis focuses on pairs of major economies for both econometric and economic reasons. From an econometric perspective, restricting the sample to major economies substantially mitigates the prevalence of zero trade flows, which is a well-known challenge in gravity estimations (Head and Mayer 2014).[9] From an economic perspective, major economies account for 59–71 percent of

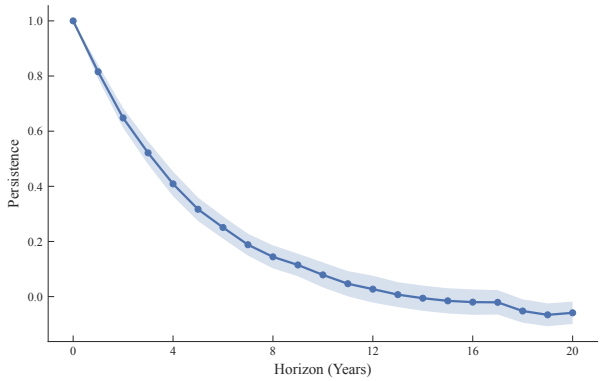
[9] Among the 32 major economies in our sample, fewer than 5% of potential bilateral trade flows are zero, compared to over 50% in the full sample. Unlike static gravity equations, where PPML offers a natural solution to zero flows (Santos Silva and Tenreyro 2006), local projections do not have a standard PPML counterpart that accommodates the

global trade over the sample period while representing fewer than 3% of all potential country pairs, making them the primary drivers of global trade patterns.

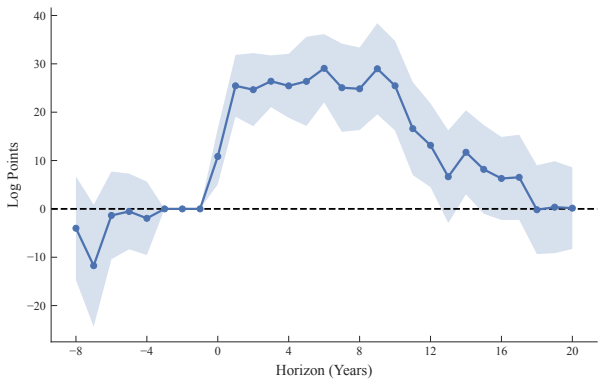
Figure 7 presents our main dynamic results. Panel A shows that shocks to geopolitical alignment are persistent but mean-reverting. Following a one-unit improvement in alignment, roughly half of the effect remains after three years, and it largely dissipates within a decade. This persistence drives the cumulative trade response documented below.

FIGURE 7. Dynamic Effect of Geopolitical Alignment on Trade

A. Persistence of Geopolitical Alignment



B. Response of Trade to Geopolitical Alignment



Notes: Panel A reports estimates $\{\phi_h\}$ from: $S_{od,t+h} = \phi_h S_{od,t} + \sum_{\ell=1}^{3} \phi_{h,\ell} S_{od,t-\ell} + \delta_{ot} + \delta_{dt} + \delta_{od} + \varepsilon_{od,t+h}$. Panel B shows estimates $\{\beta_h\}$ from $\ln X_{od,t+h} = \beta_h S_{od,t} + \sum_{\ell=1}^{3} \gamma_{h,\ell} \ln X_{od,t-\ell} + \sum_{\ell=1}^{3} \beta_{h,\ell} S_{od,t-\ell} + \delta_{od} + \delta_{ot} + \delta_{dt} + \varepsilon_{od,t+h}$. The sample includes country pairs among 32 major economies. Both panels report estimated coefficients with 95% confidence intervals based on Driscoll–Kraay standard errors.

Panel B highlights three features of the trade response. First, the coefficients at horizons −8 to −4 are small and statistically indistinguishable from zero, providing no evidence of pre-trends and supporting the identifying assumption.[10] Second, the effect builds up rapidly: the coefficient rises from about 10 log points on impact to approximately 28 log points within three years. This buildup indicates that geopolitical shocks trigger swift reallocation of trade flows, consistent with the rapid supply chain adjustments documented by Fajgelbaum et al. (2024) in the context of the U.S.–China trade war. Third, the response is hump-shaped, declining after year 10 as the geopolitical impulse dissipates.

Our inference employs Driscoll–Kraay standard errors to account for both serial correlation and cross-sectional dependence arising from common shocks (Driscoll and Kraay 1998). Appendix Figure A6 demonstrates robustness to alternative inference methods: clustering at the country-pair level yields nearly identical confidence intervals, while bootstrap inference produces only modestly wider bands.

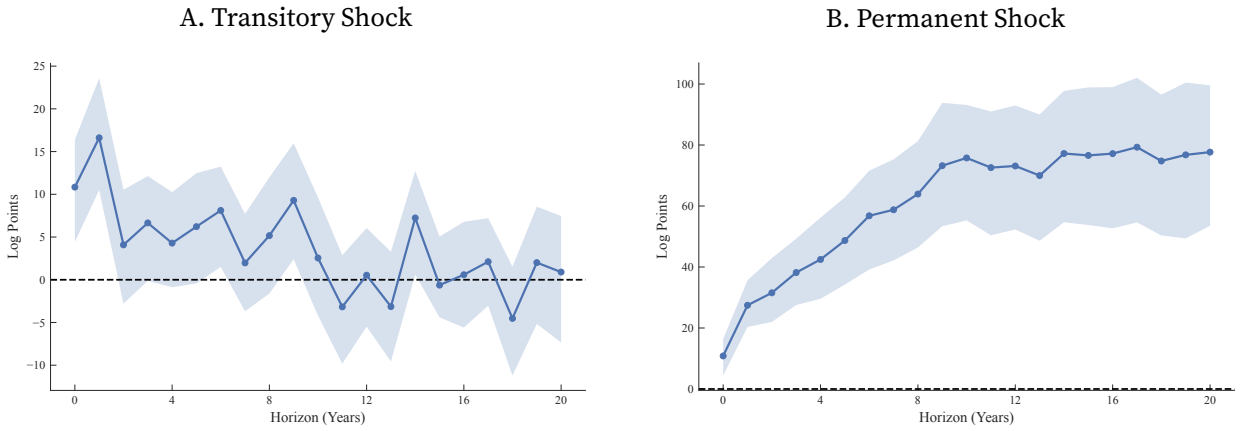
dynamic structure with leads, lags, and high-dimensional fixed effects.

[10] Because the specification includes three lags of trade as controls, the coefficients at horizons $h = -3, -2, -1$ are mechanically equal to zero.

4.2.3. Decomposing Transitory and Permanent Effects

The local projection estimates in Figure 7 combine the effect of an initial geopolitical shock with the persistence of that shock over time. To separate these margins, we decompose the responses into transitory and permanent components following Bilal and Känzig (2026). Appendix A.8 provides details of the decomposition.

FIGURE 8. Impulse Responses of Trade to Transitory and Permanent Geopolitical Shocks



Notes: Panel A reports the impulse response of log trade to a purely transitory unit shock to geopolitical alignment. Panel B reports the cumulative response to a permanent unit shock. Both panels use the baseline specification with three lags and triple fixed effects (country-pair, origin-year, destination-year). The 95% confidence intervals are based on 200 bootstrap iterations with country-pair block resampling.

Figure 8 presents the results. In Panel A, a unit transitory improvement in geopolitical alignment at $t = 0$ increases trade by approximately 11 log points on impact, peaking at about 17 log points after one year, with the effect persisting for 5–7 years before dissipating. This pattern indicates that even transitory geopolitical shocks generate meaningful and persistent effects on trade.

Panel B shows that permanent improvements in alignment produce substantially larger long-run effects. Following a permanent one-unit increase in geopolitical alignment, trade rises steadily, reaching approximately 78 log points after 20 years, with the response flattening after about 10 years. Scaling by the standard deviation of alignment (0.23 units), a permanent one-standard-deviation improvement implies a long-run increase in trade of about 18 log points, or roughly 20 percent. This magnitude is larger than the cross-sectional estimate in Table 4.

4.3. Robustness

We assess the robustness of our dynamic trade elasticities along several dimensions. First, we examine whether the effects extend to country samples beyond major economies. Second, we evaluate temporal stability across distinct global trade regimes. Third, we investigate whether the effects hold when distinguishing between economic and non-economic geopolitical events, and between positive and negative shocks. We also conduct a formal test for reverse causality and verify robustness to alternative constructions of the geopolitical measure. Figure 9 presents

the corresponding local projection estimates. The corresponding autocorrelation functions are presented in Figure A7.

4.3.1. Alternative Country Samples

Panels A and B of Figure 9 extend the analysis beyond major-economy pairs to examine whether geopolitical effects on trade are universal or concentrated among large economies.

Panel A examines trade between major and non-major economies, where power asymmetries may shape the transmission of geopolitical shocks. The peak response is approximately 17 log points, smaller than the 28 log points estimated for major–major pairs in the baseline. At the same time, the effect is more persistent, with trade remaining elevated for more than 15 years following the initial shock. This pattern suggests that geopolitical shocks may have a more muted immediate impact in asymmetric dyads but more durable effects once embedded in trading relationships.

Panel B extends the sample to all country pairs. The estimated response remains positive and statistically significant, although the peak declines to around 18 log points. This attenuation is consistent with geopolitical alignment being less consequential for trade among smaller economies. The response also evolves more gradually, reaching its peak only after approximately five years. Across both panels, the coefficients at negative horizons remain close to zero, providing no evidence of pre-trends.

4.3.2. Temporal Stability

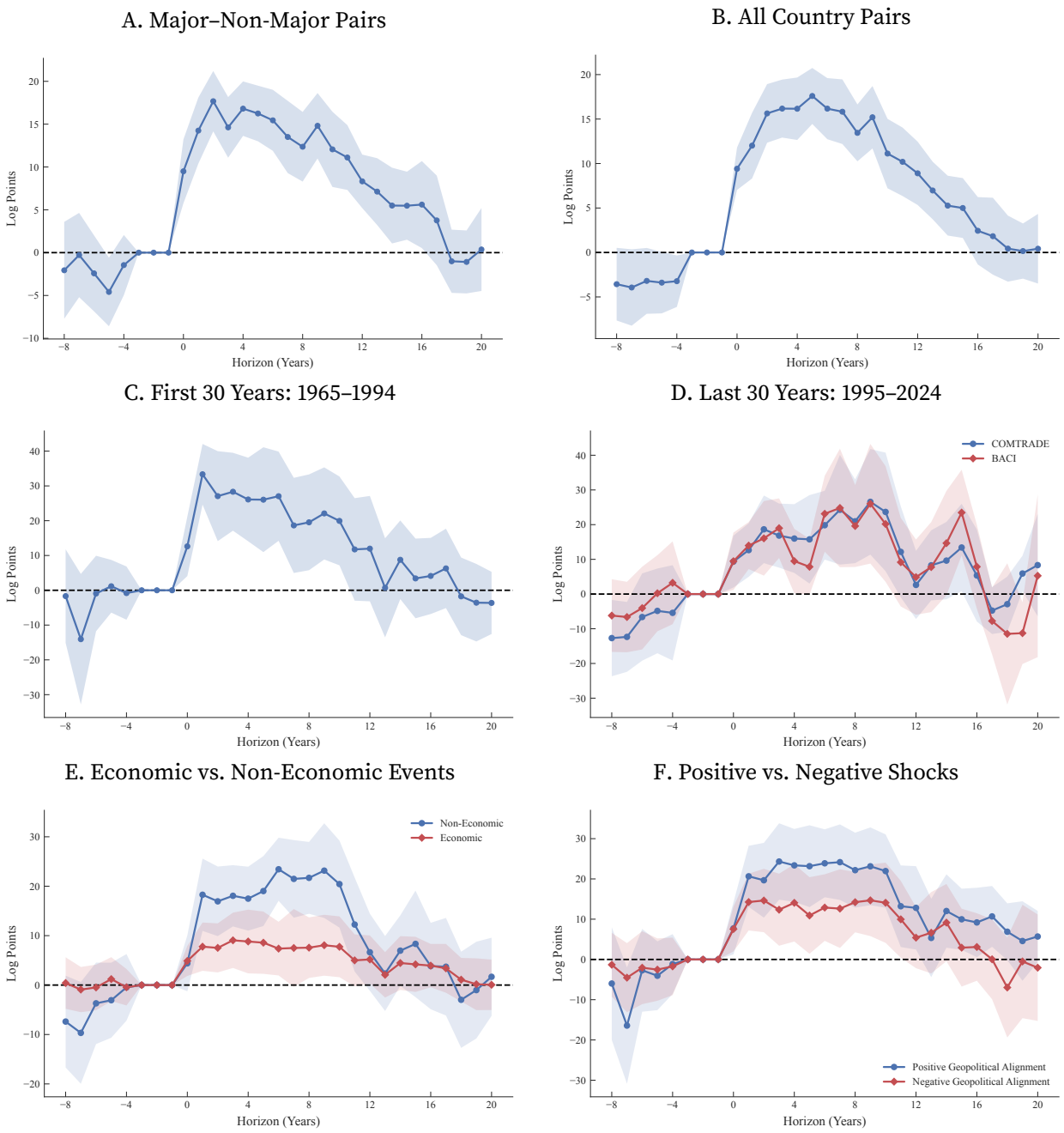
The global trading system changed substantially over our sample period, from Cold War bipolarity to WTO-centered multilateralism and, more recently, renewed fragmentation. Panels C and D of Figure 9 examine whether the effect of geopolitics on trade differs across these periods. The effect is present in both subsamples, but the adjustment dynamics differ. In the first 30-year period, which largely coincides with the Cold War, the trade response is rapid, peaking at approximately 33 log points within two to three years. In the subsequent 30-year period, the response is more gradual and hump-shaped, reaching a peak of about 26 log points at horizons 6–9; the pattern is nearly identical when using BACI trade data.

These findings suggest that the speed of adjustment changed over time, even as the overall effect of geopolitical alignment on trade remained economically meaningful in both periods. A natural interpretation is that geopolitical shocks translated more quickly into trade reallocation in the earlier period, when trade blocs and formal restrictions were more prominent. In the later period, adjustment is slower, consistent with deeper production networks and more complex trade relationships.

The corresponding results using UNGA voting similarity are less stable across periods.[11] This instability is consistent with the evidence in Section 2.5 that voting-based measures capture multilateral positioning rather than the bilateral variation most relevant for trade.

[11] Appendix Figure A11 shows that IPD-based estimates are statistically significant before 1995 but attenuate thereafter.

FIGURE 9. Dynamic Effect of Geopolitical Alignment on Trade: Robustness



Notes: Panels A–D report estimates $\{\beta_h\}$ from the regression $\ln X_{od,t+h} = \beta_h S_{od,t} + \sum_{\ell=1}^{3} \gamma_{h,\ell} \ln X_{od,t-\ell} + \sum_{\ell=1}^{3} \beta_{h,\ell} S_{od,t-\ell} + \delta_{od} + \delta_{ot} + \delta_{dt} + \varepsilon_{od,t+h}$ across four subsamples. Panel A includes country pairs between major and non-major countries; Panel B includes all country pairs; Panel C focuses on major country pairs over 1965–1994; and Panel D covers major country pairs over 1995–2024, displaying estimates using both COMTRADE (blue) and BACI (red) trade data. Panel E reports estimates $\{\beta_h^{\text{econ}}, \beta_h^{\text{non-econ}}\}$ from $\ln X_{od,t+h} = \beta_h^{\text{econ}} S_{od,t}^{\text{econ}} + \beta_h^{\text{non-econ}} S_{od,t}^{\text{non-econ}} + \sum_{\ell=1}^{3} \gamma_{h,\ell} \ln X_{od,t-\ell} + \sum_{\ell=1}^{3} \beta_{h,\ell}^{\text{econ}} S_{od,t-\ell}^{\text{econ}} + \sum_{\ell=1}^{3} \beta_{h,\ell}^{\text{non-econ}} S_{od,t-\ell}^{\text{non-econ}} + \delta_{od} + \delta_{ot} + \delta_{dt} + \varepsilon_{od,t+h}$, estimated on major country pairs. Panel F similarly reports estimates $\{\beta_h^{\text{pos}}, \beta_h^{\text{neg}}\}$ from analogous specifications. All panels display coefficient estimates with 95% confidence intervals based on Driscoll–Kraay standard errors.

4.3.3. Economic and Non-Economic Geopolitical Alignment

Economic-related events may generate a mechanical relationship between the geopolitical score and trade. To address this concern, we construct separate measures of geopolitical alignment based on economic and non-economic events. For each category, we compute the average Goldstein score and smooth the resulting series using $\lambda = 0.3$. We then estimate the following specification:

$$(6)\quad \ln X_{od,t+h} = \sum_{g\in\{\substack{\text{econ}\\\text{non-econ}}\}} \beta_h^g S_{od,t}^g + \sum_{\ell=1}^{3} \gamma_{h,\ell} \ln X_{od,t-\ell} + \sum_{g\in\{\substack{\text{econ}\\\text{non-econ}}\}} \sum_{\ell=1}^{3} \beta_{h,\ell}^g S_{od,t-\ell}^g + \delta_{od} + \delta_{ot} + \delta_{dt} + \varepsilon_{od,t+h}.$$

Panel E of Figure 9 presents the results. Non-economic geopolitical alignment exhibits effects similar in magnitude and persistence to those of the aggregate score, while the impact of economic-related alignment is weaker. This pattern suggests that the baseline results are not driven by a mechanical link between economic events and trade. Instead, non-economic interactions, including diplomatic, security, and political engagements, play a central role in shaping bilateral trade. Because non-economic shocks are less likely to be driven by contemporaneous trade flows, this specification also helps alleviate concerns about reverse causality.

4.3.4. Positive and Negative Geopolitical Alignment

We examine whether the effect of geopolitical alignment on trade is driven by positive or negative shocks. Distinguishing between them allows us to assess potential asymmetries in how trade responds to improvements versus deteriorations in relations. Using the CAMEO classification, we construct a measure of positive geopolitical shocks by averaging event scores from the verbal and material cooperation categories and smoothing the series with $\lambda = 0.3$. We construct an analogous measure of negative shocks based on the verbal and material conflict categories. We then estimate a specification analogous to equation (6), replacing $S_{od,t}^{\text{econ}}$ and $S_{od,t}^{\text{non-econ}}$ with $S_{od,t}^{\text{pos}}$ and $S_{od,t}^{\text{neg}}$.

Panel F of Figure 9 reports the results. Both positive and negative geopolitical shocks generate significant trade responses, but the effects are not symmetric. Positive shocks produce a larger and more persistent response, peaking at approximately 23 log points, while negative shocks peak at around 14 log points. This asymmetry suggests that cooperative geopolitical events, such as diplomatic agreements or alliance formation, may be more consequential for trade than conflictual events of comparable intensity. One interpretation is that cooperation opens new trading relationships and reduces uncertainty, while conflict disrupts existing flows that may be partially sustained by contractual commitments and sunk investments. Despite this asymmetry, the fact that both directions of geopolitical change produce significant trade effects strengthens confidence that our baseline estimates reflect a systematic relationship rather than a pattern driven by a specific subset of events.

4.3.5. Testing for Reverse Causality

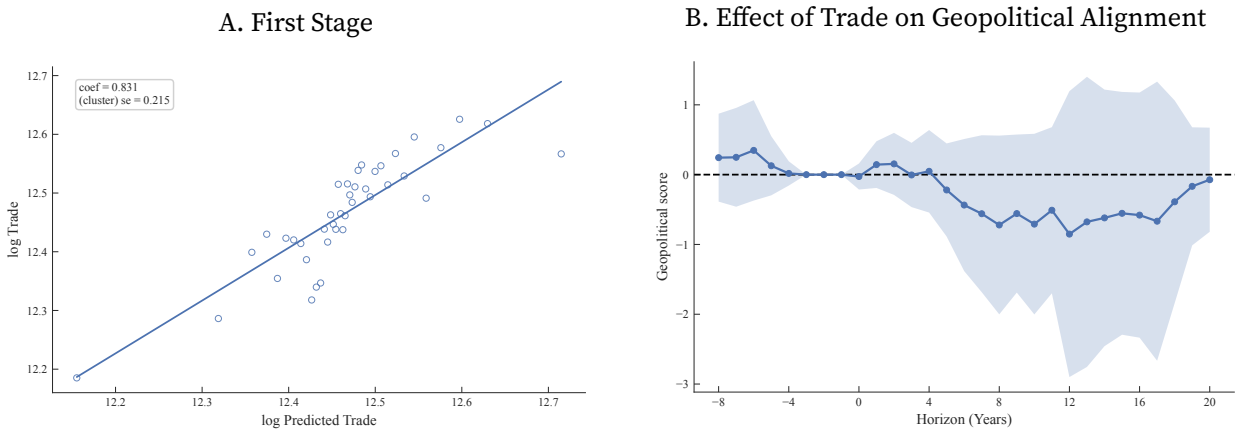
A central identification concern is reverse causality: bilateral trade may itself affect geopolitical alignment. We test whether exogenous shocks to trade generate subsequent changes in alignment.[12]

We instrument trade using predicted trade flows from a gravity equation with time-varying transportation cost coefficients, following Feyrer (2019). Specifically, we estimate:

$$\ln X_{odt} = \beta_{\text{sea},t} \times \ln \text{seadist}_{od} + \beta_{\text{air},t} \times \ln \text{airdist}_{od} + \delta_{od} + \delta_{ot} + \delta_{dt} + \epsilon_{odt}.$$

Panel A of Figure 10 reports the first stage, showing that predicted trade is highly correlated with actual trade even after controlling for bilateral, exporter-year, and importer-year fixed effects. The first-stage F-statistic is 14.9 (clustered at the country-pair level), above conventional thresholds for weak instruments. Panel B shows that instrumented trade shocks have little effect on subsequent geopolitical alignment: the estimated coefficients remain close to zero and are statistically indistinguishable from zero over a 20-year horizon.

FIGURE 10. Testing Reverse Causality: Effect of Trade on Geopolitical Alignment



Notes: This figure examines the effect of trade on geopolitical alignment. Specifically, we estimate $S_{od,t+h} = \zeta_h \ln X_{od,t} + \sum_{\ell=1}^{3} \gamma_{h,\ell} \ln X_{od,t-\ell} + \sum_{\ell=1}^{3} \phi_{h,\ell} S_{od,t-\ell} + \delta_{ot} + \delta_{dt} + \delta_{od} + \varepsilon_{od,t+h}$. Trade is instrumented using predicted trade flows from a gravity model with time-varying sea and air distance coefficients, following Feyrer (2019). The sample consists of country pairs among 32 major economies. Panel A reports the first stage. Panel B reports the estimated coefficients, with 95% confidence intervals based on Driscoll–Kraay standard errors.

These results provide little evidence that trade shocks systematically affect bilateral geopolitical alignment, supporting the interpretation that the primary direction of causality runs from geopolitics to trade. At a minimum, they indicate that greater bilateral trade alone is unlikely to generate sizable improvements in bilateral alignment.

[12]While the literature has extensively examined how economic fundamentals shape geopolitical outcomes, it typically does not focus on bilateral trade per se. Instead, existing studies emphasize broader mechanisms such as economic dependence through global trade networks (Kleinman, Liu, and Redding 2024), the opportunity cost of conflict (Mayer, Mejean, and Thoenig 2025), and trade asymmetries (Liu and Yang 2025).

4.3.6. Robustness to Alternative Geopolitical Alignment Measures

Our final robustness check examines whether the results are sensitive to the construction of the geopolitical alignment measure. We re-estimate the local projections using the unsmoothed average event score, $\tilde{S}_{od,t}$, which captures contemporaneous bilateral interactions without incorporating historical persistence. The results are reported in Figure A8. Although the unsmoothed measure exhibits rapid mean reversion, with approximately 75% of the initial shock dissipating within one year, the implied trade response remains economically meaningful. The peak elasticity declines to around 10 log points (compared to 28 log points in the baseline), consistent with the more transitory nature of individual events.

When we scale the estimates to reflect a permanent one-unit change in geopolitical alignment, the long-run trade effect converges to our baseline estimate of approximately 78 log points. This convergence across alternative constructions indicates that the relationship between geopolitics and trade is not an artifact of measurement choices but reflects a stable underlying relationship. Whether measured using smoothed indices that capture persistent relationships or raw event scores that isolate short-run shocks, geopolitical alignment emerges as a quantitatively important determinant of bilateral trade.

We further assess robustness by varying the smoothing parameter ($\lambda = 0.1$ and $\lambda = 0.5$), employing simple moving averages of the raw score, and constructing the index using the sum rather than the average of Goldstein scores. All alternative specifications yield qualitatively similar results, as reported in Figures A9 and A10.

5. Heterogeneity and Mechanisms

We examine which country pairs and sectors drive the geopolitics-trade relationship (Section 5.1) and explore the channels through which alignment affects trade (Section 5.2).

5.1. Heterogeneity

Institutional Heterogeneity Government intervention plays an important role in mediating the effect of geopolitics on trade. Deteriorating bilateral alignment increases the likelihood that countries impose restrictive trade policies, and such policies are more readily implemented where executives face fewer institutional constraints. We therefore expect the effect of geopolitical alignment on trade to be stronger among country pairs with greater executive discretionary power. Using data from the Varieties of Democracy project (V-Dem), we proxy discretionary power with the index of judicial and legislative constraints on the executive and classify 32 major economies

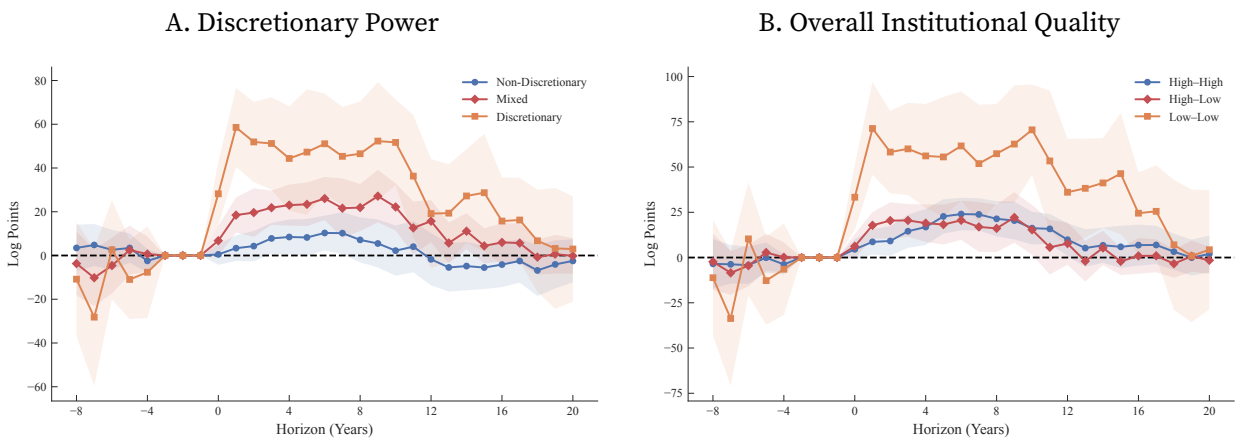
into discretionary and non-discretionary types.[13] We then estimate:

$$\ln X_{od,t+h} = \sum_{g=1}^{3} \beta_h^g S_{od,t} \times \mathbf{1}[(o,d) \in \mathcal{C}_g] + \mathbf{W}'_{od,t}\gamma_h + \delta_{od} + \delta_{ot} + \delta_{dt} + \varepsilon_{od,t+h}, \tag{7}$$

where $\mathcal{C}_1$, $\mathcal{C}_2$, and $\mathcal{C}_3$ denote country pairs in which both countries have low discretionary power, one country has high discretionary power, and both countries have high discretionary power, respectively.

Panel A of Figure 11 presents the estimates. The effect of geopolitical alignment on trade is strongest among pairs in which both countries have high discretionary power and substantially attenuated among pairs with low discretionary power. As a robustness check, we partition countries by overall institutional quality using the Worldwide Governance Indicators from the World Bank and estimate a specification analogous to equation (7).[14] Panel B confirms that the effect is largest among pairs in which both countries have low institutional quality, consistent with the discretionary power results.

FIGURE 11. Dynamic Trade Responses: Institutional Heterogeneity



Notes: This figure reports estimates $\beta_h^{g_1}, \beta_h^{g_2}, \beta_h^{g_3}$ from the regression: $\ln X_{od,t+h} = \beta_h^{g_1} S_{od,t} \times \mathbf{1}[(o,d) \in g_1] + \beta_h^{g_2} S_{od,t} \times \mathbf{1}[(o,d) \in g_2] + \beta_h^{g_3} S_{od,t} \times \mathbf{1}[(o,d) \in g_3] + \sum_{\ell=1}^{3} \gamma_{h,\ell} \ln X_{od,t-\ell} + \sum_{\ell=1}^{3} \beta_{h,\ell}^{g_1} S_{od,t-\ell} \times \mathbf{1}[(o,d) \in g_1] + \sum_{\ell=1}^{3} \beta_{h,\ell}^{g_2} S_{od,t-\ell} \times \mathbf{1}[(o,d) \in g_2] + \sum_{\ell=1}^{3} \beta_{h,\ell}^{g_3} S_{od,t-\ell} \times \mathbf{1}[(o,d) \in g_3] + \delta_{od} + \delta_{ot} + \delta_{dt} + \varepsilon_{od,t+h}$, estimated on major country pairs. In Panel A, g_1 denotes country pairs in which both origin and destination have low discretionary power, g_2 denotes pairs in which one country has high discretionary power, and g_3 denotes pairs in which both countries have high discretionary power. In Panel B, g_1 denotes pairs in which both countries have high institutional quality, g_2 denotes pairs in which one country has low institutional quality, and g_3 denotes pairs in which both countries have low institutional quality. Both panels report coefficient estimates with 95% confidence intervals based on Driscoll–Kraay standard errors.

[13] Countries with low discretionary power include Australia, Austria, Belgium, Canada, Denmark, France, Germany, India, Italy, Japan, the Netherlands, Sweden, Switzerland, the United Kingdom, and the United States. Countries with high discretionary power include Argentina, Brazil, China, Indonesia, Iran, Iraq, Mexico, Nigeria, the Philippines, Poland, Russia, Saudi Arabia, South Africa, South Korea, Spain, Türkiye, and Venezuela.

[14] Countries classified as having high institutional quality include Australia, Austria, Belgium, Canada, Denmark, France, Germany, Italy, Japan, the Netherlands, Poland, South Korea, Spain, Sweden, Switzerland, the United Kingdom, and the United States. Countries classified as having lower institutional quality include Argentina, Brazil, China, India, Indonesia, Iran, Iraq, Mexico, Nigeria, the Philippines, Russia, Saudi Arabia, South Africa, Türkiye, and Venezuela.

Formal Alliances The effect of geopolitical alignment on trade is attenuated among countries linked through formal alliances. Institutionalized cooperation within alliances may dampen the transmission of geopolitical shocks into trade flows in both directions. Alliance members are less likely to impose restrictive policies in response to temporary bilateral deterioration, as formal coordination and dispute resolution mechanisms help contain conflicts. At the same time, improvements in alignment generate more limited trade expansion within alliances, since member countries already exhibit high baseline integration and low policy uncertainty.

Appendix Figure A12 presents the dynamic effects of geopolitical alignment on trade within the European Union and NATO. Consistent with this interpretation, the estimated responses are substantially weaker and statistically insignificant among alliance members, indicating that formal institutional ties reduce the sensitivity of trade to geopolitical shocks.

Sectoral Heterogeneity We examine how the effects of geopolitical alignment vary across sectors. Grouping industries by their 2-digit North American Industry Classification System (NAICS) codes, we estimate effects separately for agriculture, energy and mining, and three manufacturing subsectors. Figure A13 presents the results. The effects are positive across all sectors except energy and mining. The largest and most persistent responses occur in manufacturing, particularly in NAICS sector 33 (primary metals, machinery, electronics, and transportation equipment).

We also examine whether our findings are concentrated in sectors that the U.S. International Trade Administration classifies as "critical." The effects are positive in both critical and non-critical sectors, with no statistically significant difference between the two (Figure A13 Panel F). The sizable effects in sectors not explicitly targeted by government policy suggest that our results are not primarily driven by directed intervention.

5.2. Mechanisms

Trade Policies: Tariffs and Sanctions We turn to whether the effect of geopolitical alignment on trade operates through policy instruments such as tariffs and sanctions. A deterioration in bilateral relations may increase the likelihood of restrictive policy measures, which in turn reduce trade. To investigate this channel, we compile data on three types of restrictive policies: tariffs from Teti (2024), sanctions from the Global Sanctions Database (Felbermayr et al. 2020; Yalcin et al. 2025),[15] and other restrictive trade policies from the Global Trade Alert (GTA) Database. We estimate how geopolitical alignment is associated with the imposition of these policies.

As shown in Column 1 of Table 5, a deterioration in geopolitical alignment is associated with higher tariffs. However, the estimates are imprecise and we cannot reject the null of no effect. One explanation is that tariff setting largely takes place within multilateral frameworks, limiting the role of bilateral geopolitical relations.[16] In contrast, the likelihood of imposing sanctions rises

[15] The GSDB records both comprehensive and partial trade sanctions, encompassing a broader set of restrictive measures than simple trade embargoes.

[16] Among the 32 major economies, 13% of observations have zero tariffs. To account for this, we also use $\ln(1+\text{tariff rate})$ as the dependent variable, yielding a coefficient of −0.003 (0.003).

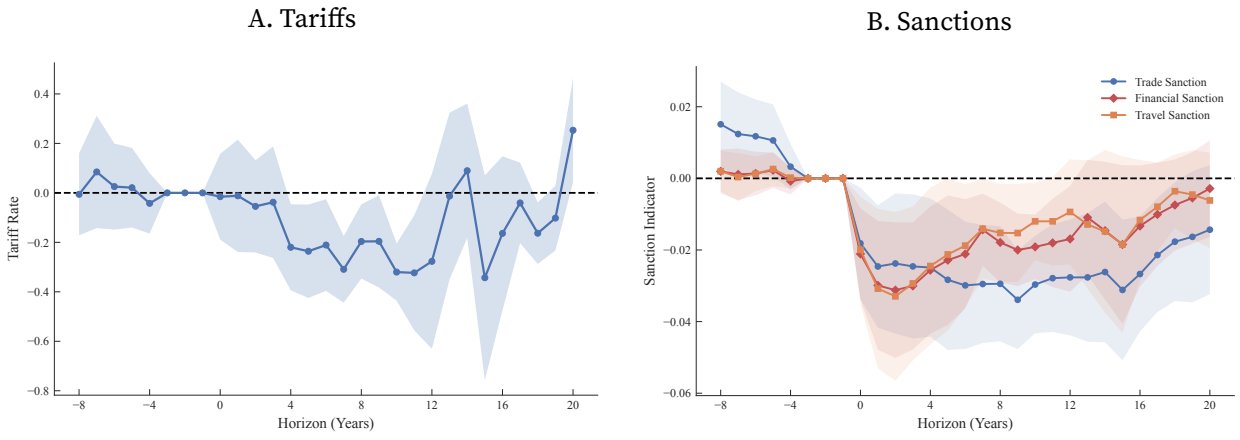
TABLE 5. Geopolitical Alignment and Policies

Dependent Variable:	(1) log Tariff	(2)	(3) **1** [Sanction]	(4)	(5) Restricting Trade Policy	(6)
		Trade	Financial	Travel	≥ 1 Product	≥ 20 Products
Geopolitical Alignment	-0.087	-0.051	-0.052	-0.050	-4.24	-2.16
	(0.130)	(0.009)	(0.006)	(0.005)	(2.02)	(0.88)
Mean Dep. Var.	0.73	0.049	0.037	0.019	21.4	3.24
Observations	21640	74400	74400	74400	16864	16864
Imposer × Year FE	Yes	Yes	Yes	Yes	Yes	Yes
Receiver × Year FE	Yes	Yes	Yes	Yes	Yes	Yes
Imposer × Receiver FE	Yes	Yes	Yes	Yes	Yes	Yes

Notes: The unit of observation is an imposer–receiver country pair in a given year. The dependent variables are the log tariff (column 1); indicators for the presence of trade, financial, and travel sanctions (columns 2–4, respectively); and the number of restrictive trade policies (columns 5–6). The sample includes country pairs among 32 major countries. Standard errors are clustered at the country-pair level.

as geopolitical relations deteriorate. A one-standard-deviation decline in alignment is associated with a 1.4 percentage point increase in the probability of imposing trade, financial, or travel sanctions. Columns 5–6 indicate that worsening relations also increase the number of restrictive trade measures: a one-standard-deviation decline raises the count by about 1.2, with roughly half covering more than 20 products. Taken together, these results suggest that geopolitical alignment shapes the use of restrictive policies, which in turn affect trade flows. Table A6 shows similar results when we use non-economic geopolitical alignment as the independent variable.

FIGURE 12. Dynamic Effect of Geopolitical Alignment on Policies



Notes: This figure shows estimates $\{\beta_h\}$ from: $Y_{od,t+h} = \beta_h S_{od,t} + \sum_{\ell=1}^{3} \gamma_{h,\ell} Y_{od,t-\ell} + \sum_{\ell=1}^{3} \beta_{h,\ell} S_{od,t-\ell} + \delta_{ot} + \delta_{dt} + \delta_{od} + \epsilon_{od,t+h}$, where the dependent variable is log tariff in Panel A and indicators for trade, financial, or travel sanctions in Panel B. The sample includes country pairs among 32 major economies. Both panels report coefficient estimates with 95% confidence intervals based on Driscoll–Kraay standard errors.

Figure 12 examines the dynamic responses of tariffs and sanctions to geopolitical shocks.[17] The responses differ sharply across the two instruments. Panel A shows little systematic response of tariffs to bilateral geopolitical shocks, consistent with Table 5. One interpretation is that the GATT/WTO system and its Most Favored Nation commitments limited the scope for bilateral tariff adjustment over this period.

By contrast, Panel B shows that sanctions respond systematically to geopolitical deterioration. A one-standard-deviation decline in alignment increases the probability of sanctions by about 0.6 percentage points on impact, with the effect persisting for up to a decade.

These results clarify how geopolitical tensions translate into economic decoupling through restrictive policy instruments. While tariffs appear insulated by multilateral rules, sanctions remain flexible tools of bilateral statecraft. At the same time, sanctions account for roughly 18 percent of the total trade response.[18]

Beyond Formal Policies: Uncertainty and Social Attitudes Although we cannot quantify the contribution of other restrictive trade policies, the evidence suggests that formal policy measures explain only part of the broader relationship between geopolitics and trade. Geopolitical tensions can increase uncertainty about future tariffs, sanctions, or regulatory disruptions, inducing firms to adjust supply chains, sourcing decisions, and investment plans in advance. They may also shape consumer demand and firm behavior through changes in social attitudes or political sentiment.

We provide suggestive evidence on this latter channel using bilateral attitude data from the Pew Research Center's *Global Attitudes and Trends Survey*, which measures views toward other countries for a limited sample beginning in 2002. We rescale the index to lie between 0 and 1, with higher values indicating more favorable attitudes. Table 6 reports the results. Among major economies, country pairs with higher geopolitical alignment exhibit more favorable bilateral attitudes. Columns 2 and 3 show that more favorable attitudes are associated with larger bilateral trade flows, and controlling for attitudes reduces the estimated effect of geopolitical alignment on trade.[19] Similar patterns emerge in the full sample of countries.

6. Model and Quantitative Results

To quantify the aggregate and distributional implications of geopolitical change for trade, we embed reduced-form elasticities from Section 4 in an Armington model with perfect competition. There

[17] The GTA data begin in 2008 and therefore do not permit local projections over a sufficiently long horizon.

[18] Following the approach in Appendix A.8, we estimate that the long-run impulse responses of a permanent shock to trade, financial, and travel sanctions on trade value are approximately −0.4, −0.5, and −0.6, respectively. A permanent one-unit deterioration in geopolitical alignment increases the probability of trade, financial, and travel sanctions by roughly 12, 9, and 8 percentage points. Combining these estimates implies that the sanctions channel explains at most $(0.4 \times 0.12 + 0.5 \times 0.09 + 0.6 \times 0.08)/0.78 \approx 18\%$ of the total effect of geopolitical alignment on trade. Sanctions may also affect trade indirectly through exchange rate and financial channels (Itskhoki and Mukhin 2025).

[19] The social attitudes measure is directional, and in the Global Attitudes and Trends Survey most country pairs are observed in only one direction. When estimating the trade regressions, we assign the attitude for each origin–destination pair using the available directional measure; if both directions are observed, we take their average. As a result, the number of observations in columns 2 and 3 is less than double that in column 1.

TABLE 6. Geopolitical Alignment and Social Attitudes

Dependent Variable:	(1) Attitudes	(2) log Trade	(3)	(4) Attitudes	(5) log Trade	(6)
	Major Countries			All Countries		
Geopolitical Alignment	0.147	0.427	0.309	0.140	0.254	0.144
	(0.017)	(0.143)	(0.149)	(0.016)	(0.109)	(0.112)
Attitudes			0.763			0.829
			(0.341)			(0.241)
Mean Dep. Var.	0.48	15.8	15.8	0.49	14.6	14.6
Observations	1665	3048	3048	2772	5138	5138
Origin × Year FE	Yes	Yes	Yes	Yes	Yes	Yes
Destination × Year FE	Yes	Yes	Yes	Yes	Yes	Yes
Origin × Destination FE	Yes	Yes	Yes	Yes	Yes	Yes

Notes: The unit of observation is an origin–destination country pair in a given year. The dependent variables are the preference index (columns 1 and 4) and the log trade value (columns 2–3 and 5–6). Columns 1–3 report results for country pairs among 32 major countries, while columns 4–6 include all country pairs. Standard errors are clustered at the country-pair level.

are N countries indexed by $o, d \in \{1, \ldots, N\}$, where o denotes origin and d destination. Each country produces a unique variety using labor as the only input. Country d is endowed with labor ℓ_d.

6.1. Model

Preferences and Consumption. Country d consumes varieties from all countries with constant elasticity of substitution (CES) preferences,

$$C_d = \left[\sum_{o=1}^{N} c_{od}^{\frac{\sigma-1}{\sigma}} \right]^{\frac{\sigma}{\sigma-1}}, \tag{8}$$

where c_{od} is consumption in d of the variety produced by o, and $\sigma > 1$ is the elasticity of substitution.

Production Technology. Labor is the only input. Producers in country o operate technology $y_o = z_o \ell_o$, where z_o denotes productivity and w_o the wage. Bilateral trade is subject to trade costs $d_{od} \geq 1$, which enter multiplicatively: $d_{od} = d_{od}^{\text{iceberg}} \cdot \tilde{\tau}_{od} \cdot d_{od}^{\text{geo}}$, where d_{od}^{iceberg} captures transportation costs, $\tilde{\tau}_{od} \equiv 1 + \tau_{od}$ is the ad valorem tariff factor, and d_{od}^{geo} reflects geopolitical frictions. The expenditure share of country d on varieties from country o is

$$\pi_{od} = \left(\frac{p_{od}}{P_d} \right)^{1-\sigma}, \qquad p_{od} = \frac{w_o d_{od}}{z_o}, \qquad P_d = \left[\sum_{o=1}^{N} p_{od}^{1-\sigma} \right]^{\frac{1}{1-\sigma}}. \tag{9}$$

Market Clearing. Total expenditure in country d equals wage income plus tariff revenue rebated

lump sum:

$$X_d = w_d \ell_d + \sum_{o=1}^{N} X_d \pi_{od} \left(1 - \frac{1}{\tilde{\tau}_{od}}\right) = \frac{w_d \ell_d}{\sum_{o=1}^{N} \pi_{od}/\tilde{\tau}_{od}}. \tag{10}$$

Define $\iota_d \equiv \sum_o \pi_{od}/\tilde{\tau}_{od} \leq 1$ as the share of expenditure received by producers. When tariffs are zero, $\iota_d = 1$ and expenditure equals wage income. Labor-market clearing requires

$$w_o \ell_o = \sum_{d=1}^{N} \frac{X_d \pi_{od}}{\tilde{\tau}_{od}}. \tag{11}$$

Welfare. Real income in country d is $\omega_d = \frac{X_d}{P_d} = \frac{w_d \ell_d}{\iota_d P_d}$. Welfare changes satisfy

$$\hat{\omega}_d = \frac{\hat{X}_d}{\hat{P}_d}, \qquad \hat{X}_d = \hat{w}_d \cdot \frac{\iota_d}{\iota'_d}, \tag{12}$$

where $\iota'_d = \sum_o \pi'_{od}/\tilde{\tau}'_{od}$ is the producer share in the counterfactual equilibrium. When tariffs fall, ι'_d rises, so $\hat{X}_d < \hat{w}_d$: consumers gain from lower prices but lose tariff revenue.

Equilibrium in Changes. We solve counterfactuals using exact hat algebra (Dekle, Eaton, and Kortum 2008). Let $\hat{x} = x'/x$, where x denotes the initial equilibrium and x' the counterfactual. Given an exogenous shock to trade costs $\hat{d}_{od}$, we solve for the implied changes in endogenous variables using the system reported in Appendix A.13. We fix one country's wage as numeraire to close the system.

6.2. Bringing the Model to the Data

We implement the model using OECD Inter-Country Input-Output (ICIO) data for 78 countries from 1995 to 2021 and decompose trade flow changes into contributions from geopolitics, tariffs, and residual trade barriers.

Trade Cost Decomposition. We parameterize trade costs as

$$\ln d_{od,t} = \text{Geo}_{od,t} + \ln \tilde{\tau}_{od,t} + \mathbf{Z}_{od}\boldsymbol{\beta} + \varepsilon_{od,t},$$

where $\text{Geo}_{od,t}$ captures geopolitical factors, $\boldsymbol{Z}_{od}$ includes time-invariant bilateral characteristics, and $\varepsilon_{od,t}$ captures residual barriers. Relative to base year t_0,

$$\ln \hat{d}_{od,t} = \Delta\text{Geo}_{od,t} + \ln \hat{\tilde{\tau}}_{od,t} + \hat{\varepsilon}_{od,t}.$$

Dynamic Geopolitical Effects. Because geopolitical shocks affect trade with persistence, we map changes in alignment into cumulative trade-cost effects:

$$(1-\sigma)\Delta\text{Geo}_{od,t} = \sum_{s=1}^{t-t_0} \hat{\beta}^{\text{geo}}_{t-s} \left(S_{od,t_0+s} - S_{od,t_0+s-1}\right),$$

where $\hat{\beta}^{\text{geo}}_{t-s}$ is estimated from the local projections in Section 4.2.3.[20] We set $\sigma - 1 = 3$, based on the impulse response of trade to tariffs reported in Appendix A.11.

Unobserved Cost Shocks. Following Head and Ries (2001) and assuming symmetric residual trade-cost shocks, $\hat{\varepsilon}_{od,t} = \hat{\varepsilon}_{do,t}$, and unchanged domestic trade costs, $\hat{d}_{oo,t} = 1$, we recover unobserved trade-cost changes from bilateral trade flows:

$$\hat{\varepsilon}_{od,t} = \left[\frac{\hat{\pi}_{od,t}\hat{\pi}_{do,t}}{\hat{\pi}_{oo,t}\hat{\pi}_{dd,t}}\right]^{\frac{1}{2(1-\sigma)}} \left[\hat{\tilde{\tau}}_{od,t}\hat{\tilde{\tau}}_{do,t}\right]^{-1/2} \exp(-\Delta\text{Geo}_{od,t}), \tag{13}$$

where $\hat{\pi}_{od,t}$ denotes the change in trade shares. Total trade-cost changes then satisfy

$$\hat{d}_{od,t} = \hat{\varepsilon}_{od,t} \times \hat{\tilde{\tau}}_{od,t} \times \exp(\Delta\text{Geo}_{od,t}), \tag{14}$$

which separates residual frictions, observable tariffs, and geopolitical factors. This decomposition allows us to quantify the contribution of each force to the evolution of global trade between 1995 and 2021.

6.3. Counterfactual Framework

To decompose the evolution of global trade from 1995 to 2021, we consider four counterfactuals that isolate the roles of geopolitics, tariffs, and residual barriers. Productivity is fixed at its 1995 value throughout.

For each year $t \in \{1996, \ldots, 2021\}$, we consider:

a. **Baseline:**
$$\hat{d}^{\text{baseline}}_{od,t} = \hat{\varepsilon}_{od,t} \times \hat{\tilde{\tau}}_{od,t} \times \exp(\Delta\text{Geo}_{od,t});$$

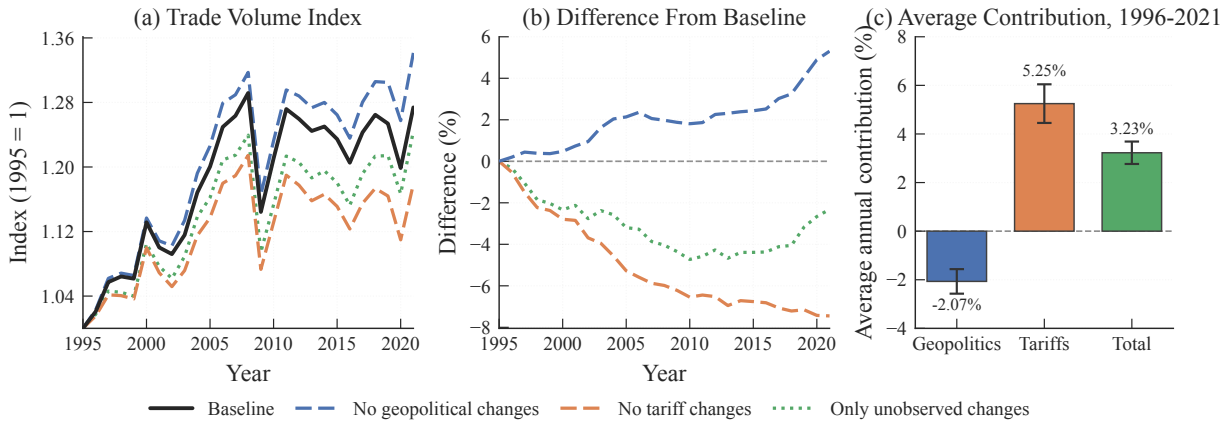
b. **No geopolitical change:**
$$\hat{d}^{\text{no-geo}}_{od,t} = \hat{\varepsilon}_{od,t} \times \hat{\tilde{\tau}}_{od,t};$$

c. **No tariff change:**
$$\hat{d}^{\text{no-tariff}}_{od,t} = \hat{\varepsilon}_{od,t} \times \exp(\Delta\text{Geo}_{od,t});$$

d. **Residual barriers only:**
$$\hat{d}^{\text{only-unobs}}_{od,t} = \hat{\varepsilon}_{od,t}.$$

Comparing outcomes across these scenarios isolates the effects of geopolitical change, tariff liberalization, and residual barriers.

FIGURE 13. Counterfactual Analysis of Global Trade Flows, 1995–2021



Notes: Panel A plots global trade volume, indexed to 1995 = 1, under four scenarios: baseline, no geopolitical changes, no tariff changes, and residual barriers only. Panel B reports percentage differences relative to the baseline. Panel C reports average annual contributions to trade growth with 95% confidence intervals. Productivity is fixed at its 1995 level in all scenarios.

6.4. Aggregate Trade Effects

Figure 13 reports global trade under the four counterfactuals. Holding productivity fixed at its 1995 level, global trade rises by 27.4 percent between 1995 and 2021 in the baseline.

We measure the contribution of each factor as the difference between baseline growth and counterfactual growth when that factor is shut down. Panel A and Table 7 report the results. Without tariff liberalization, trade would have grown by 17.9 percent rather than 27.4 percent, implying a contribution of 9.5 percentage points. Had geopolitical relations remained at their 1995 levels, trade would have grown by 34.1 percent. Geopolitical deterioration therefore subtracted 6.8 percentage points from trade growth. Panel B traces the year-by-year percentage difference from the baseline. By 2021, removing geopolitical frictions raises trade by 5.3 percent, while removing tariff liberalization lowers it by 7.4 percent.

Panel C reports average annual contributions. Tariff liberalization raised trade volumes by 5.25 percent per year relative to the baseline, while geopolitical deterioration lowered them by 2.07 percent.[21] Together, tariffs and geopolitics contributed 3.18 percent per year.

These results shed light on the slowdown in globalization documented by Antràs (2021) and Goldberg and Reed (2023). Tariff liberalization continued to support trade integration, but geopolitical deterioration offset a substantial share of those gains.

[20] Because we observe the full path of bilateral geopolitical alignment, $\hat{\beta}(\sigma - 1)$ corresponds to the impulse response of trade to a permanent change in the geopolitical score.

[21] These are annual averages of the percentage difference between each counterfactual and the baseline over 1996–2021, not annualized growth rates.

TABLE 7. Decomposition of Trade Growth, 1995–2021

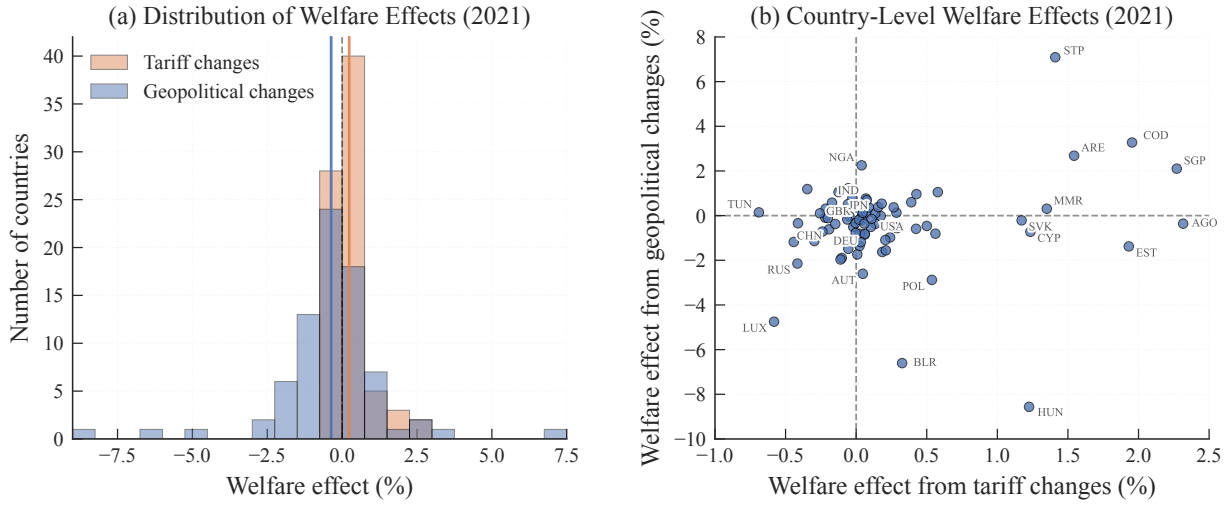
Scenario	2000	2010	2021	Total Growth
Baseline (all changes)	1.131	1.211	1.274	27.4%
No geopolitical changes	1.137	1.232	1.341	34.1%
No tariff changes	1.100	1.131	1.179	17.9%
Residual barriers only	1.105	1.153	1.244	24.4%
Contribution to trade growth (percentage points):				
Geopolitical deterioration				−6.8
Tariff liberalization				+9.5
Combined				+3.0

Notes: The table decomposes global trade growth from 1995 to 2021. Trade volumes are indexed to 1995 = 1.00. Productivity is fixed at its 1995 level in all scenarios. Contributions are computed as baseline growth minus counterfactual growth when the factor is shut down.

6.5. Country-Level Welfare Effects

We next examine welfare. For country d, welfare changes are given by $\hat{\omega}_d = \hat{X}_d/\hat{P}_d$, where $\hat{X}_d$ incorporates both wage changes and tariff-revenue adjustments.

FIGURE 14. Distribution and Heterogeneity of Welfare Effects, 1995–2021



Notes: Panel A plots histograms of welfare changes from tariff liberalization and geopolitical realignment. Panel B plots country-level welfare gains from tariff changes on the horizontal axis and gains from geopolitical changes on the vertical axis. Welfare is measured as $\hat{\omega}_d = \hat{X}_d/\hat{P}_d$, where $\hat{X}_d$ accounts for tariff-revenue changes.

Figure 14 and Table 8 report welfare effects in 2021. We define the welfare effect of factor k as

$$\left(\frac{\hat{\omega}_d^{\text{Baseline}}}{\hat{\omega}_d^{\text{No-}k}} - 1\right) \times 100.$$

A positive value indicates that the factor raised welfare.

TABLE 8. Distribution of Welfare Effects, 2021

	Welfare Effect (%)	
	Tariff Changes	Geopolitical Changes
Mean	+0.24	−0.37
Median	+0.06	−0.27
Std. Deviation	0.61	1.88
Skewness	1.86	−0.76
Countries gaining	50 (64.1%)	30 (38.5%)
Countries losing	28 (35.9%)	48 (61.5%)
Range of effects	[−0.69%, +2.32%]	[−8.56%, +7.09%]

Notes: The table reports the distribution of welfare effects from tariff liberalization and geopolitical realignment between 1995 and 2021. Positive values indicate that the factor raised welfare. Welfare gains from tariff changes are smaller than wage-based measures because lower tariffs also reduce tariff revenue.

Tariff changes generate modest average welfare gains. The mean effect is 0.24 percent, and 64.1 percent of countries gain. These gains are smaller than wage-based measures would imply because lower tariffs also reduce tariff revenue. The distribution is right-skewed, with the largest gains accruing to small open economies such as Angola, Singapore, and the Democratic Republic of the Congo.

Geopolitical realignment generates a wider distribution. The mean effect is −0.37 percent, and the range extends from −8.56 percent to +7.09 percent. About 61.5 percent of countries experience welfare losses from geopolitical deterioration.

Panel B of Figure 14 reveals substantial heterogeneity across countries. The largest group, 38.5 percent of countries, gains from tariff liberalization but loses from geopolitical change. Another 25.6 percent gains from both forces, while 23.1 percent loses from both. The remaining 12.8 percent loses from tariffs but gains from geopolitical shifts.

These cross-country differences align with observed geopolitical trajectories. Hungary records the largest welfare loss from geopolitical change (−8.56 percent), consistent with its increasing geopolitical isolation within the EU framework. Belarus loses 6.60 percent, reflecting the economic consequences of its alignment with Russia. At the other end, São Tomé and Príncipe gains 7.09 percent, and the United Arab Emirates gains 2.68 percent.

Overall, tariff liberalization generates small and broadly shared gains, partly offset by lost tariff revenue, whereas geopolitical change produces more dispersed welfare effects. The cross-sectional standard deviation of welfare effects is 1.88 percent for geopolitics and 0.61 percent for tariffs. Geopolitical alignment therefore produces more heterogeneous welfare consequences than tariff policy, even though its contribution to the cross-sectional variance of bilateral trade-cost changes

TABLE 9. Sensitivity to the Elasticity of Substitution

	$\sigma = 3$	$\sigma = 4$	$\sigma = 5$	$\sigma = 6$	$\sigma = 8$
Average contribution to global trade, 1996–2021 (pp)					
Geopolitical	−2.09	−2.07	−2.05	−2.04	−2.01
Tariff	3.33	5.25	7.04	8.73	11.75
Trade volume difference from baseline at 2021 (%)					
No geopolitical	5.36	5.30	5.27	5.25	5.22
No tariff	−4.70	−7.45	−10.00	−12.34	−16.27
Welfare effects at 2021 (%)					
Geopolitical: mean	−0.54	−0.37	−0.28	−0.22	−0.16
[min, max]	[−12.2, 10.7]	[−8.6, 7.1]	[−6.6, 5.4]	[−5.4, 4.3]	[−3.9, 3.2]
Tariff: mean	0.16	0.24	0.30	0.36	0.44
[min, max]	[−1.1, 2.4]	[−0.7, 2.3]	[−0.6, 2.3]	[−0.5, 2.4]	[−1.1, 2.6]

Notes: The baseline specification sets $\sigma = 4$. Each column solves the full model under the indicated elasticity. Average contributions to trade are computed as the negative percentage difference between the counterfactual and baseline trade volumes, averaged over 1996–2021. Welfare effects are the ratio of baseline to counterfactual real expenditure at 2021, expressed in percent.

is modest.[22]

6.6. Sensitivity Analysis

Table 9 reports counterfactual results for $\sigma \in \{3, 4, 5, 6, 8\}$, spanning a standard range in the trade literature. The geopolitical contribution to trade is nearly unchanged across specifications, varying only from −2.09 to −2.01 percentage points. This follows from the construction of the geopolitical trade-cost component: because the IRF convolution weights scale with $1/(\sigma - 1)$, the implied trade response is approximately invariant to σ.

Tariff effects, by contrast, increase with the elasticity, since the trade response to a given tariff change is proportional to $\sigma - 1$. Welfare losses from geopolitical frictions become smaller in absolute value as σ rises, while welfare gains from tariff changes increase. The qualitative conclusions are unchanged throughout.

7. Conclusion

This paper shows that geopolitical fragmentation constitutes a major barrier to trade globalization. Using an event-based measure constructed from 833,485 political events across 193 countries from 1950 to 2024, we estimate that a one-standard-deviation permanent improvement in bilateral alignment raises trade by approximately 20 percent in the long run. These effects are robust

[22]The single-sector Armington framework abstracts from several features that could affect the quantitative results. Intermediate inputs would likely amplify trade-cost effects (Caliendo and Parro 2015). A multi-sector structure could redistribute effects across industries. The static model does not capture the adjustment dynamics visible in the impulse responses. Finally, the trade elasticities are estimated on 32 major economies and applied to all 78 countries under the assumption of a common geopolitical trade elasticity.

across country samples, time periods, identification strategies, and alternative constructions of the geopolitical measure. Embedding the estimated elasticities in a quantitative trade model, we find that tariff liberalization contributed 9.5 percentage points to global trade growth from 1995 to 2021, while geopolitical deterioration subtracted 6.8 percentage points. Tariff changes generate modest and broadly shared welfare gains, whereas geopolitical realignment produces more dispersed welfare effects, with most countries losing from the deterioration in bilateral relations observed over recent decades.

These findings are subject to important caveats. Our identification strategy exploits within-dyad variation and therefore speaks to the effects of changes in geopolitical alignment, not the level effects of sustained cooperation or isolation. The event-based measure, while more comprehensive than alternatives based on UN voting or binary indicators, relies on LLM-compiled data that may introduce measurement error. And while the absence of pre-trends, the reverse causality test, and the robustness to non-economic events support the interpretation that geopolitics drives trade rather than the reverse, the exclusion of all possible confounders cannot be guaranteed.

Our estimates show that bilateral geopolitical relations shape trade with magnitudes comparable to tariffs and geography. An important avenue for future research is to study the microeconomic channels through which geopolitical fragmentation affects trade, including how firms adjust supply chains and governments deploy policy instruments in response to geopolitical shocks.

References

Aghion, Philippe, Xavier Jaravel, Torsten Persson, and Dorothée Rouzet. 2019. "Education and military rivalry." *Journal of the European Economic Association* 17 (2): 376–412.

Ahn, Daniel P and Rodney D Ludema. 2020. "The sword and the shield: The economics of targeted sanctions." *European Economic Review* 130 (103587): 103587.

Airaudo, Florencia, Francois De Soyres, Keith Richards, and Ana Maria Santacreu. 2025. "Measuring Geopolitical Fragmentation: Implications for Trade, Financial Flows, and Economic Policy." *Federal Reserve Bank of St. Louis Review* .

Aiyar, Shekhar and Franziska Ohnsorge. 2024. "Geoeconomic Fragmentation and" Connector" Countries." *Working Paper* .

Alesina, Alberto, Enrico Spolaore, and Romain Wacziarg. 2000. "Economic integration and political disintegration." *American Economic Review* 90 (5): 1276–1296.

Alfaro, Laura, Harald Fadinger, Jan Schymik, and Virananda Gede. 2025. "Trade and Industrial Policy in Supply Chains: Directed Technological Change in Rare Earths." .

Anderson, James E and Eric Van Wincoop. 2003. "Gravity with gravitas: A solution to the border puzzle." *American economic review* 93 (1): 170–192.

Anderson, James E and Eric Van Wincoop. 2004. "Trade costs." *Journal of Economic literature* 42 (3): 691–751.

Antràs, Pol. 2021. "De-Globalisation? Global Value Chains in the Post-COVID-19 Age."

Baier, Scott L and Jeffrey H Bergstrand. 2007. "Do free trade agreements actually increase members' international trade?" *Journal of international economics* 71 (1): 72–95.

Bailey, Michael A, Anton Strezhnev, and Erik Voeten. 2017. "Estimating dynamic state preferences from united Nations voting data." *Journal of Conflict Resolution* 61 (2): 430–456.

Baker, Scott R, Nicholas Bloom, and Steven J Davis. 2016. "Measuring economic policy uncertainty." *The Quarterly Journal of Economics* 131 (4): 1593–1636.

Becko, John Sturm and Daniel O'Connor. 2024. "Strategic (dis) integration." Tech. rep., Working paper.

Bilal, Adrien and Diego R Känzig. 2026. "The Macroeconomic Impact of Climate Change: Global Versus Local Temperature." *The Quarterly Journal of Economics* p. qjag011. 10.1093/qje/qjag011.

Boehm, Christoph E, Andrei A Levchenko, and Nitya Pandalai-Nayar. 2023. "The long and short (run) of trade elasticities." *American Economic Review* 113 (4): 861–905.

Bonadio, Barthélémy, Zhen Huo, Elliot Kang, Andrei A. Levchenko, Nitya Pandalai-Nayar, Hiroshi Toma, and Petia Topalova. 2025. "Playing with blocs: Quantifying decoupling." *Journal of International Economics* p. 104204. https://doi.org/10.1016/j.jinteco.2025.104204.

Boschee, Elizabeth, Jennifer Lautenschlager, Sean O'Brien, Steve Shellman, James Starz, and Michael Ward. 2015. "ICEWS coded event data."

Broner, Fernando, Alberto Martin, Josefin Meyer, Christoph Trebesch, and Jiaxian Zhou Wu. 2025a. "Hegemony and international alignment." *AEA papers and proceedings. American Economic Association* 115: 593–598.

Broner, Fernando, Alberto Martín, Julian Meyer, and Christoph Trebesch. 2025b. "Hegemonic Globalization." Discussion Paper DP20339, CEPR, Paris and London.

Cai, Sheng, Wei Xiang, and Yu Zhao. 2025. "Quantifying Decoupling in Global Production and Trade." *Available at SSRN 5520518* .

Caldara, Dario and Matteo Iacoviello. 2022. "Measuring geopolitical risk." *American economic review* 112 (4): 1194–1225.

Caliendo, L and F Parro. 2015. "Estimates of the trade and welfare effects of NAFTA." *The Review of Economic Studies* 82 (1): 1–44.

Chang, Pao-Li, Tomoki Fujii, and Wei Jin. 2022. "Good names beget favors: The impact of country image on trade flows and welfare." *Management Science* 68 (10): 7555–7596.

Chen, Tuo, Chang-Tai Hsieh, and Zheng Michael Song. 2022. "Non-tariff barriers in the US-China trade war." Tech. rep., National Bureau of Economic Research.

Clayton, Christopher, Antonio Coppola, Matteo Maggiori, and Jesse Schreger. 2025. "Geoeconomic Pressure." Research paper, Columbia Business School and Stanford University Graduate School of Business.

Clayton, Christopher, Matteo Maggiori, and Jesse Schreger. 2025. "A Theory of Economic Coercion and Fragmentation." Tech. rep., National Bureau of Economic Research.

Couttenier, Mathieu, Julien Marcoux, Thierry Mayer, and Mathias Thoenig. 2024. "The Gravity of Violence." CEPR Discussion Paper 19527, Centre for Economic Policy Research, Paris and London. https://cepr.org/publications/dp19527.

Dekle, Robert, Jonathan Eaton, and Samuel Kortum. 2008. "Global rebalancing with gravity: Measuring the burden of adjustment." *IMF Staff papers* 55 (3): 511–540.

Dell, Melissa. 2025. "Deep learning for economists." *Journal of Economic Literature* 63 (1): 5–58.

Disdier, Anne-Célia and Keith Head. 2008. "The puzzling persistence of the distance effect on bilateral trade." *The Review of Economics and Statistics* 90 (1): 37–48.

Driscoll, John C and Aart C Kraay. 1998. "Consistent covariance matrix estimation with spatially dependent panel data." *The Review of Economics and Statistics* 80 (4): 549–560.

Fajgelbaum, Pablo, Pinelopi Goldberg, Patrick Kennedy, Amit Khandelwal, and Daria Taglioni. 2024. "The US-China trade war and global reallocations." *American Economic Review: Insights* 6 (2): 295–312.

Fan, Tianyu. 2025. "The Geopolitical Determinants of Economic Growth, 1960-2019." Working paper,

arXiv:2507.04833.

Fang, Hanming, Ming Li, and Guangli Lu. 2025. "Decoding China's Industrial Policies." Working Paper 33814, National Bureau of Economic Research.

Federle, Jonathan, André Meier, Gernot J Müller, Willi Mutschler, and Moritz Schularick. 2026. "The price of war." *American Economic Review* 116 (3): 791–827.

Felbermayr, Gabriel, Alexandra Kirilakha, Constantinos Syropoulos, Erdal Yalcin, and Yoto V. Yotov. 2020. "The Global Sanctions Data Base." *European Economic Review* 129. 10.1016/j.euroecorev.2020.103561.

Felbermayr, Gabriel, T Clifton Morgan, Constantinos Syropoulos, and Yoto V Yotov. 2021. "Understanding economic sanctions: Interdisciplinary perspectives on theory and evidence." *European Economic Review* 135 (103720): 103720.

Fernández-Villaverde, Jesús, Tomohide Mineyama, and Dongho Song. 2024. "Are we fragmented yet? Measuring geopolitical fragmentation and its causal effect." Tech. rep., National Bureau of Economic Research.

Feyrer, James. 2019. "Trade and Income—Exploiting Time Series in Geography." *American Economic Journal: Applied Economics* 11(4): 1–35.

Flynn, Joel P, Antoine B Levy, Jacob Moscona, and Mai Wo. 2025. "Foreign political risk and technological change." Tech. rep., National Bureau of Economic Research.

Gibler, Douglas M. 2008. "The costs of reneging: Reputation and alliance formation." *Journal of Conflict Resolution* 52 (3): 426–454.

Goldberg, Pinelopi and Michele Ruta. 2025. "The Changing Nature of International Trade and Its Implications for Development." Tech. rep., CESifo.

Goldberg, Pinelopi K and Tristan Reed. 2023. "Is the global economy deglobalizing? If so, why? And what is next?" *Brookings Papers on Economic Activity* 2023 (1): 347–423.

Goldstein, Joshua S. 1992. "A conflict-cooperation scale for WEIS events data." *Journal of Conflict Resolution* 36 (2): 369–385.

Gopinath, Gita, Pierre-Olivier Gourinchas, Andrea F Presbitero, and Petia Topalova. 2025. "Changing global linkages: A new Cold War?" *Journal of International Economics* 153: 104042.

Grossman, Gene M. and Elhanan Helpman. 1994. "Protection for Sale." *American Economic Review* 84 (4): 833–850.

Hassan, T A, S Hollander, Lent L Van, and A Tahoun. 2019. "Firm-level political risk: Measurement and effects." *The Quarterly Journal of Economics* 134 (4): 2135–2202.

Head, Keith and Thierry Mayer. 2014. "Gravity equations: Workhorse, toolkit, and cookbook." In *Handbook of international economics*, vol. 4, pp. 131–195. Elsevier.

Head, Keith and John Ries. 2001. "Increasing returns versus national product differentiation as an explanation for the pattern of US–Canada trade." *American Economic Review* 91 (4): 858–876.

Helpman, Elhanan, Marc Melitz, and Yona Rubinstein. 2008. "Estimating trade flows: Trading partners and trading volumes." *The Quarterly Journal of Economics* 123 (2): 441–487.

Hirschman, Albert O. 1945. *National power and the structure of foreign trade*, vol. 105. Univ of California Press.

Itskhoki, Oleg and Dmitry Mukhin. 2025. "Sanctions and the Exchange Rate." *The Review of Economic Studies* 10.1093/restud/rdaf085.

Jordà, Òscar. 2005. "Estimation and inference of impulse responses by local projections." *American Economic Review* 95 (1): 161–182.

Jordà, Òscar and Alan M Taylor. 2025. "Local projections." *Journal of Economic Literature* 63 (1): 59–110.

Kleinman, Benny, Ernest Liu, and Stephen J Redding. 2024. "International friends and enemies." *American Economic Journal: Macroeconomics* 16 (4): 350–385.

Korovkin, Vasily and Alexey Makarin. 2023. "Conflict and intergroup trade: Evidence from the 2014 Russia-Ukraine crisis." *American economic review* 113 (1): 34–70.

Leetaru, Kalev and Philip A Schrodt. 2013. "GDELT: Global data on events, location, and tone, 1979–2012." *International Studies Quarterly* 57 (4): 1–16.

Liu, Ernest and David Y Yang. 2025. "International Power." Tech. rep., National Bureau of Economic Research.

Looi Kee, Hiau, Alessandro Nicita, and Marcelo Olarreaga. 2009. "Estimating trade restrictiveness indices." *Economic journal (London, England)* 119 (534): 172–199.

Mansfield, Edward D, Helen V Milner, and B Peter Rosendorff. 2000. "Free to trade: Democracies, autocracies, and international trade." *American political science review* 94 (2): 305–321.

Martin, Philippe, Thierry Mayer, and Mathias Thoenig. 2008. "Make trade not war?" *The Review of Economic Studies* 75 (3): 865–900.

Mayer, Thierry, Isabelle Mejean, and Mathias Thoenig. 2025. "The fragmentation paradox: De-risking trade and global safety." Tech. rep., working paper.

Melitz, Jacques. 2008. "Language and foreign trade." *European Economic Review* 52 (4): 667–699.

Mohr, Cathrin and Christoph Trebesch. 2025. "Geoeconomics." *Annual Review of Economics* 17.

Montiel Olea, José Luis and Mikkel Plagborg-Møller. 2021. "Local projection inference is simpler and more robust than you think." *Econometrica: journal of the Econometric Society* 89 (4): 1789–1823.

Morrow, James D, Randolph M Siverson, and Tressa E Tabares. 1998. "The political determinants of international trade: the major powers, 1907–1990." *American political science review* 92 (3): 649–661.

Pellegrino, Bruno, Enrico Spolaore, and Romain Wacziarg. 2025. "Barriers to Global Capital Allocation*." *The Quarterly Journal of Economics* p. qjaf031. 10.1093/qje/qjaf031.

Plagborg-Møller, Mikkel and Christian K Wolf. 2021. "Local projections and VARs estimate the same impulse responses." *Econometrica: journal of the Econometric Society* 89 (2): 955–980.

Qiu, Han, Dora Xia, and James Yetman. 2024. "Deconstructing global trade: the role of geopolitical alignment." *BIS Quarterly Review* pp. 35–50.

Santos Silva, J. M. C. and Silvana Tenreyro. 2006. "The Log of Gravity." *Review of Economics and Statistics* 88 (4): 641–658.

Schrodt, Philip A and Omur Yilmaz. 2012. "CAMEO: Conflict and Mediation Event Observations Event and Actor Codebook." Tech. rep., Pennsylvania State University.

Signorino, Curtis S and Jeffrey M Ritter. 1999. "Tau-b or not tau-b: Measuring the similarity of foreign policy positions." *International Studies Quarterly* 43: 115–144.

Sims, C. 1986. "Are forecasting models usable for policy analysis." *Quarterly Review* 10 (Win): 2–16.

Teti, Feodora A. 2024. "Missing Tariffs." Tech. Rep. 11590, CESifo Working Papers. Feodora Teti's Global Tariff Database (v_beta1-2024-12).

Thompson, William R. 2001. "Identifying rivals and rivalries in world politics." *International Studies Quarterly* 45 (4): 557–586.

Voeten, Erik. 2026. "Conceptualizing and Measuring Geopolitical Alignments." *Annual Review of Political Science* https://doi.org/10.1146/annurev-polisci-041924-012436.

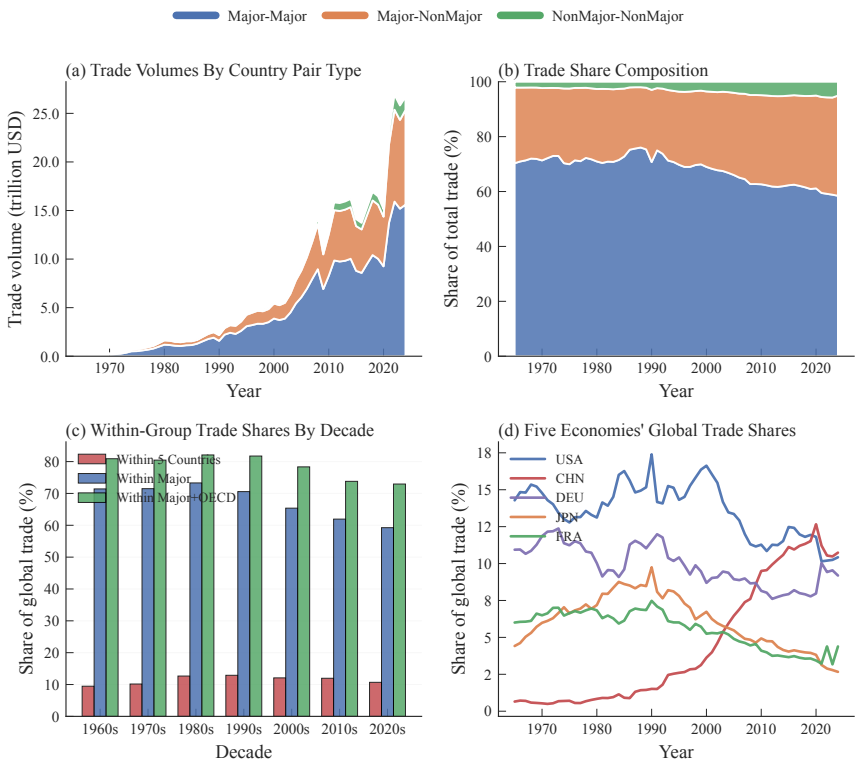
Yalcin, Erdal, Gabriel Felbermayr, Heba Kariem, Alexandra Kirilakha, Ohyun Kwon, Constantinos Syropoulos, and Yoto V. Yotov. 2025. "The Global Sanctions Data Base - Release 4: The Heterogeneous Effects of the Sanctions on Russia." *The World Economy* 10.1111/twec.13729.

Appendix A. Additional Empirical Results

A.1. Trade Decomposition: Major Countries

Our empirical analysis focuses on 32 major countries that have ranked among the world's top 20 economies by GDP at any point since 1960.[23] This restriction mitigates extensive-margin concerns in trade data (Helpman, Melitz, and Rubinstein 2008; Head and Mayer 2014) while capturing the bulk of global commerce. Figure A1 demonstrates that these major economies dominate global trade patterns, validating our sample selection.

FIGURE A1. Trade Flow Decomposition by Country Groups, 1962–2024



Notes: Panel A shows absolute trade volumes by country-pair type. Panel B displays the corresponding shares. Panel C presents within-group trade concentration by decade. Panel D tracks individual country shares of global trade. Major economies are defined as countries ever ranking in the top 20 by GDP since 1960.

Three key patterns emerge from Figure A1. First, trade among major economies accounts for approximately 70% of world trade throughout our sample period, despite these dyads representing fewer than 3% of potential country pairs. This concentration reflects both size effects and deeper economic integration among developed economies.

[23]The 32 major economies in our sample are: Argentina, Australia, Austria, Belgium, Brazil, Canada, China, Denmark, France, Germany, India, Indonesia, Iran, Iraq, Italy, Japan, Mexico, Netherlands, Nigeria, Philippines, Poland, Russia, Saudi Arabia, South Korea, Spain, Sweden, Switzerland, Türkiye, United Kingdom, United States, Venezuela, and South Africa.

Second, concentration has declined over time, indicating broadening participation in global trade. Trade shares within the five largest economies decreased from 13% in the 1980s to 11% in the 2020s, while the overall major economy share fell from 71% to 59%. This trend reflects the integration of emerging markets into global value chains and the geographic dispersion of production networks.

Third, China's rise has restructured global trade geography. China's share increased from near zero in 1970 to 12% by 2024, matching the United States' stable 12–15% share and surpassing Japan, whose share declined from 10% to 5%.

A.2. Additional Case Studies: U.S. Trading Partners

We examine four distinct U.S. bilateral relationships—China, Brazil, Saudi Arabia, and Colombia—that illustrate how geopolitical alignment and trade co-move across different political contexts: strategic rivalry, ideological divergence, energy interdependence, and security cooperation. These cases complement the main text by demonstrating that the relationship between residualized geopolitical alignment and residualized bilateral trade persists across a wide range of U.S. partnerships, despite substantial heterogeneity in the underlying political drivers.

China-U.S.: Strategic rivalry and weakening economic ties. Figure A2Aa highlights the evolution from engagement to strategic rivalry. The period following the Nixon opening and around WTO accession is characterized by strong trade growth alongside relatively favorable geopolitical alignment. By contrast, since the late 2000s, intensifying strategic competition is mirrored in a joint decline in both alignment and trade. Consistent with the notion of strategic rivalry, the figure suggests that deep commercial interdependence provides only limited insulation against deteriorating geopolitical relations.

Brazil-U.S.: Ideological distance and attenuated trade integration. Figure A2Ab illustrates how shifts in ideological distance shape economic linkages within the Western Hemisphere. In particular, the late 1970s and parts of the first Lula administration represent periods of heightened ideological divergence between Brazil and the United States. In both episodes, greater ideological distance is associated with weaker geopolitical alignment and reduced trade integration. By contrast, periods characterized by closer ideological alignment coincide with stronger bilateral trade flows.

Saudi Arabia-U.S.: Energy interdependence and political volatility. Figure A2Ac shows a relationship marked by substantial political volatility alongside enduring economic linkages. The 1973 embargo, post-9/11 tensions, and the Khashoggi episode coincide with declines in geopolitical alignment and are accompanied by noticeable reductions in bilateral trade, even if trade does not collapse entirely. Relative to other U.S. dyads, the Saudi case suggests that while strong complementarities in strategic commodities sustain the relationship, trade remains meaningfully affected by geopolitical strain rather than fully insulated from it.

Colombia-U.S.: Security cooperation and economic integration. Figure A2Ad presents a case where sustained security cooperation aligns with deepening economic integration. The strengthening of bilateral ties around Plan Colombia and the subsequent free trade agreement is

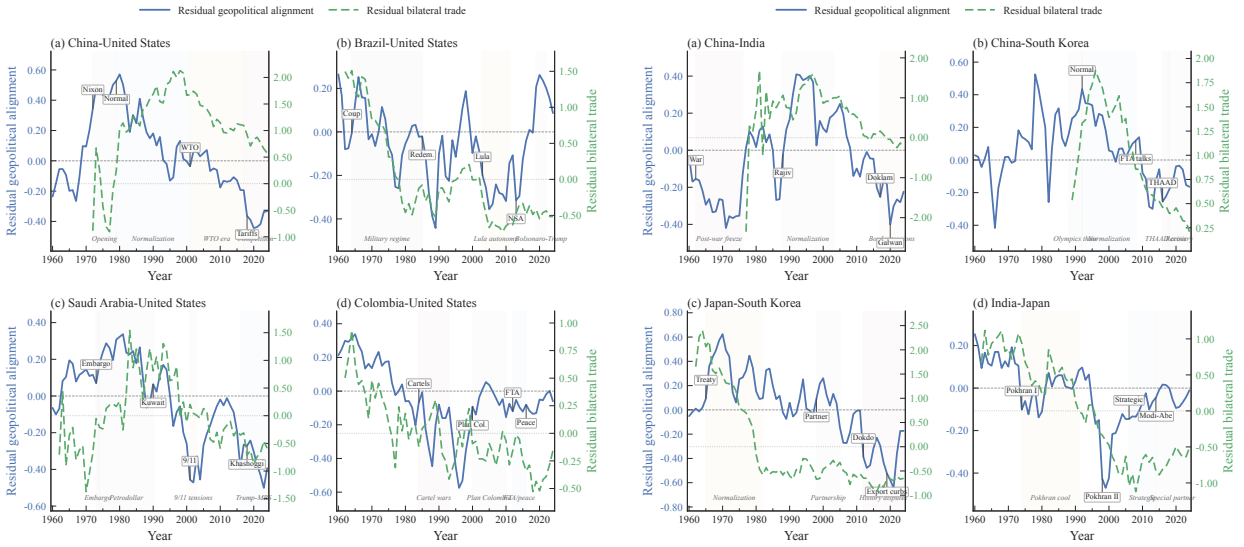
associated with improvements in both geopolitical alignment and trade. In line with the notion of security cooperation, this case suggests that strategic partnerships can reinforce broader economic linkages.

Taken together, these cases reinforce that the relationship between geopolitics and trade is not confined to a single type of bilateral interaction. While the underlying mechanisms differ—ranging from rivalry and ideology to resource dependence and security alliances—each case exhibits a consistent pattern: stronger geopolitical alignment is associated with stronger bilateral trade.

FIGURE A2. Bilateral Relations: Geopolitical Alignment and Trade

A. U.S. Trading Partners

B. Asian Trading Networks



Notes: Each panel plots residualized geopolitical relations against residualized bilateral trade flows. All variables are residualized following the methodology in Figure 4. In Panel A, the China–U.S. trade series begins in 1970, following the normalization of relations under the Nixon administration. In Panel B, the China–South Korea trade series begins in 1985, when indirect trade through Hong Kong became quantitatively significant, despite formal normalization occurring in 1992. Shaded regions indicate major diplomatic periods with distinct geopolitical characteristics.

A.3. Additional Case Studies: Asian Trading Networks

Intra-Asian trade accounts for a substantial share of global commerce, yet it unfolds within a political environment that differs markedly from many U.S.-centered relationships. We examine four dyads—China–India, China–South Korea, Japan–South Korea, and India–Japan—that illustrate three recurring features of Asian trade networks: persistent historical tensions, security considerations that often outweigh economic complementarities, and pronounced volatility in bilateral relations. Despite these regional characteristics, residualized geopolitical alignment and residualized bilateral trade display a systematic positive association across these Asian dyads.

China-India: Territorial disputes and constrained integration. Figure A2Ba illustrates how per-

sistent geopolitical tensions shape economic interactions between the world's two most populous economies. The 1962 war established a fragile political baseline, and subsequent episodes—such as the Doklam standoff in 2017 and the Galwan Valley clash in 2020—have reinforced this pattern. Consistent with these geopolitical frictions, residualized alignment remains persistently low, and residualized trade also weakens in the latter part of the sample. Overall, the figure underscores how enduring strategic rivalry continues to constrain the economic relationship between these neighboring markets.

China-South Korea: Security tensions and economic exposure. Figure A2Bb highlights how geopolitical tensions shape a highly integrated trade relationship. Following normalization in 1992, both geopolitical alignment and trade strengthened substantially. However, the relationship begins to deteriorate in the 2000s, when rising security tensions coincide with weaker bilateral trade residuals. The figure underscores how shifts in the geopolitical environment can translate into a deterioration of economic ties, even in deeply integrated markets.

Japan-South Korea: Historical memory and repeated bilateral strain. Figure A2Bc shows that even between two advanced U.S. allies, historical grievances continue to shape bilateral economic relations. Residualized trade declines alongside geopolitical alignment after 1970 and remains persistently low thereafter, with no clear recovery trend. Overall, the pattern suggests that unresolved historical disputes have had a lasting constraining effect on bilateral economic integration.

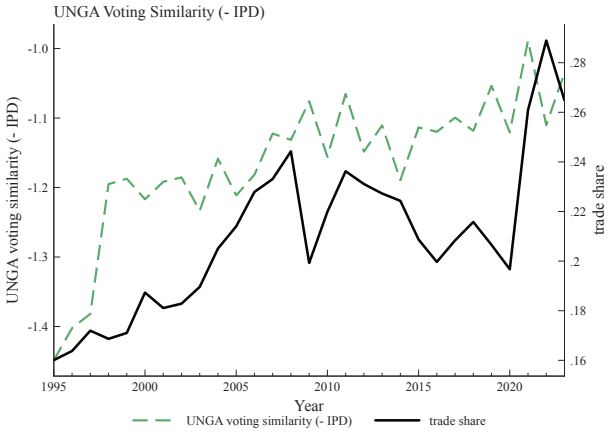
India-Japan: Strategic convergence. Figure A2Bd presents the case of Japan and India, where trade co-moves closely with geopolitical alignment. Following India's nuclear tests, bilateral relations deteriorated, accompanied by a decline in trade. Since the mid-2000s, however, the gradual strengthening of ties—reflected in deeper security cooperation, more frequent high-level engagement, and agreements such as the Strategic and Global Partnership—coincides with improved trade performance. Overall, the pattern suggests that closer alignment in foreign policy priorities and security interests can support economic integration.

Taken together, these Asian cases show that geopolitical alignment and bilateral trade comove across a range of political contexts, from territorial disputes to security partnerships.

A.4. UNGA Voting Similarity and Trade Globalization

Figure A3 illustrates a divergence between multilateral voting patterns and trade flows. From 1995 to 2007, UNGA voting similarity and global trade share moved broadly in tandem, both rising with deepening post–Cold War integration. After 2007, however, the two series diverge: UNGA voting similarity continues to increase through 2022, while trade as a share of GDP plateaus and subsequently declines. This pattern is consistent with the evidence in Section 2.5 that UNGA voting primarily reflects multilateral positioning rather than the bilateral relationships most relevant for trade. The continued convergence in voting may instead capture the growing influence of developing-country coalitions in multilateral forums, a dynamic that is largely orthogonal to the bilateral geopolitical frictions that increasingly constrain trade flows.

FIGURE A3. UNGA Voting Similarity and Trade Globalization, 1995–2021



Notes: The green dashed line plots the trade-weighted average UNGA voting similarity (negative Ideal Point Distance) across country pairs. The black solid line plots trade as a share of GDP.

A.5. Variance Decomposition of Gravity Determinants

We decompose the variance of bilateral trade flows to quantify the relative importance of geopolitical alignment vis-à-vis traditional gravity determinants. Specifically, by excluding each determinant from equation 3, we assess its marginal contribution to explaining cross-dyadic variation in trade. Table A1 reports the estimated coefficients alongside the reduction in R^2 associated with the exclusion of each variable. Two main findings emerge.

TABLE A1. Gravity Equation Coefficients and Variance Decomposition

	Regression Coefficients (S.E.)				R^2 Loss (%)			
Sample	Geo Score	Distance (log)	Border	Linguistic Dist.	Geo Score	Distance	Border	Ling. Dist.
Panel A: All Countries								
Full Period (1962–2024)	1.10 (0.027)	-1.45 (0.016)	0.84 (0.079)	-1.70 (0.075)	3.4	42.5	1.1	2.6
Pre-1990	1.08 (0.043)	-1.29 (0.023)	0.54 (0.104)	-0.88 (0.112)	4.8	48.1	0.4	0.9
Post-1990	1.08 (0.032)	-1.50 (0.017)	1.02 (0.082)	-2.10 (0.076)	2.5	40.0	1.1	3.2
Panel B: Major Economies								
Full Period	0.46 (0.106)	-0.81 (0.052)	0.23 (0.171)	-1.10 (0.330)	2.2	49.7	0.6	2.8
Pre-1990	0.78 (0.141)	-0.68 (0.069)	0.10 (0.213)	-0.91 (0.422)	8.6	44.8	0.0	2.6
Post-1990	0.20 (0.139)	-0.92 (0.052)	0.33 (0.172)	-1.24 (0.332)	0.4	50.6	0.8	3.1
Full R^2 (Full Period)		All: 0.268	Major: 0.179		Observations: 1,087,543 / 58,948			

Notes: Left panel: coefficients from gravity equation with origin-year, destination-year, and standard gravity controls. Standard errors clustered by dyad in parentheses. Right panel: percentage point reduction in R^2 when variable excluded. Major economies defined as countries ever ranking in top 20 by GDP since 1960.

First, geopolitical alignment is quantitatively comparable to standard trade frictions such as language. In the full sample, it accounts for 3.4% of the variation in bilateral trade, exceeding the

contribution of linguistic distance (2.6%) and more than tripling that of shared borders (1.1%). Among major economies, geopolitical alignment explains 2.2% of trade variation, a magnitude broadly similar to that of linguistic distance (2.8%).

Second, the decomposition reveals substantial heterogeneity across samples, pointing to important structural shifts over time. Among major economies, the sensitivity of trade to geopolitical alignment declines markedly: the estimated coefficient falls from 0.78 in the pre-1990 period to 0.20 thereafter, while its explanatory power decreases from 8.6% to 0.4%. This attenuation is consistent with the view that global integration after the Cold War insulated economies from geopolitical fluctuations. However, recent episodes—such as sanctions on Russia and the decoupling between the United States and China—suggest that such insulation is incomplete, and that geopolitical constraints reassert themselves when political tensions intensify.

A.6. Additional Cross-Sectional Estimates

This section provides robustness checks for the cross-sectional gravity results in Section 4.1.

PPML and Inverse Hyperbolic Sine. Table A2 addresses concerns about zero trade flows. PPML estimates (columns 1–4) confirm a positive effect of geopolitical alignment on trade, though the coefficient for major economies is imprecisely estimated. The inverse hyperbolic sine specification (columns 5–8) yields qualitatively similar results, with larger coefficients in the full sample. In both specifications, UNGA voting similarity enters with the wrong sign, consistent with the main text finding that it captures multilateral positioning rather than bilateral relations.

TABLE A2. The Effect of Geopolitical Alignment on Trade: PPML and Inverse Hyperbolic Sine

	PPML (Dep. Var.: Trade Value)				IHS (Dep. Var.: asinh(Trade Value))			
	Major Countries		All Countries		Major Countries		All Countries	
	(1)	(2)	(3)	(4)	(5)	(6)	(7)	(8)
Geopolitical Score	0.161		0.236		0.499		1.490	
	(0.092)		(0.076)		(0.144)		(0.030)	
UNGA Voting Similarity:		-0.020		-0.029		-0.423		-0.163
Negative Ideal Point Distance		(0.041)		(0.028)		(0.056)		(0.015)
Mean Dep. Var.	43.1[a]	46.7[a]	1.82[a]	2.41[a]	12.5	12.8	3.71	4.87
Observations	62,496	53,554	2,334,528	1,599,544	62,496	53,554	2,334,528	1,599,544
Origin × Year FE	Yes	Yes	Yes	Yes	Yes	Yes	Yes	Yes
Destination × Year FE	Yes	Yes	Yes	Yes	Yes	Yes	Yes	Yes

Notes: The unit of observation is an origin-destination country pair in a year. Odd columns use our geopolitical alignment measure; even columns use UNGA voting similarity. Columns 1–2 and 5–6 report results for country pairs among 32 major countries; columns 3–4 and 7–8 include all country pairs. Columns 1–4 report PPML estimates; columns 5–8 use the inverse hyperbolic sine transformation. All specifications control for geographic distance, contiguity, and linguistic distance (coefficients not reported). [a]Mean dependent variable $\times 10^5$. Standard errors are clustered at the country pair level.

Country-Pair Fixed Effects. Table A3 adds country-pair fixed effects, so that identification relies on within-pair temporal variation rather than cross-sectional differences. The coefficient on geopolitical alignment remains positive and precisely estimated. For major economies, the estimate (0.595) is larger than the baseline without pair fixed effects, suggesting that time-invariant confounders, if anything, attenuate the cross-sectional relationship. The UNGA voting similarity coefficient switches sign and becomes positive in this specification.

TABLE A3. The Effect of Geopolitical Alignment on Trade: with Country Pair FEs

	(1)	(2)	(3)	(4)
Dependent Variable:	log Trade Value			
	Major Countries		All Countries	
Geopolitical Score	0.595		0.357	
	(0.077)		(0.017)	
UNGA Voting Similarity:		0.323		0.170
Negative Ideal Point Distance		(0.045)		(0.011)
Mean Dep. Var.	12.52	12.72	7.23	7.27
Observations	58,948	50,946	1,087,543	991,266
Origin × Year FE	Yes	Yes	Yes	Yes
Destination × Year FE	Yes	Yes	Yes	Yes
Origin × Destination FE	Yes	Yes	Yes	Yes

Notes: The unit of observation is an origin-destination country pair in a year. Columns 1–2 report results for country pairs among 32 major countries, while Columns 3–4 include all country pairs. Standard errors are clustered at the country pair level.

Alternative Trade Data Sources. Table A4 validates the results using BACI (1995–2023) and IMF Direction of Trade Statistics (1948–2024) as alternative data sources. The positive effect of geopolitical alignment is robust across both datasets, with coefficients of similar magnitude to the baseline UN Comtrade estimates. The IMF data, which extend back to 1948, confirm that the relationship holds over a longer time horizon.

Alternative Geopolitical Measures. Table A5 confirms that the results are robust to alternative constructions of the geopolitical alignment measure. The coefficient on geopolitical alignment is positive and significant across all specifications: raw scores without smoothing, alternative depreciation rates ($\lambda = 0.1$ and $\lambda = 0.5$), four-period moving averages, and cumulative sum scores. The coefficients attenuate when gravity controls are added (even columns) but remain precisely estimated throughout.

TABLE A4. The Effect of Geopolitical Alignment on Trade: Alternative Trade Measures

Dependent Variable: log Trade Value	BACI (1995–2023)						IMF (1948–2024)					
	Major Countries			All Countries			Major Countries			All Countries		
	(1)	(2)	(3)	(4)	(5)	(6)	(7)	(8)	(9)	(10)	(11)	(12)
Geopolitical Score	0.276	0.177		2.806	1.114		0.660	0.446		2.483	1.022	
	(0.172)	(0.149)		(0.050)	(0.034)		(0.106)	(0.088)		(0.042)	(0.027)	
UNGA Voting Similarity:			-0.210			-0.170			-0.219			-0.018
Negative Ideal Point Distance			(0.053)			(0.014)			(0.041)			(0.012)
Mean Dep. Var.	13.94	13.94	14.03	7.57	7.57	7.60	12.26	12.26	12.49	7.45	7.45	7.48
Observations	27,451	27,451	26,601	668,849	668,849	632,568	64,691	64,691	54,701	1,078,076	1,078,076	947,751
Origin × Year FE	Yes	Yes	Yes	Yes	Yes	Yes	Yes	Yes	Yes	Yes	Yes	Yes
Destination × Year FE	Yes	Yes	Yes	Yes	Yes	Yes	Yes	Yes	Yes	Yes	Yes	Yes

Notes: The unit of observation is an origin-destination country pair in a year. Columns 1–3 and 7–9 report results for country pairs among 32 major countries, while Columns 4–6 and 10–12 include all country pairs. All specifications control for geographic distance, contiguity, and linguistic distance (coefficients not reported). Standard errors are clustered at the country pair level.

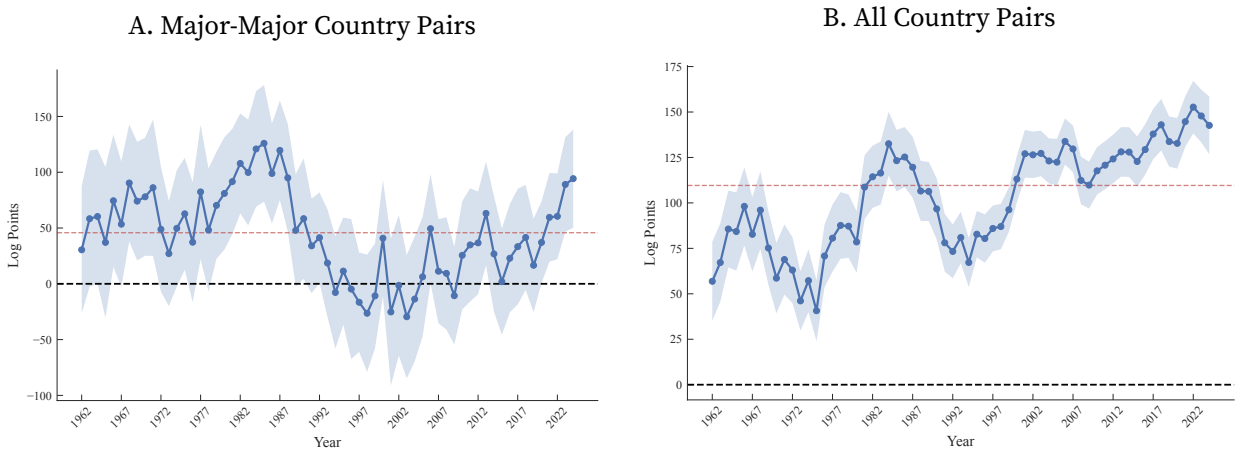
TABLE A5. The Effect of Geopolitical Alignment on Trade: Alternative Geo Measures

Dependent Variable:	log Trade Value, Major Countries									
	Raw Score		$\lambda = 0.1$		$\lambda = 0.5$		MA(4)		Sum Score	
	(1)	(2)	(3)	(4)	(5)	(6)	(7)	(8)	(9)	(10)
Geopolitical Score	0.388	0.223	0.902	0.555	0.599	0.368	0.823	0.488	0.115	0.063
	(0.058)	(0.049)	(0.178)	(0.158)	(0.095)	(0.083)	(0.115)	(0.100)	(0.014)	(0.012)
Mean Dep. Var.	12.52	12.52	12.52	12.52	12.52	12.52	12.52	12.52	12.52	12.52
Observations	58948	58948	58948	58948	58948	58948	58948	58948	58948	58948
Origin × Year FE	Yes	Yes	Yes	Yes	Yes	Yes	Yes	Yes	Yes	Yes
Destination × Year FE	Yes	Yes	Yes	Yes	Yes	Yes	Yes	Yes	Yes	Yes

Notes: The unit of observation is an origin-destination country pair in a year. All columns report results for country pairs among 32 major countries. Columns 1–2 use the raw geopolitical score. Columns 3–4 use a smoothed geopolitical score with $\lambda = 0.1$, while columns 5–6 use a smoothed score with $\lambda = 0.5$. Columns 7–8 report results based on a four-period moving average of the raw score. Columns 9–10 use the smoothed sum score with $\lambda = 0.3$. Even columns control for geographic distance, contiguity, and linguistic distance (coefficients not reported). Standard errors are clustered at the country pair level.

Gravity Estimates by Year. Figure A4 plots the estimated coefficient of geopolitical alignment on trade by year. The coefficients are consistently positive and display a U-shaped pattern: larger during the Cold War, smaller during the globalization period, and rising again after 2018. This temporal variation suggests that while the geopolitics-trade relationship persists across international regimes, its magnitude responds to the prevailing level of geopolitical tension.

FIGURE A4. The Effect of Geopolitical Alignment on Trade: Gravity by Year



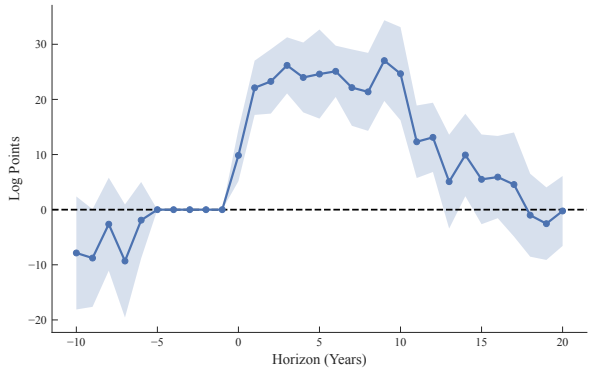
Notes: This figure plots the estimated coefficients of geopolitical alignment on log trade values by year. Specifically, we estimate $\ln X_{odt} = \delta_{ot} + \delta_{dt} + \sum_{\tau=1962}^{2024} \beta_\tau S_{odt} \times \mathbf{1}[t = \tau] + \text{Controls} + \epsilon_{odt}$, where controls include geographic distance, contiguity, and linguistic distance. The red dashed lines depict the corresponding estimates obtained from pooling all years. Panel A shows results for major-major country pairs (corresponding to column 2 in Table 4), while Panel B shows results for all countries (corresponding to column 5 in Table 4). Standard errors are clustered at the country-pair level.

A.7. Robustness of Dynamic Results

This section provides robustness tests supporting the main dynamic results from Section 4.2.

Alternative Lag Structure. Figure A5 validates our baseline three-lag specification by extending to five lags. The trade impulse responses remain virtually unchanged, with identical peak timing and comparable magnitudes throughout the horizon. This stability confirms that three lags capture the relevant dynamics without overfitting.

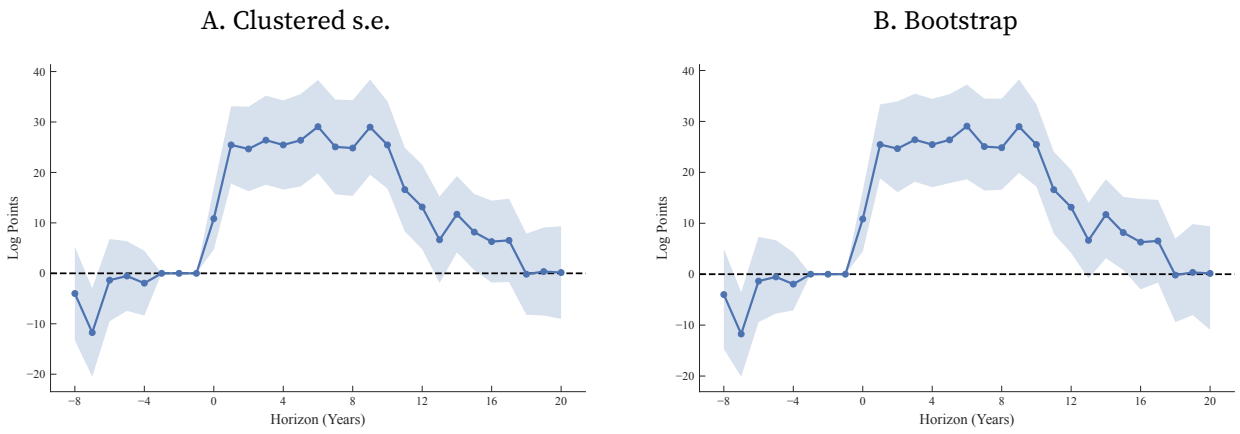
FIGURE A5. Dynamic Effect of Geopolitical Alignment on Trade: Alternative Lags



Notes: This figure reports estimates $\{\beta_h\}$ from $\ln X_{od,t+h} = \beta_h S_{od,t} + \sum_{\ell=1}^{5} \gamma_{h,\ell} \ln X_{od,t-\ell} + \sum_{\ell=1}^{5} \beta_{h,\ell} S_{od,t-\ell} + \delta_{od} + \delta_{ot} + \delta_{dt} + \varepsilon_{od,t+h}$. The sample includes country pairs among 32 major economies. Estimated coefficients are shown with 95% confidence intervals based on Driscoll-Kraay standard errors.

Alternative Inference. Figure A6 examines robustness to alternative standard error constructions. Panel A uses standard errors clustered at the country-pair level. Panel B implements block bootstrap resampling (200 iterations). Both methods yield confidence intervals closely matching our baseline Driscoll–Kraay approach, with bootstrap intervals widening marginally at longer horizons.

FIGURE A6. Dynamic Effect of Geopolitical Alignment on Trade: Alternative Inference

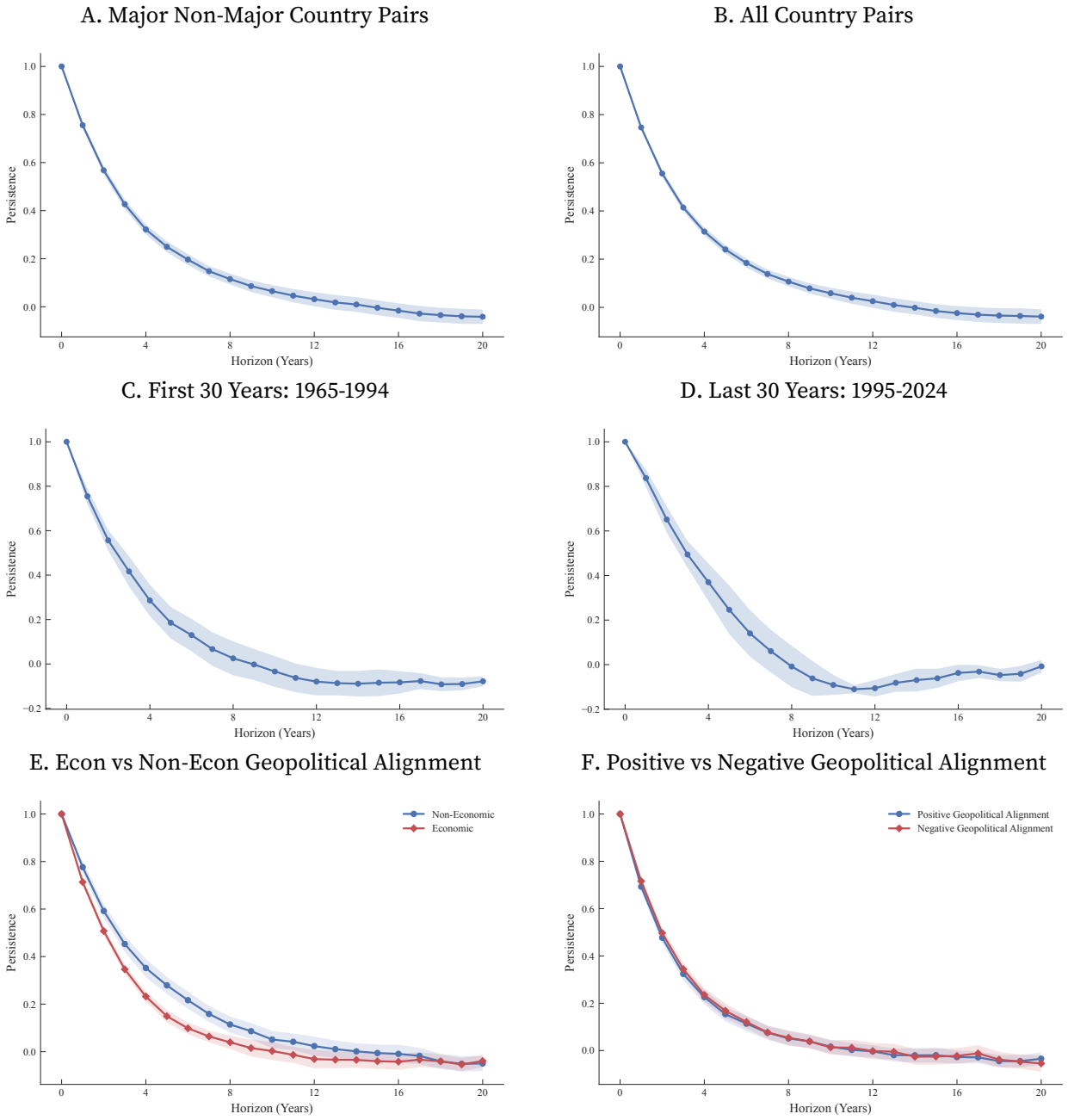


Notes: This figure reports estimates $\{\beta_h\}$ from $\ln X_{od,t+h} = \beta_h S_{od,t} + \sum_{\ell=1}^{3} \gamma_{h,\ell} \ln X_{od,t-\ell} + \sum_{\ell=1}^{3} \beta_{h,\ell} S_{od,t-\ell} + \delta_{od} + \delta_{ot} + \delta_{dt} + \varepsilon_{od,t+h}$. The sample includes country pairs among 32 major economies. Panel A reports estimated coefficients and 95% confidence intervals with standard errors clustered at the country-pair level. Panel B reports estimated coefficients and 95% confidence intervals from 200 bootstrap iterations with country-pair block resampling.

Autocorrelation Functions Across Samples Figure A7 documents the persistence of geopolitical shocks across country samples and time periods. Panels A and B extend the autocorrelation analysis to major–non-major pairs and all country pairs, respectively. In both cases, shocks are persistent but less so than in the baseline major-economy sample. Panels C and D show that persistence is similar across the Cold War and post-Cold War periods, indicating that the dynamics are a stable feature of the data rather than an artifact of a particular geopolitical regime. Panels E and F decompose persistence by event type and sign.

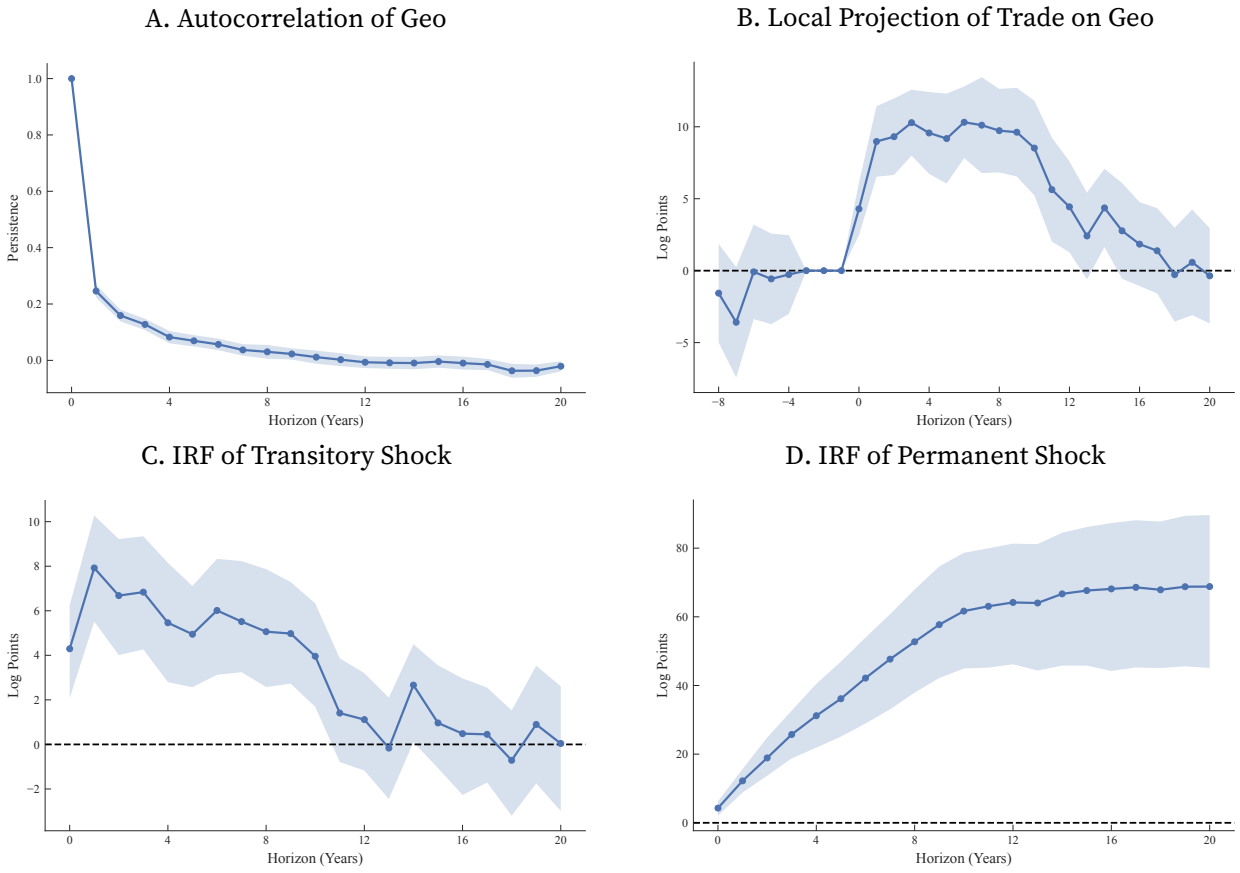
Alternative Geopolitical Measures. Figure A8 examines robustness using unsmoothed average event scores. These unsmoothed measures exhibit low persistence, with autocorrelation falling below 0.2 after two years (Panel A), yet they still generate economically meaningful trade responses, with peak elasticities of around 0.12 at horizons of 4–6 years (Panel B). Although the local projection produces somewhat smaller estimates, a one-unit permanent geopolitical shock implies a cumulative increase in trade of about 70 log points after 20 years (Panel D), close to the baseline estimate of 78 log points. This similarity indicates that permanent geopolitical realignments yield comparable long-run trade effects regardless of the measurement approach.

FIGURE A7. Autocorrelation of Geopolitical Alignment: Robustness



Notes: Panels A–D report estimates $\{\phi_h\}$ from: $S_{od,t+h} = \phi_h S_{od,t} + \sum_{\ell=1}^{3} \phi_{h,\ell} S_{od,t-\ell} + \delta_{ot} + \delta_{dt} + \delta_{od} + \varepsilon_{od,t+h}$ across four subsamples. Panel A includes country pairs between major and non-major countries; Panel B includes all country pairs; Panel C focuses on major country pairs over 1965–1994; and Panel D covers major country pairs over 1995–2024. Panel E reports estimates $\{\phi_h^{\text{econ}}, \phi_h^{\text{non-econ}}\}$ from $S_{od,t+h}^{\text{econ}} = \phi_h^{\text{econ}} S_{od,t}^{\text{econ}} + \phi_h^{\text{en}} S_{od,t}^{\text{non-econ}} + \sum_{\ell=1}^{3} \phi_{h,\ell}^{\text{ee}} S_{od,t-\ell}^{\text{econ}} + \sum_{\ell=1}^{3} \phi_{h,\ell}^{\text{en}} S_{od,t-\ell}^{\text{non-econ}} + \delta_{ot} + \delta_{dt} + \delta_{od} + \varepsilon_{od,t+h}$, and $S_{od,t+h}^{\text{non-econ}} = \phi_h^{\text{non-econ}} S_{od,t}^{\text{non-econ}} + \phi_h^{\text{ne}} S_{od,t}^{\text{econ}} + \sum_{\ell=1}^{3} \phi_{h,\ell}^{\text{ne}} S_{od,t-\ell}^{\text{econ}} + \sum_{\ell=1}^{3} \phi_{h,\ell}^{\text{nn}} S_{od,t-\ell}^{\text{non-econ}} + \delta_{ot} + \delta_{dt} + \delta_{od} + \varepsilon_{od,t+h}$, both estimated on major country pairs. Panel F similarly reports estimates $\{\phi_h^{\text{pos}}, \phi_h^{\text{neg}}\}$ from analogous specifications. All panels display coefficient estimates with 95% confidence intervals based on Driscoll–Kraay standard errors.

FIGURE A8. Dynamic Effect of Geopolitical Alignment on Trade: Raw Geo Scores

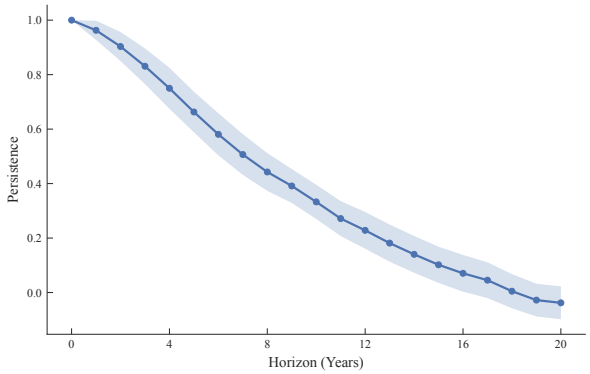


Notes: This figure uses the raw geopolitical score. Panel A reports estimates $\{\phi_h\}$ from: $S_{od,t+h} = \phi_h S_{od,t} + \sum_{\ell=1}^{3} \phi_{h,\ell} S_{od,t-\ell} + \delta_{ot} + \delta_{dt} + \delta_{od} + \varepsilon_{od,t+h}$. Panel B shows estimates $\{\beta_h\}$ from $\ln X_{od,t+h} = \beta_h S_{od,t} + \sum_{\ell=1}^{3} \gamma_{h,\ell} \ln X_{od,t-\ell} + \sum_{\ell=1}^{3} \beta_{h,\ell} S_{od,t-\ell} + \delta_{od} + \delta_{ot} + \delta_{dt} + \varepsilon_{od,t+h}$. The sample includes country pairs among 32 major economies. Both panels report estimated coefficients with 95% confidence intervals based on Driscoll-Kraay standard errors. Panel C presents the impulse response of log trade to a purely transitory unit shock in raw geopolitical score. Panel D shows the cumulative response to a permanent unit shock. 95% confidence intervals are from 200 bootstrap iterations with country-pair block resampling.

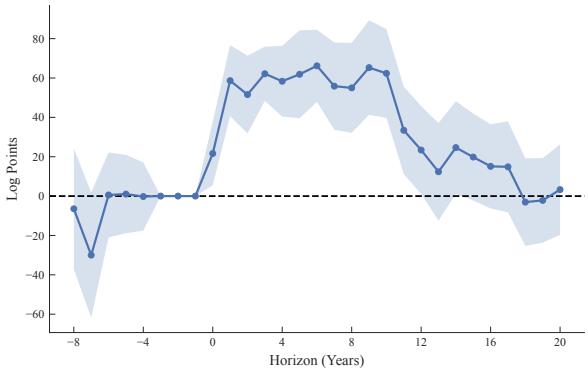
Figure A9 tests robustness to alternative depreciation rates ($\lambda = 0.1$, $\lambda = 0.5$) and a four-period moving average. Results remain qualitatively similar across specifications, confirming that our findings do not depend on the particular smoothing parameter. Figure A10 shows that using the sum rather than the average of event scores also produces consistent results.

FIGURE A9. Dynamic Effect of Geopolitical Alignment on Trade: Alternative Geo Scores

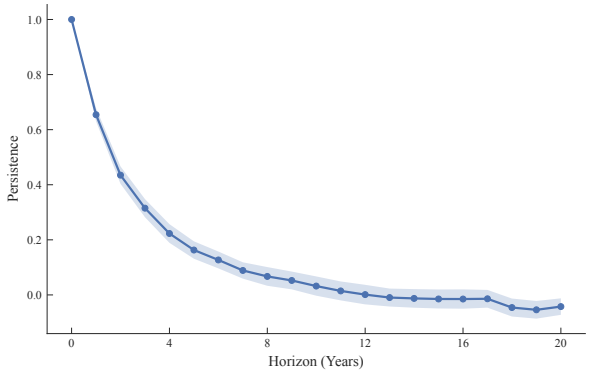
A. Autocorrelation of Geo: λ = 0.1



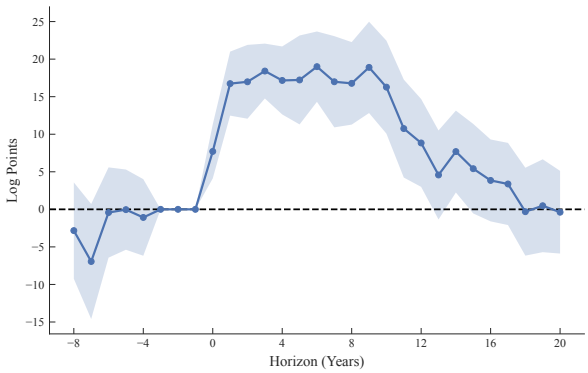
B. Local Projection of Trade on Geo: λ = 0.1



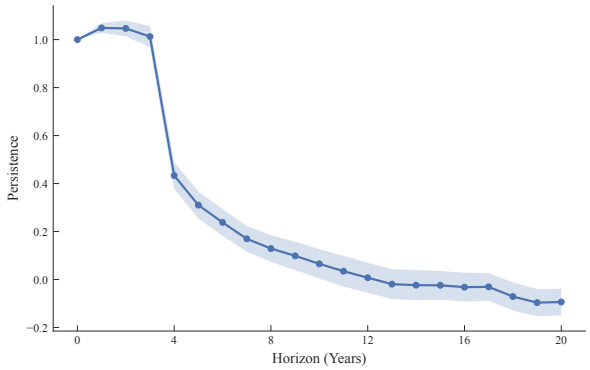
C. Autocorrelation of Geo: λ = 0.5



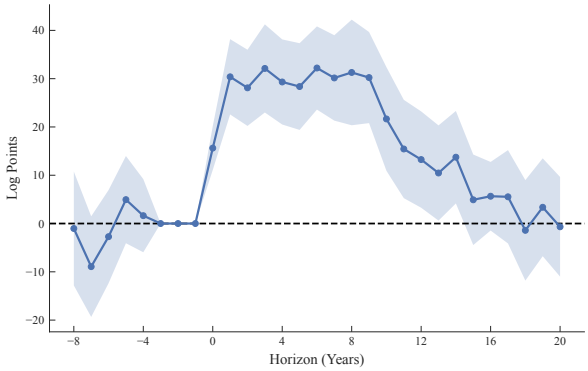
D. Local Projection of Trade on Geo: λ = 0.5



E. Autocorrelation of Geo: MA(4)



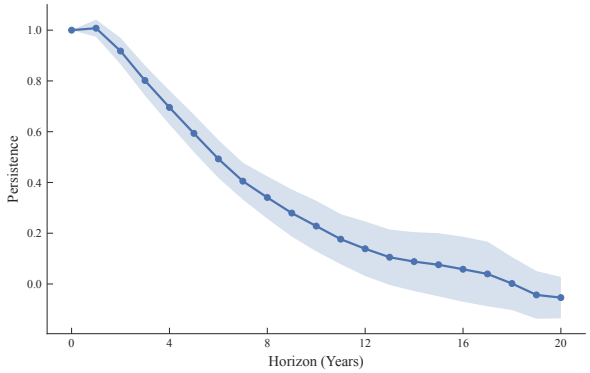
F. Local Projection of Trade on Geo: MA(4)



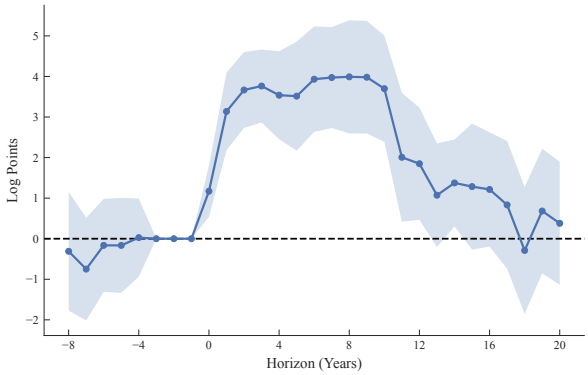
Notes: Panel A, C, E report estimates $\{\phi_h\}$ from: $S_{od,t+h} = \phi_h S_{od,t} + \sum_{\ell=1}^{3} \phi_{h,\ell} S_{od,t-\ell} + \delta_{ot} + \delta_{dt} + \delta_{od} + \varepsilon_{od,t+h}$. Panel B, D, F show estimates $\{\beta_h\}$ from $\ln X_{od,t+h} = \beta_h S_{od,t} + \sum_{\ell=1}^{3} \gamma_{h,\ell} \ln X_{od,t-\ell} + \sum_{\ell=1}^{3} \beta_{h,\ell} S_{od,t-\ell} + \delta_{od} + \delta_{ot} + \delta_{dt} + \varepsilon_{od,t+h}$. The sample includes country pairs among 32 major economies. Panel A and B use a smoothed geopolitical score with λ = 0.1, while Panel C and D use a smoothed score with λ = 0.5. Panel E and F report results based on a four-period moving average of the raw score. All panels report estimated coefficients with 95% confidence intervals based on Driscoll-Kraay standard errors.

FIGURE A10. Dynamic Effect of Geopolitical Alignment on Trade: Sum of Event Scores

A. Autocorrelation of Geo



B. Local Projection of Trade on Geo



Notes: This figure uses the smoothed sum score with $\lambda = 0.3$. Panel A reports estimates $\{\phi_h\}$ from: $S_{od,t+h} = \phi_h S_{od,t} + \sum_{\ell=1}^{3} \phi_{h,\ell} S_{od,t-\ell} + \delta_{ot} + \delta_{dt} + \delta_{od} + \varepsilon_{od,t+h}$. Panel B shows estimates $\{\beta_h\}$ from $\ln X_{od,t+h} = \beta_h S_{od,t} + \sum_{\ell=1}^{3} \gamma_{h,\ell} \ln X_{od,t-\ell} + \sum_{\ell=1}^{3} \beta_{h,\ell} S_{od,t-\ell} + \delta_{od} + \delta_{ot} + \delta_{dt} + \varepsilon_{od,t+h}$. The sample includes country pairs among 32 major economies. Both panels report estimated coefficients with 95% confidence intervals based on Driscoll-Kraay standard errors.

A.8. Decomposition of Transitory and Permanent Shocks

The local projection estimates in Section 4.2 combine the initial shock's direct impact with effects from its subsequent persistence. We decompose these components by constructing counterfactual responses to purely transitory versus permanent geopolitical improvements.

A.8.1. Methodology

Following Sims (1986) and Bilal and Känzig (2026), we implement a two-step decomposition. First, we estimate the autocorrelation function of geopolitical alignment:

$$S_{od,t+h} = \phi_h S_{od,t} + \sum_{\ell=1}^{L} \phi_{h,\ell} S_{od,t-\ell} + \delta_{od} + \delta_{ot} + \delta_{dt} + \mu_{od,t+h} \tag{A1}$$

where $\{\phi_h\}_{h=0}^{H}$ captures shock persistence.

To generate a purely transitory shock (one at $h = 0$, zero thereafter), we solve for the auxiliary shock sequence $\mathbf{p} = \{p_0, p_1, \ldots, p_H\}$:

$$\mathbf{p} = (\mathbf{\Phi})^{-1} \mathbf{e}_1 \tag{A2}$$

where $\mathbf{\Phi}$ is the lower triangular matrix with elements $\Phi_{ij} = \phi_{i-j}$ for $i \geq j$ (zero otherwise), and $\mathbf{e}_1 = (1, 0, \ldots, 0)'$ represents the targeted transitory shock pattern.

The trade response to this transitory geopolitical shock becomes:

$$\tilde{\beta}_h = \sum_{s=0}^{h} p_s \beta_{h-s} \tag{A3}$$

where $\{\beta_h\}$ are baseline local projection estimates from equation (4). For permanent shocks, we compute cumulative responses: $\sum_{s=0}^{h} \tilde{\beta}_s$.

A.8.2. Implementation and Inference

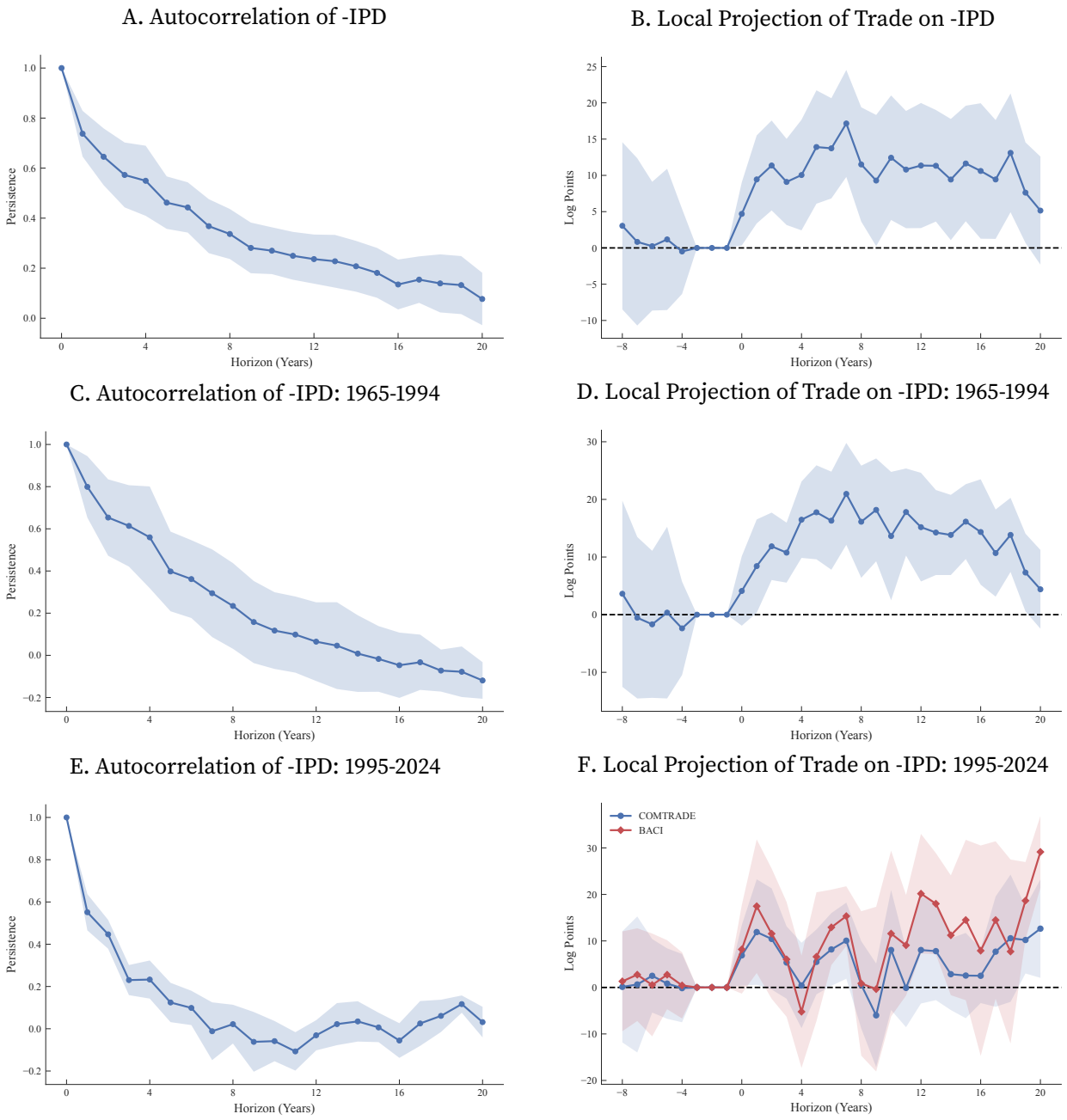
We implement this decomposition using local projection estimates from our baseline specification with $L = 3$. Statistical inference employs block bootstrap with 200 iterations: 1. Resample country pairs with replacement (block bootstrap); 2. Re-estimate both geopolitical autocorrelation (A1) and trade responses (4); 3. Compute decomposed impulse responses for each bootstrap sample; 4. Construct 95% confidence intervals using the 2.5th and 97.5th percentiles. This procedure accounts for estimation uncertainty in both stages while preserving within-pair correlation structure.

A.9. Temporal Variation in IPD-Based Estimates

Figure A11 illustrates how the relationship between UN voting–based measures and trade varies across periods. We use negative IPD as a measure of geopolitical alignment, so that higher values correspond to closer alignment. Panels A–B report full-period estimates. Negative IPD exhibits greater persistence over time, and this persistence is reflected in more sustained estimated effects on trade. During the Cold War (Panels C–D), the local projection estimates display the expected relationship, with lower alignment (that is, more divergent UN voting) associated with lower trade. This pattern is consistent with the evidence in Section 2.5 that UNGA voting primarily captures multilateral positioning, which during the Cold War was more closely linked to bilateral relations because bloc membership shaped both voting behavior and trade linkages. In the post–Cold War period (Panels E–F), the estimated trade responses are smaller and less precisely estimated, consistent with a weaker connection between multilateral voting patterns and bilateral economic relationships as trade networks became less dependent on geopolitical blocs.

The comparison with our event-based measure is useful in highlighting the different information contained in the two measures. While the association between IPD and trade varies across periods, our event-based measure yields positive trade elasticities in both subsamples (see figures in Section 4.2). This pattern is consistent with the broader finding in Section 2.5 that bilateral and multilateral dimensions of geopolitical alignment are distinct and need not move together over time.

FIGURE A11. Dynamic Effect of -IPD on Trade

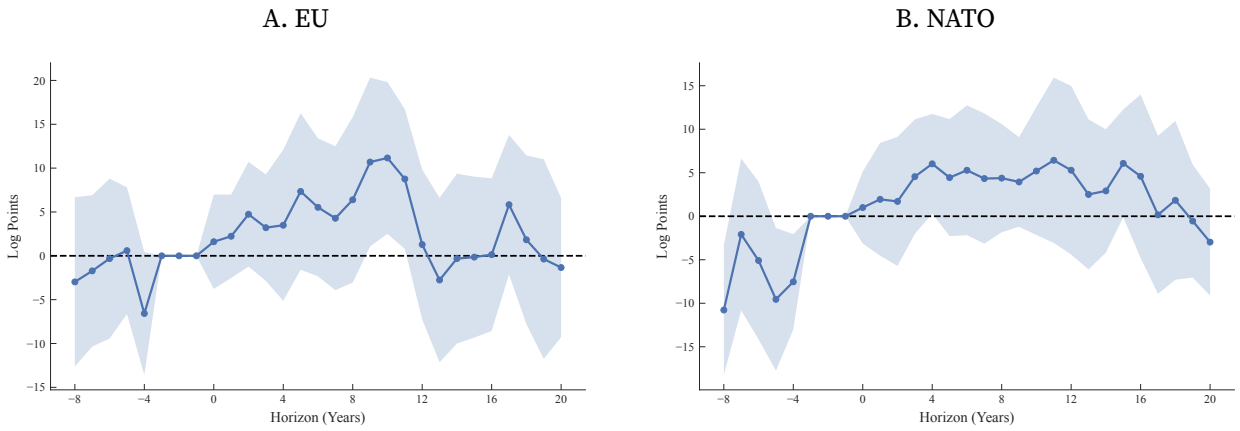


Notes: This figure uses negative IPD as measure of geopolitical alignment. Panel A, C, E report estimates $\{\phi_h\}$ from: $S_{od,t+h} = \phi_h S_{od,t} + \sum_{\ell=1}^{3} \phi_{h,\ell} S_{od,t-\ell} + \delta_{ot} + \delta_{dt} + \delta_{od} + \varepsilon_{od,t+h}$. Panels B, D, F report estimates β_h from the regression $\ln X_{od,t+h} = \beta_h S_{od,t} + \sum_{\ell=1}^{3} \gamma_{h,\ell} \ln X_{od,t-\ell} + \sum_{\ell=1}^{3} \beta_{h,\ell} S_{od,t-\ell} + \delta_{od} + \delta_{ot} + \delta_{dt} + \varepsilon_{od,t+h}$. The sample includes country pairs among 32 major economies. Panel A and B includes all years; Panel C and D focuses on 1965–1994; and Panel E and F covers 1995–2024. All panels report estimated coefficients with 95% confidence intervals based on Driscoll-Kraay standard errors.

A.10. Heterogeneity: Alliances and Sectors

Figure A12 examines heterogeneity by EU and NATO membership. The estimated responses are substantially weaker and statistically insignificant among alliance members, consistent with the view that formal institutional ties reduce the sensitivity of trade to bilateral geopolitical shocks.

FIGURE A12. Dynamic Trade Responses: EU and NATO



Notes: This figure reports estimates β_h from the regression $\ln X_{od,t+h} = \beta_h S_{od,t} + \sum_{\ell=1}^{3} \gamma_{h,\ell} \ln X_{od,t-\ell} + \sum_{\ell=1}^{3} \beta_{h,\ell} S_{od,t-\ell} + \delta_{od} + \delta_{ot} + \delta_{dt} + \varepsilon_{od,t+h}$. The sample consists of country pairs among EU in panel A, and among NATO in panel B. All panels display coefficient estimates with 95% confidence intervals based on Driscoll–Kraay standard errors.

Figure A13 reports dynamic trade responses by NAICS sector. The effects are positive across all sectors except energy and mining (NAICS 21). The largest and most persistent responses occur in manufacturing, particularly NAICS 33 (primary metals, machinery, electronics, and transportation equipment). Panel F shows that the effects are similar in critical and non-critical sectors, suggesting that the results are not driven by targeted government intervention.

A.11. The Trade Effects of Trade Policies

A.11.1. Econometric Specification

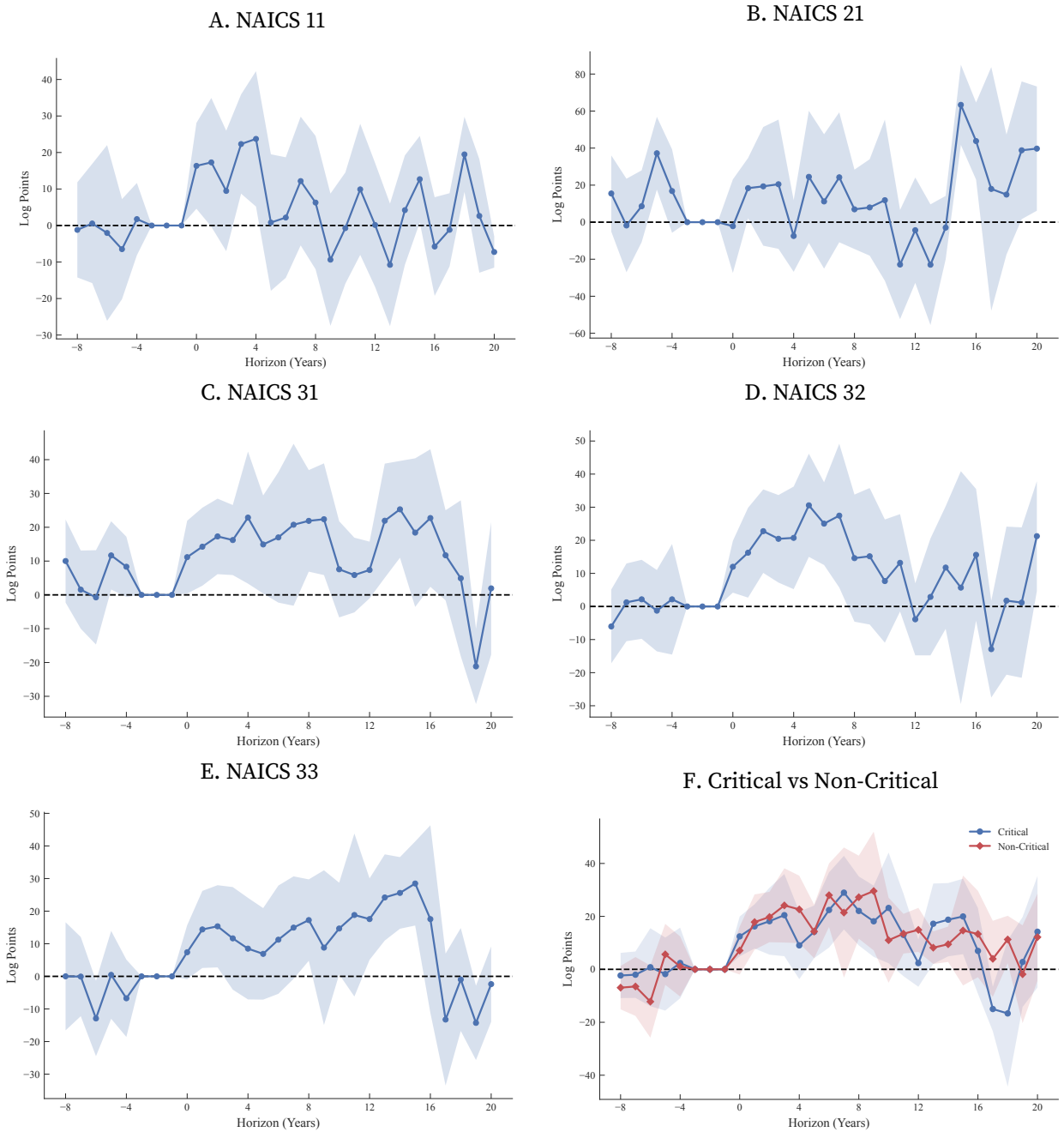
We estimate dynamic impacts of trade policies on bilateral flows and policy persistence using local projections. For tariffs, we estimate the trade response to tariffs as:

$$\ln X_{od,t+h} = \beta_h \ln(1+\tau_{od,t}) + \sum_{\ell=1}^{3} \gamma_{h,\ell} \ln X_{od,t-\ell} + \sum_{\ell=1}^{3} \beta_{h,\ell} \ln(1+\tau_{od,t-\ell}) + \delta_{ot} + \delta_{dt} + \delta_{od} + \varepsilon_{od,t+h}.$$

And we estimate tariff persistence as:

$$\ln(1+\tau_{od,t+h}) = \phi_h \ln(1+\tau_{od,t}) + \sum_{\ell=1}^{3} \phi_{h,\ell} \ln(1+\tau_{od,t-\ell}) + \delta_{ot} + \delta_{dt} + \delta_{od} + \varepsilon_{od,t+h}.$$

FIGURE A13. Dynamic Trade Responses: Sector Heterogeneity



Notes: This figure reports estimates β_h from the regression $\ln X_{od,t+h} = \beta_h S_{od,t} + \sum_{\ell=1}^{3} \gamma_{h,\ell} \ln X_{od,t-\ell} + \sum_{\ell=1}^{3} \beta_{h,\ell} S_{od,t-\ell} + \delta_{od} + \delta_{ot} + \delta_{dt} + \varepsilon_{od,t+h}$, using sector-specific trade flows. The sample consists of country pairs among 32 major economies. Panels A–E report estimates for NAICS sectors 11, 21, 31, 32, and 33, respectively. Panel F reports estimates for trade in critical and non-critical sectors. All panels display coefficient estimates with 95% confidence intervals based on Driscoll–Kraay standard errors.

For sanctions, we estimate analogously the trade response to sanctions as:

$$\ln X_{od,t+h} = \beta_h \mathbf{1}[\text{sanction}_{od,t}] + \sum_{\ell=1}^{3} \gamma_{h,\ell} \ln X_{od,t-\ell} + \sum_{\ell=1}^{3} \beta_{h,\ell} \mathbf{1}[\text{sanction}_{od,t-\ell}] + \delta_{ot} + \delta_{dt} + \delta_{od} + \varepsilon_{od,t+h},$$

and the sanction persistence as:

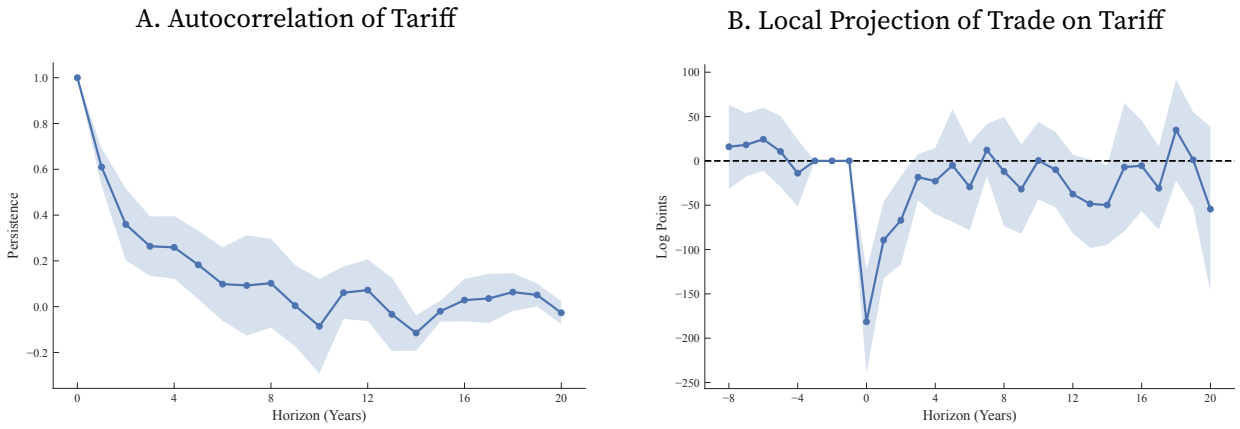
$$\mathbf{1}[\text{sanction}_{od,t+h}] = \phi_h \mathbf{1}[\text{sanction}_{od,t}] + \sum_{\ell=1}^{3} \phi_{h,\ell} \mathbf{1}[\text{sanction}_{od,t-\ell}] + \delta_{ot} + \delta_{dt} + \delta_{od} + \varepsilon_{od,t+h}.$$

A.11.2. Results

Figures A14 and A15 present estimated dynamic effects for tariffs and sanctions, displaying both policy persistence and trade impacts.

Tariff Effects. Figure A14 reveals limited persistence and transitory trade impacts. Tariff shocks decay rapidly (Panel A), with autocorrelation falling below 0.3 after two years and approaching zero by year five. Trade responses are similarly short-lived (Panel B): a one percentage point tariff increase reduces bilateral trade by approximately 2% initially, but effects dissipate within 3–4 years. This transitory nature reflects firms' rapid adjustment through supply chain reorganization and product differentiation.

FIGURE A14. Dynamic Effects of Tariff on Trade

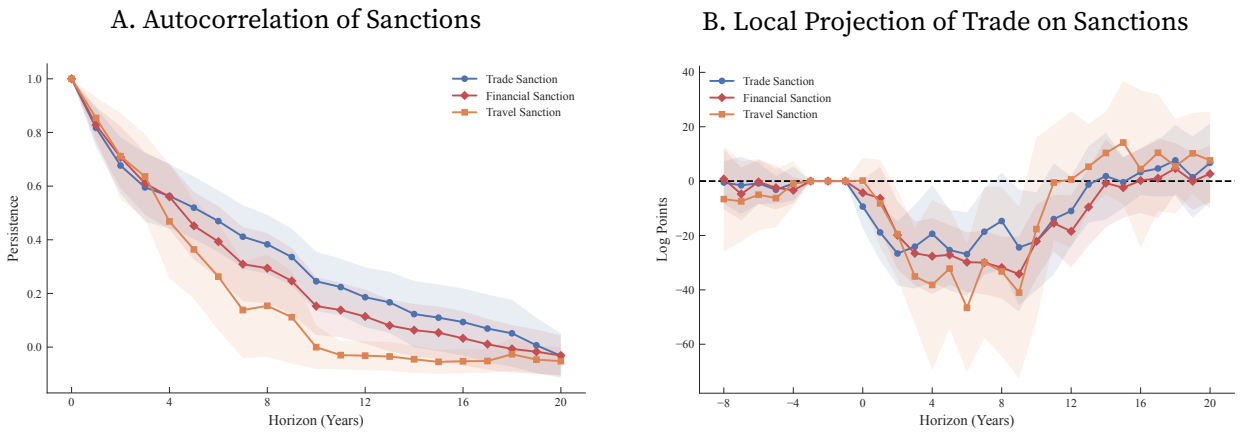


Notes: Panel A reports estimates $\{\phi_h\}$ from: $\ln(1+\tau_{od,t+h}) = \phi_h \ln(1+\tau_{od,t}) + \sum_{\ell=1}^{3} \phi_{h,\ell} \ln(1+\tau_{od,t-\ell}) + \delta_{ot} + \delta_{dt} + \delta_{od} + \varepsilon_{od,t+h}$. Panel B shows estimates $\{\beta_h\}$ from $\ln X_{od,t+h} = \beta_h \ln(1+\tau_{od,t}) + \sum_{\ell=1}^{3} \gamma_{h,\ell} \ln X_{od,t-\ell} + \sum_{\ell=1}^{3} \beta_{h,\ell} \ln(1+\tau_{od,t-\ell}) + \delta_{od} + \delta_{ot} + \delta_{dt} + \varepsilon_{od,t+h}$. The sample includes country pairs among 32 major economies. Both panels report estimated coefficients with 95% confidence intervals based on Driscoll-Kraay standard errors.

Sanction Effects. Figure A15 shows markedly different dynamics. Sanctions exhibit strong persistence (Panel A), with autocorrelation remaining above 0.5 after five years and declining toward zero by year 15. This persistence reflects the political and institutional nature of sanctions—they signal diplomatic ruptures tied to prolonged conflicts rather than temporary economic protection.

Trade impacts are correspondingly large and durable (Panel B): sanctions reduce bilateral trade by nearly 20% on impact, with effects remaining substantial for over a decade. Unlike the transitory effects of tariffs, sanctions generate persistent trade reductions extending well beyond the initial shock.

FIGURE A15. Dynamic Effects of Sanctions on Trade

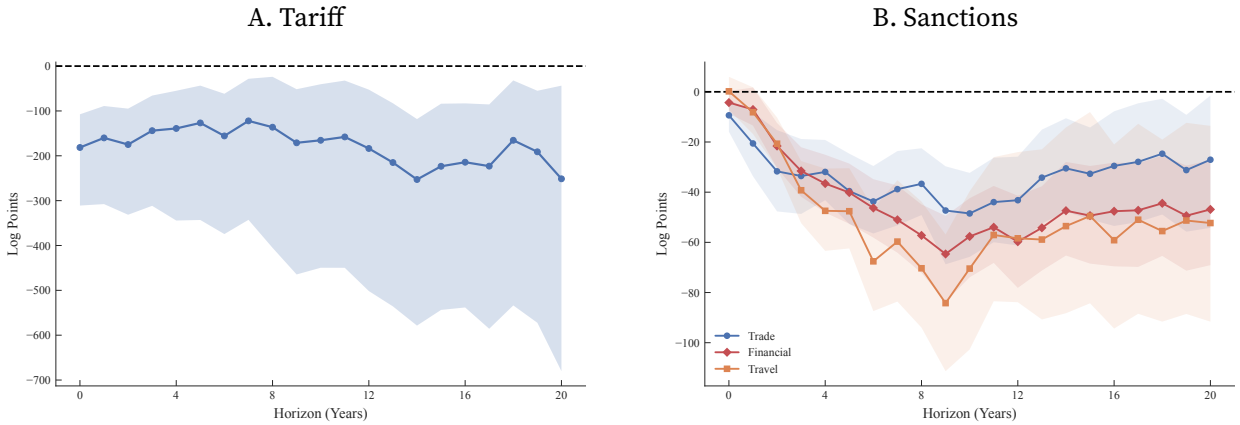


Notes: Panel A reports estimates $\{\phi_h\}$ from: $\mathbf{1}[\text{sanction}_{od,t+h}] = \phi_h \mathbf{1}[\text{sanction}_{od,t}] + \sum_{\ell=1}^{3} \phi_{h,\ell} \mathbf{1}[\text{sanction}_{od,t-\ell}] + \delta_{ot} + \delta_{dt} + \delta_{od} + \varepsilon_{od,t+h}$. Panel B shows estimates $\{\beta_h\}$ from $\ln X_{od,t+h} = \beta_h \mathbf{1}[\text{sanction}_{od,t}] + \sum_{\ell=1}^{3} \gamma_{h,\ell} \ln X_{od,t-\ell} + \sum_{\ell=1}^{3} \beta_{h,\ell} \mathbf{1}[\text{sanction}_{od,t-\ell}] + \delta_{od} + \delta_{ot} + \delta_{dt} + \varepsilon_{od,t+h}$. The sample includes country pairs among 32 major economies. Both panels report estimated coefficients with 95% confidence intervals based on Driscoll-Kraay standard errors.

Economic Interpretation. These contrasting dynamics are consistent with institutional differences in how the two policy instruments operate. Tariffs are largely set within multilateral frameworks, and firms can adjust through supply chain reorganization, so effects dissipate within a few years. Sanctions, by contrast, signal broader diplomatic ruptures and trigger wider economic disengagement. Their persistence suggests that even partial sanctions can create lasting disruptions to bilateral trade.

Figure A16 quantifies these differences through permanent shock responses. A permanent 1% tariff increase reduces trade by approximately 2% on impact, stabilizing at a 3% long-run decline. This implies a trade elasticity of 3, corresponding to a substitution elasticity of $\sigma \approx 4$ in our quantitative framework. Permanent sanctions produce substantially larger effects, reducing bilateral trade by nearly 40%-60% in the long run. This difference in magnitude is consistent with the view that sanctions disrupt a broader set of commercial relationships than tariffs.

FIGURE A16. IRF: Trade to Permanent Policy Shocks



Notes: Panel A presents the cumulative impulse response of log trade to a permanent unit shock in tariff. Panel B shows the cumulative response to a permanent unit shock in sanctions. Both panels use the baseline specification with three lags and three two-way fixed effects. 95% confidence intervals are from 200 bootstrap iterations with country-pair block resampling.

A.12. Non-Economic Geopolitical Score and Policies

Table A6 confirms that the relationship between geopolitical alignment and policy instruments holds when using only the non-economic component of the geopolitical score, which excludes trade agreements, sanctions, and commercial disputes.

TABLE A6. Geopolitical Alignment and Policies: Non-Economic Geo Score

	(1)	(2)	(3)	(4)	(5)	(6)
Dependent Variable:	log Tariff	**1** [Sanction]			Restricting Trade Policy	
		Trade	Financial	Travel	≥ 1 Product	≥ 20 Products
Geopolitical Alignment	-0.147	-0.045	-0.043	-0.041	-3.38	-1.50
	(0.124)	(0.008)	(0.006)	(0.004)	(2.04)	(0.79)
Mean Dep. Var.	0.73	0.049	0.037	0.019	21.4	3.24
Observations	21640	74400	74400	74400	16864	16864
Imposer × Year FE	Yes	Yes	Yes	Yes	Yes	Yes
Receiver × Year FE	Yes	Yes	Yes	Yes	Yes	Yes
Imposer × Receiver FE	Yes	Yes	Yes	Yes	Yes	Yes

Notes: The unit of observation is an imposer–receiver country pair in a given year. The dependent variables are the log tariff (column 1); indicators for the presence of trade, financial, and travel sanctions (columns 2–4, respectively); and the number of restrictive trade policies (columns 5–6). The geopolitical alignment measure uses only non-economic events. The sample includes country pairs among 32 major countries. Standard errors are clustered at the country-pair level.

A.13. Hat Algebra

Using exact hat algebra, we denote proportional changes as $\hat{x} = x'/x$ and define $\tilde{\tau}_{od} \equiv 1 + \tau_{od}$.

Price index:

$$\hat{P}_d = \left[\sum_{o=1}^{N} \pi_{od} \left(\hat{w}_o \hat{\tilde{d}}_{od} \right)^{1-\sigma} \right]^{\frac{1}{1-\sigma}}.$$

Trade shares:

$$\hat{\pi}_{od} = \left(\frac{\hat{w}_o \hat{\tilde{d}}_{od}}{\hat{P}_d} \right)^{1-\sigma}.$$

Budget constraint:

$$X'_d = \frac{\hat{w}_d \, w_d \, \ell_d}{\sum_{o=1}^{N} \frac{\hat{\pi}_{od} \, \pi_{od}}{\hat{\tilde{\tau}}_{od} \, \tilde{\tau}_{od}}}.$$

Labor market clearing:

$$\hat{w}_o \, w_o \, \ell_o = \sum_{d=1}^{N} \frac{\hat{\pi}_{od} \, \pi_{od}}{\hat{\tilde{\tau}}_{od} \, \tilde{\tau}_{od}} \, X'_d.$$

Appendix B. Construction of the Geopolitical Alignment Measure

This appendix details the construction and validation of our bilateral geopolitical alignment measure. Building on Fan (2025), we employ large language models to compile comprehensive event data across all country pairs from 1950–2024. Section B.1 presents the full taxonomy of event categories. Section B.2 describes event compilation and classification. Section B.3 demonstrates robustness to the choice of LLM. Section B.4 provides validation through case studies. Section B.5 documents the evolution of geopolitical event scores globally. Section B.6 compares our measure with the Geopolitical Risk index. Section B.7 documents the LLM prompt design.

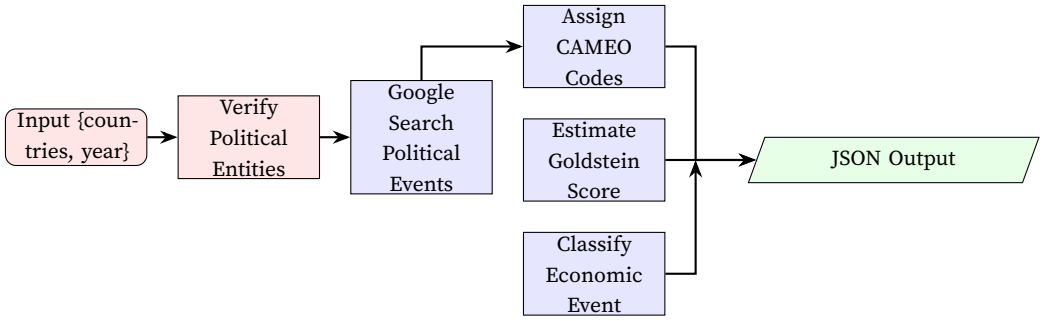
B.1. Event Categories

Table B1 presents the full taxonomy of bilateral geopolitical events used in our database. Events span six major categories and 22 subcategories, covering the principal dimensions of interstate interaction.

B.2. Event Compilation Using Large Language Models

Major bilateral geopolitical events form core elements of LLM training corpora, appearing extensively across news archives, government publications, and scholarly databases. We employ Gemini 2.5 Pro with web search capabilities to systematically compile and analyze these events through structured prompt engineering. Figure B1 illustrates our analysis procedure, with the complete prompt specification documented in Section B.7.

FIGURE B1. LLM Geopolitical Event Analysis Procedure



The LLM performs five sequential tasks: (i) verify historical political entities accounting for state succession (e.g., Soviet Union to Russian Federation); (ii) search knowledge base and internet sources for major bilateral events from authoritative sources; (iii) classify events using the Conflict and Mediation Event Observations (CAMEO) framework; (iv) assign Goldstein scores from −10 (maximum conflict) to +10 (maximum cooperation); and (v) categorize economic content when applicable.

TABLE B1. Categories of Bilateral Geopolitical Events

Subcategory	Representative Events	Subcategory	Representative Events
A. Economic Relations		*D. Legal, Territorial & Movement*	
A1. Trade Policy	Tariff imposition/removal; non-tariff barriers; FTA negotiations, signing, ratification, withdrawal	D1. Legal Actions	ICJ/WTO disputes; international arbitration; extradition; law enforcement cooperation
A2. Financial Relations	Asset freezes; SWIFT exclusions; capital market denial; currency swaps; FDI restrictions; investment treaties	D2. Territorial & Maritime	EEZ/continental shelf disputes; freedom of navigation operations; border demarcation; sovereignty claims
A3. Economic Coercion	Trade embargoes; sectoral sanctions; Entity List designations; export controls; foreign aid; debt relief	D3. Movement of People	Visa regime changes; travel bans; guest worker programs; refugee/asylum policies
A4. Strategic Sectors	Energy supply agreements; pipeline projects; nuclear cooperation; 5G bans; rare earth controls		
A5. Integration	BRI/B3W infrastructure; port concessions; friendshoring; supply chain arrangements; customs unions	*E. Multilateral & Global Governance*	
A6. Other Economic	Regulatory harassment; boycott campaigns; government procurement restrictions; gray zone pressures	E1. Int'l Organizations	UNSC confrontations; GA coalition building; regional bloc membership changes
		E2. Global Issues	Climate cooperation; pandemic coordination; vaccine diplomacy; human rights
B. Diplomatic & Political Relations		*F. Other Significant Events*	
B1. Formal Diplomacy	Embassy/consulate openings and closures; ambassador recalls; staff expulsions; démarches	F1. Historical & Symbolic	Apologies for historical wrongs; memorial visits; monument disputes
B2. High-Level Interactions	Presidential visits; bilateral summits; summit boycotts; ministerial meetings; strategic dialogues	F2. Humanitarian	Disaster aid offers/rejections; joint rescue operations; evacuation cooperation
B3. Public Diplomacy	Policy speeches; parliamentary resolutions; propaganda campaigns	F3. Sports & Events	Olympic boycotts; joint hosting; World Expo participation
B4. Cultural & Educational	Cultural agreements/boycotts; scholarship programs; university partnerships; student visa policies	F4. Technology & Space	Joint space missions; tech theft accusations; research terminations
		F5. Environment	Transboundary river/pollution disputes; conservation conflicts
C. Security & Defense		F6. Communications	Journalist expulsions; broadcasting restrictions; information warfare
C1. Military Cooperation	Alliances; defense pacts; base arrangements; arms sales/embargoes; joint exercises; military aid	F7. Other	Emerging forms of bilateral interaction
C2. Security Incidents	Border skirmishes; airspace/maritime violations; naval encounters; hybrid warfare		
C3. Intelligence & Cyber	Espionage revelations; intel officer expulsions; intel-sharing pacts; state-sponsored cyber attacks		

Table B2 illustrates a year of sharp swings in U.S.-China relations rather than uniformly rising cooperation or conflict. The Hainan Island incident (−8.5) and the U.S. arms sale to Taiwan (−5.0) generated severe security tensions in the first half of the year. Yet these shocks were followed by a marked improvement in bilateral relations through post-9/11 counterterrorism cooperation (+6.0), the Jiang-Bush APEC summit (+5.0), and China's WTO accession (+8.0). The 2001 pattern is informative for our measure because it shows that bilateral geopolitical alignment can incorporate

both acute political crises and major trade-relevant breakthroughs within the same year. This combination of security conflict and economic integration is precisely the type of nuance that aggregate voting-based measures struggle to capture.

TABLE B2. Major U.S.-China Bilateral Events in 2001: LLM Analysis Results

Event Name	Event Description	CAMEO Class.	Econ. Type	Goldstein Score
Hainan Island Incident	A U.S. EP-3 surveillance aircraft collided with a Chinese fighter near Hainan on Apr. 1, triggering a major diplomatic crisis, emergency landing, and prolonged crew detention	Material Conflict (17-173)	Not econ.	−8.5
U.S. Arms Sale to Taiwan	The Bush administration approved a major arms package for Taiwan on Apr. 24, including submarines, destroyers, and surveillance aircraft, provoking sharp objections from Beijing	Material Conflict (17-170)	Not econ.	−5.0
Jiang-Bush APEC Summit	Presidents Jiang Zemin and George W. Bush met at the APEC summit in Shanghai on Oct. 19, helping stabilize relations after the Hainan crisis and opening space for renewed dialogue	Verbal Coop. (04-043)	Not econ.	+5.0
China Joins the WTO	China formally entered the World Trade Organization on Dec. 11 after fifteen years of negotiations, with U.S. support playing a central role in the accession process	Material Coop. (06-061)	Trade	+8.0
Post-9/11 Counterterrorism Cooperation	Following the Sept. 11 attacks, China expressed support for the U.S.-led campaign against terrorism, creating a temporary period of strategic cooperation despite earlier tensions	Verbal Coop. (03-032)	Not econ.	+6.0

Comparing Table B2 with the 2024 U.S.-China example in the main text highlights the dynamic range of our measure within a single bilateral relationship. In 2001, severe security frictions—the Hainan incident (−8.5) and the Taiwan arms sale (−5.0)—coexisted with substantial cooperation through post-9/11 coordination, the Jiang-Bush summit, and China's WTO accession (+8.0). By 2024, that mixed pattern had shifted toward managed rivalry: conflict remained pronounced through tariffs, sanctions, export controls, and military tensions over Taiwan, while the cooperative events were narrower and primarily aimed at crisis management rather than deeper integration. This contrast shows that our event-based framework captures not only overall relationship valence, but also changes in the substantive channels through which geopolitics affects economic exchange.

Comparison with Existing Event Databases Our approach differs fundamentally from GDELT (Leetaru and Schrodt 2013) and ICEWS (Boschee et al. 2015). First, we leverage LLMs' contextual understanding to focus exclusively on major bilateral political events that define geopolitical relationships, rather than attempting comprehensive coverage of all international interactions.[24] This targeted approach yields more precise measurement of relationship intensity. Second, our compilation spans 1950–2024, aligning with economic data availability for panel analysis.[25]

B.2.1. Statistics of Geopolitical Events

Our comprehensive compilation of bilateral geopolitical events spans seven and a half decades (1950–2024) and encompasses 833,485 individual events across all 193×192/2 country pairs. Table B3 and Figure B2 provide detailed statistics revealing both the scale and evolution of international political interactions over this extended period.

TABLE B3. Summary Statistics of Geopolitical Events by Decade, 1950–2024

	1950s	1960s	1970s	1980s	1990s	2000s	2010s	2020s	Total
CAMEO Event Classification									
Verbal Cooperation	21,709	33,113	43,108	39,089	45,930	70,549	113,422	71,141	438,061
Material Cooperation	13,423	18,314	22,087	22,664	28,743	44,521	58,045	32,899	240,696
Verbal Conflict	11,484	13,953	12,810	14,064	8,241	11,863	16,754	10,104	99,273
Material Conflict	5,598	6,924	6,505	7,782	6,705	6,606	9,556	5,779	55,455
Goldstein Scale Statistics									
Mean	2.02	2.41	3.06	2.61	3.83	4.00	3.76	3.62	3.38
Std. Dev.	5.45	5.12	4.71	4.85	4.35	3.86	3.69	3.66	4.33
Median	4.00	4.50	5.00	4.00	5.00	5.00	4.00	4.00	4.50
Event Categories									
Economic Relations	8,631	12,264	16,324	16,419	22,470	35,396	46,383	25,946	183,833
Diplomatic & Political	19,324	25,498	29,274	28,522	29,716	49,028	87,932	55,222	324,516
Security & Defense	9,267	9,978	9,498	9,817	7,857	10,398	14,940	8,483	80,238
Legal & Territorial	3,061	2,811	3,310	2,813	3,821	6,743	10,031	5,434	38,024
Multilateral Governance	10,562	19,951	23,771	21,353	22,201	26,460	29,560	18,178	172,036
Other Events	1,369	1,802	2,333	4,675	3,554	5,514	8,931	6,660	34,838
Summary									
Total Events	52,214	72,304	84,510	83,599	89,619	133,539	197,777	119,923	833,485

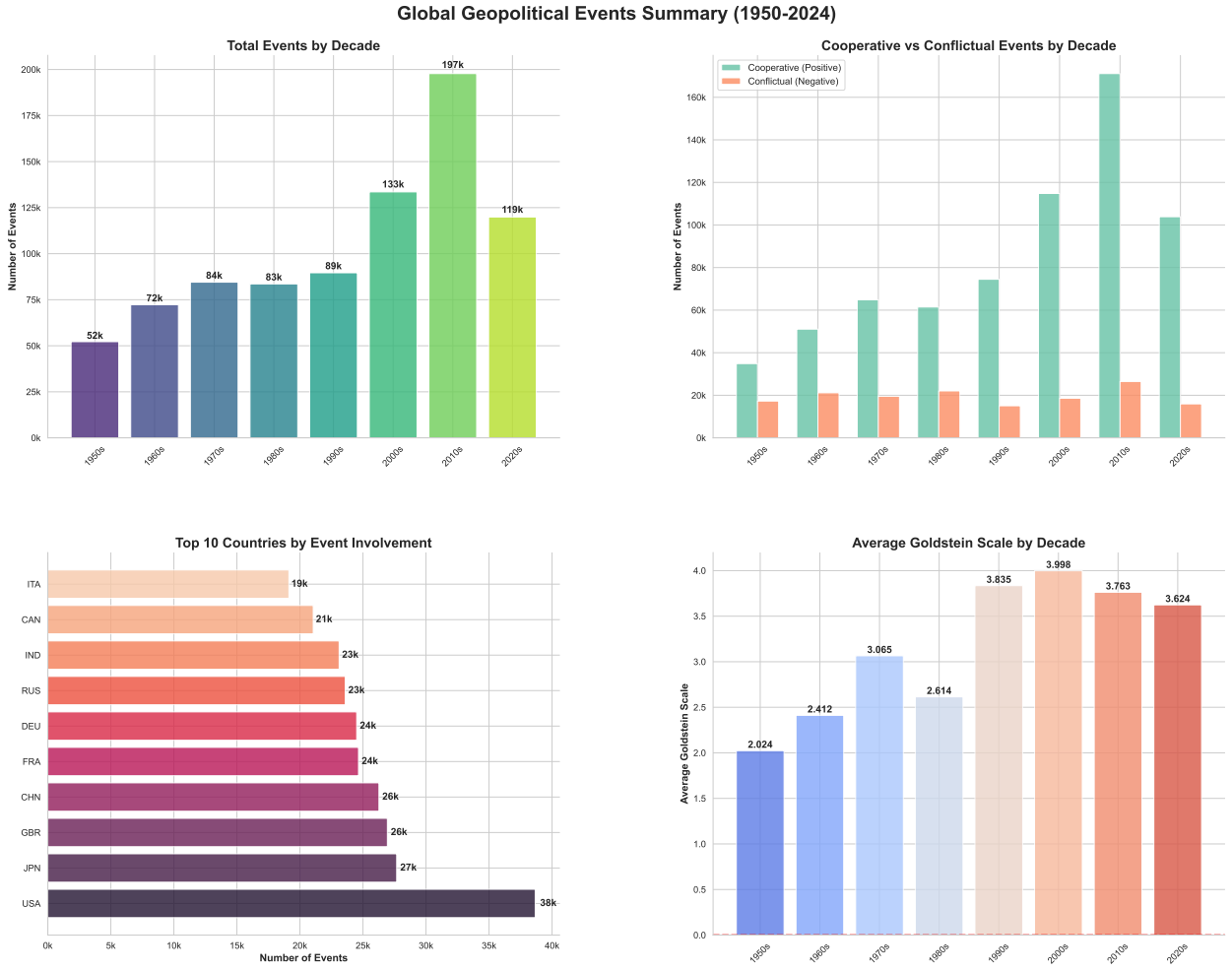
Notes: CAMEO classifications follow the Conflict and Mediation Event Observations framework. Goldstein Scale ranges from −10 (most conflictual) to +10 (most cooperative). Event Categories: Economic Relations, Diplomatic & Political Relations, Security & Defense, Legal & Territorial, Multilateral Governance, and Other Events. The 2020s column covers 2020–2024. All figures represent event counts except Goldstein Scale statistics.

The data reveal a persistent cooperative bias in international relations, with cooperative events

[24] GDELT and ICEWS collect all global events across actors and issue areas, complicating aggregation into meaningful bilateral relationship measures.

[25] GDELT begins in 1979 and ICEWS covers only 1995–present, limiting historical economic analysis.

FIGURE B2. Geopolitical Events Summary (1950–2024)



(both verbal and material) comprising 81.5% of all recorded interactions (678,757 events) compared to 18.5% for conflictual events (154,728 events). Verbal cooperation represents the single largest category with 438,061 events (52.6%), followed by material cooperation with 240,696 events (28.9%). Diplomatic communications and cooperative actions—such as trade agreements, aid provision, and joint initiatives—account for the majority of recorded interactions.

The temporal evolution demonstrates substantial growth in event frequency, with total events nearly quadrupling from 52,214 in the 1950s to a peak of 197,777 in the 2010s. The 2020s show 119,923 events despite covering only five years (2020–2024), suggesting continued high interaction intensity. Notably, the growth concentrates in cooperative categories: verbal cooperation increases more than fivefold from the 1950s (21,709) to the 2010s (113,422), while material cooperation quadruples (from 13,423 to 58,045). Conflict events show more modest variation, with the ratio of cooperation to conflict remaining stable across decades.

The Goldstein Scale statistics document shifts in relationship intensity over time. The early

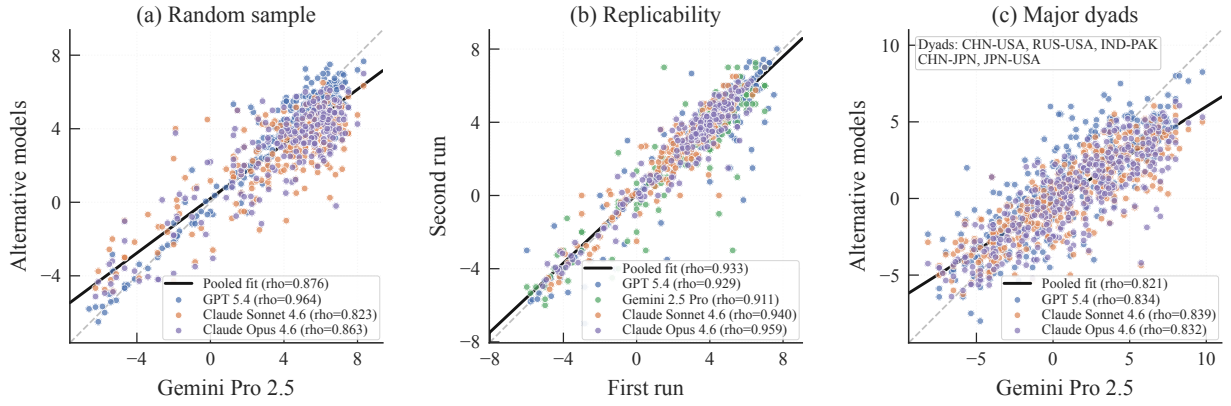
Cold War (1950s) exhibits the lowest mean cooperation score (2.02) with the highest volatility (standard deviation of 5.45), reflecting the bipolar tensions and uncertainty of the period. Mean scores improve through the 1970s (3.06) before declining in the 1980s (2.61) amid renewed Cold War tensions. The post-Cold War transformation is pronounced: mean scores nearly double from 2.61 in the 1980s to 3.83 in the 1990s, peaking at 4.00 in the 2000s with reduced volatility (standard deviation of 3.86). The 2010s and early 2020s show modest declines (3.76 and 3.62 respectively), suggesting emerging fragmentation while maintaining cooperation levels well above Cold War norms.

Event categories reveal the multifaceted nature of contemporary international relations. Diplomatic and political relations dominate with 324,516 events (38.9%), reflecting the primacy of state-to-state engagement. Economic relations account for 183,833 events (22.1%), underscoring the centrality of economic interdependence—particularly relevant for our analysis of trade flows. The substantial growth in economic events from 8,631 in the 1950s to 46,383 in the 2010s parallels the expansion of global trade networks. Multilateral governance events (172,036 total, 20.6%) highlight the rise of international institutions, while security and defense interactions (80,238 events, 9.6%) remain relatively stable across decades, suggesting that military considerations, while important, no longer dominate bilateral relationships as they did during the Cold War.

B.3. Model Robustness

A potential concern with LLM-based measurement is that results may depend on the specific model used or vary across runs. We address this through three complementary exercises using three frontier LLMs: Gemini 2.5 Pro (our baseline), GPT 5.4, and Claude (Opus 4.6 and Sonnet 4.6).

FIGURE B3. Model Robustness and Replicability of Geopolitical Alignment Scores



Notes: Each point represents the mean Goldstein score for a country-pair-year observation. Panel (a) compares scores from alternative models (vertical axis) against Gemini 2.5 Pro (horizontal axis) for 300 randomly selected dyad-years. Panel (b) tests within-model replicability by running each model twice on the same dyad-years. Panel (c) compares scores across models for five major bilateral relationships (CHN-USA, RUS-USA, IND-PAK, CHN-JPN, JPN-USA) across all years.

Figure B3 presents the results. Panel (a) compares scores from alternative LLMs against our baseline Gemini 2.5 Pro for 300 randomly selected dyad-years. Scores cluster tightly along the 45-degree line, with correlation coefficients exceeding 0.82 in all pairwise comparisons (pooled $\rho = 0.88$). Panel (b) tests within-model replicability by running each model twice on the same inputs.[26] Within-model correlations are higher than cross-model correlations (pooled $\rho = 0.93$), as expected: the only source of variation is stochastic decoding, while cross-model comparisons additionally reflect differences in training data and scoring tendencies. Newer frontier models achieve higher stability, with Opus 4.6 reaching $\rho = 0.96$ and Sonnet 4.6 reaching $\rho = 0.94$, compared to $\rho = 0.93$ for GPT 5.4 and $\rho = 0.91$ for Gemini 2.5 Pro. Panel (c) provides a more demanding test by comparing scores for five major bilateral relationships across all years. The pooled correlation ($\rho = 0.82$) is lower than for random dyad-years, reflecting greater judgment involved in scoring volatile major-power relationships. Across all three exercises, correlation coefficients exceed 0.82, suggesting that major bilateral geopolitical events are sufficiently well-documented that different LLMs converge on similar assessments.

B.4. Validation

This section validates our event-based measure through bilateral case studies, geographic visualization, and statistical tests demonstrating its economic relevance.

B.4.1. Case Studies Across Regions

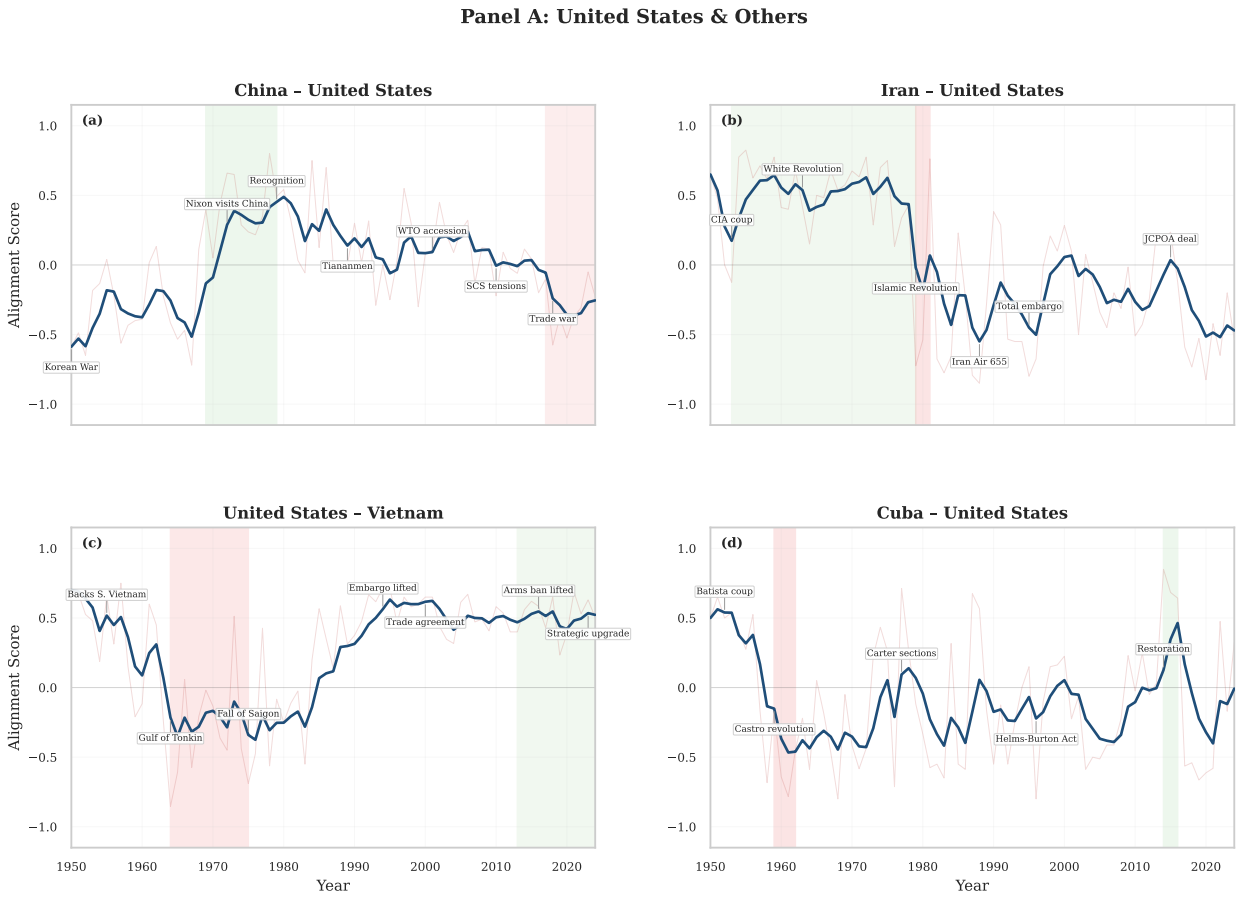
Beyond the U.S.-China trajectory presented in Section 2, we validate our measure across 16 additional bilateral relationships spanning four regions. Each panel plots the dynamic alignment score alongside the yearly event score from 1950 to 2024, with key historical events annotated.

Figure B4 presents four U.S. bilateral relationships that illustrate the measure's ability to capture sharp reversals. The China–U.S. trajectory (panel a) traces the full arc from Korean War hostility through Nixon's rapprochement to the recent deterioration driven by trade war and strategic rivalry. The Iran–U.S. relationship (panel b) exhibits one of the sharpest discontinuities in our dataset: the 1979 Islamic Revolution transforms the score from sustained cooperation to deep hostility, with only the brief 2015 JCPOA episode registering a partial recovery. The U.S.–Vietnam trajectory (panel c) captures the mirror image—from Cold War conflict through post-embargo normalization to the 2023 strategic upgrade. Cuba–U.S. relations (panel d) show persistent hostility following the Castro revolution, punctuated by the short-lived Obama-era opening in 2014–2016 and its subsequent reversal.

Figure B5 covers four Asian relationships characterized by ideological realignments and territorial disputes. The China–Russia trajectory (panel a) captures the Sino-Soviet alliance, the Sino-Soviet split and 1969 border clashes, gradual rapprochement, and the contemporary partnership. China–India relations (panel b) show an early cooperative phase shattered by the 1962 border war, followed

[26] All models are run with temperature = 0.1 to reduce stochastic variation while preserving some flexibility in event retrieval and summary.

FIGURE B4. Geopolitical Alignment Trajectories: United States & Others



Notes: Dynamic alignment scores (dark blue) and yearly event scores (light red) for four U.S. bilateral relationships, 1950–2024. Green shading denotes cooperative eras; red shading denotes conflictual eras. Key geopolitical events are annotated along the dynamic score series.

by decades of cautious engagement disrupted by standoffs at Doklam (2017) and Galwan Valley Clash (2020). The China–Japan score (panel c) tracks post-war hostility, the 1972 normalization, and the deterioration following the Senkaku/Diaoyu crisis of 2012. India–Pakistan (panel d) exhibits persistent tension punctuated by wars (1965, 1971), nuclear tests (1998), and rare cooperative windows.

Figure B6 illustrates relationships shaped by revolutionary regime changes and prolonged conflicts. The Egypt–Israel trajectory (panel a) captures the transformation from repeated wars to the Camp David peace. Iran–Israel relations (panel b) exhibit another revolutionary discontinuity: the Pahlavi-era peripheral pact gives way to sustained enmity after 1979. Iran–Saudi Arabia (panel c) follows a similar pattern of pre-revolutionary cooperation, post-1979 hostility, and the 2023 China-brokered rapprochement. The Iran–Iraq score (panel d) captures the eight-year war (1980–1988) and the post-2003 reversal as regime change in Baghdad transformed the bilateral relationship.

Figure B7 presents European relationships that exhibit meaningful variation driven by insti-

FIGURE B5. Geopolitical Alignment Trajectories: Asia



Notes: Dynamic alignment scores (dark blue) and yearly event scores (light red) for four Asian bilateral relationships, 1950–2024. Green shading denotes cooperative eras; red shading denotes conflictual eras.

tutional integration and strategic disagreements. The UK–U.S. "special relationship" (panel a) maintains consistently positive scores, with the Suez crisis of 1956 representing the most notable disruption. Greece–Turkey relations (panel b) show the most volatile European trajectory, driven by the Cyprus crises, the Aegean disputes, and renewed tensions over Eastern Mediterranean resources. France–UK relations (panel c) fluctuate around a cooperative baseline, with De Gaulle's EEC veto and Brexit producing the largest dips. France–Turkey (panel d) exhibits a sustained decline from NATO-era cooperation through progressive disagreements over EU accession, Libya, and Eastern Mediterranean sovereignty.

Across all 16 dyads, the measure consistently tracks well-documented historical turning points, captures both gradual trends and sharp discontinuities, and distinguishes between sustained regime shifts (e.g., Iran–U.S. post-1979) and temporary disruptions (e.g., UK–U.S. during Suez).

FIGURE B6. Geopolitical Alignment Trajectories: Middle East



Notes: Dynamic alignment scores (dark blue) and yearly event scores (light red) for four Middle Eastern bilateral relationships, 1950–2024. Green shading denotes cooperative eras; red shading denotes conflictual eras.

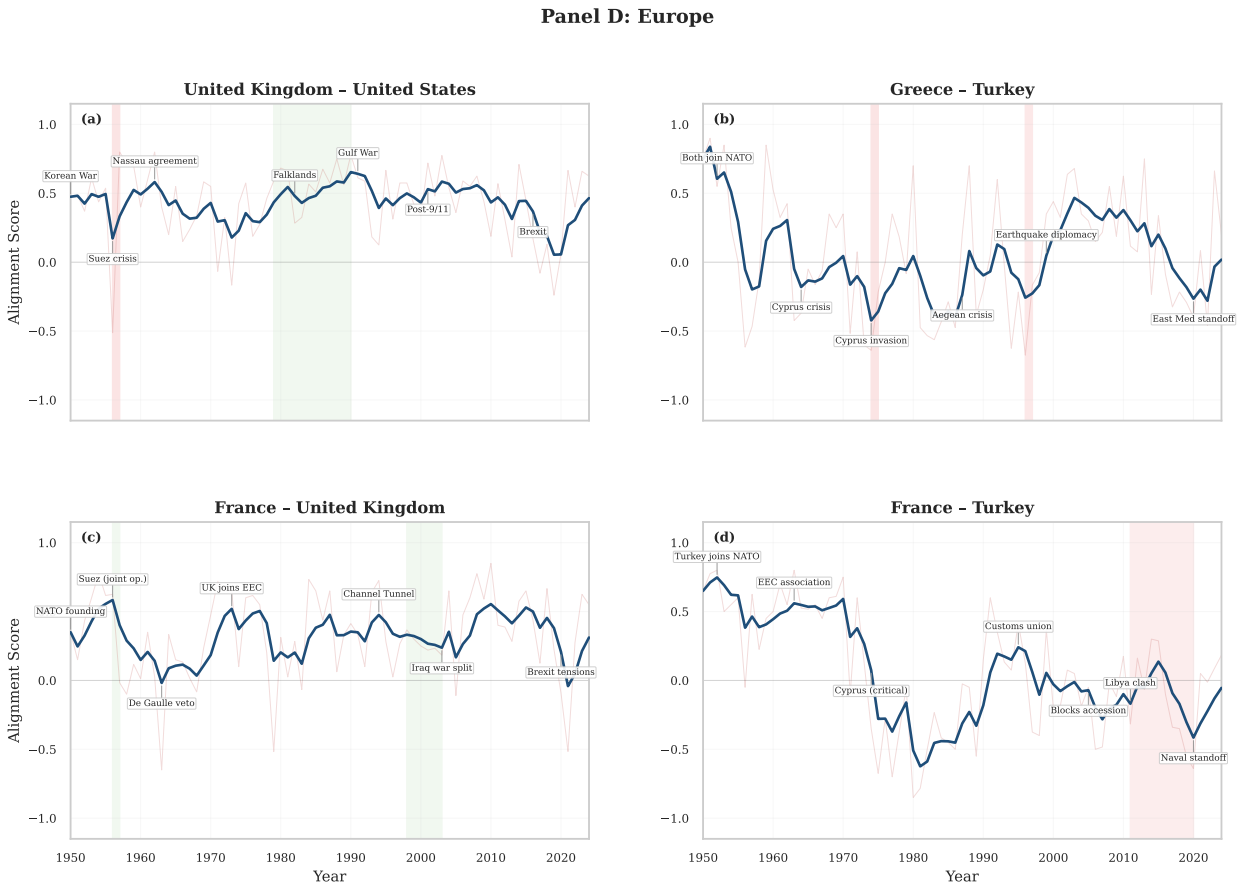
B.4.2. Geographic Validation Through Maps

We validate our measure's ability to capture geopolitical dynamics by examining three pivotal moments in great power competition: Cold War bipolarity (USA-USSR, 1980), emerging multipolarity (USA-China, 2019), and contemporary regional conflict (Ukraine-Russia, 2024).

The 1980 maps (Figure B8) exhibit canonical Cold War alignment patterns: the two superpowers' scores are strongly negatively correlated across partners, consistent with zero-sum competition. The United States dominates NATO Europe, Pacific allies, and the Western Hemisphere, while the USSR controls Eastern Europe, Cuba, Vietnam, Ethiopia, and Afghanistan. Countries displaying positive relations with one superpower show negative relations with the other—validating our measure's ability to capture mutually exclusive alignment. Notable exceptions such as India and Egypt correctly reflect Non-Aligned Movement membership despite their practical tilts.

The 2019 comparison (Figure B9) reveals transformed competition patterns. While the United States maintains traditional alliances (NATO, Japan, Australia), sharp bipolar divisions have dissolved. China achieves positive relations across most of Africa and Southeast Asia through economic

FIGURE B7. Geopolitical Alignment Trajectories: Europe



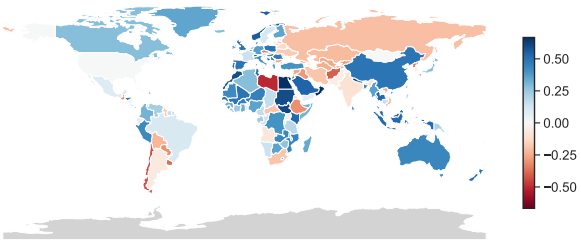
Notes: Dynamic alignment scores (dark blue) and yearly event scores (light red) for four European bilateral relationships, 1950–2024. Green shading denotes cooperative eras; red shading denotes conflictual eras.

engagement rather than military alliances. Many countries maintain positive relations with both powers—the "connector states" that enable continued globalization despite strategic rivalry. China's most negative scores concentrate among U.S. treaty allies, while the United States shows deteriorated relations primarily with Russia, Iran, and Venezuela.

The 2024 Ukraine-Russia maps (Figure B10) demonstrate how regional conflicts generate global polarization. Ukraine achieves very high Western alignment—exceeding even U.S. levels across NATO members—reflecting wartime solidarity. Russia faces near-total isolation from developed democracies while maintaining positive relations with China, India, and parts of Africa resistant to Western pressure. The clear geographic clustering—democratic alignment with Ukraine versus authoritarian and non-aligned support for Russia—validates our measure's sensitivity to how regional crises restructure global alignments. Belarus and Central Asian states' positioning accurately reflects their delicate balance between historical ties and sanctions pressure.

FIGURE B8. Cold War Bipolarity: USA vs. USSR, 1980

A. United States, 1980



B. Soviet Union, 1980

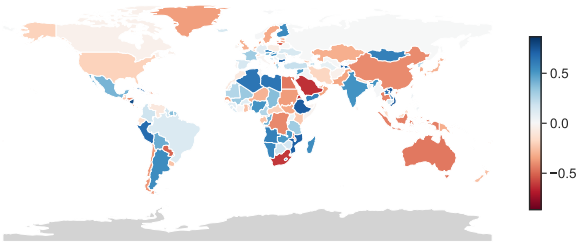
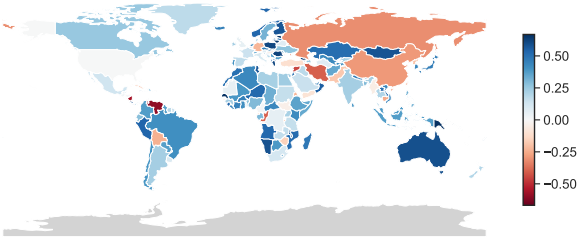


FIGURE B9. Emerging Multipolarity: USA vs. China, 2019

A. United States, 2019



B. China, 2019

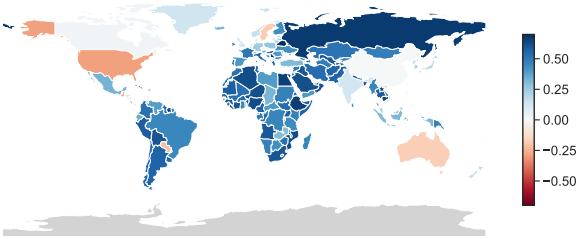
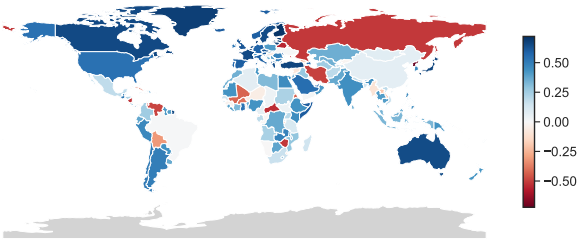
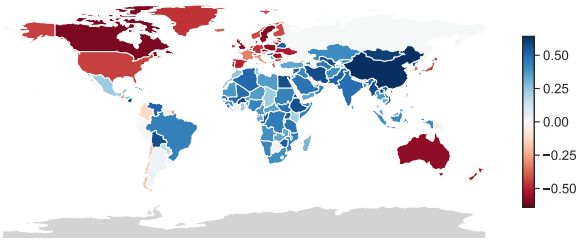


FIGURE B10. Regional Conflict Polarization: Ukraine vs. Russia, 2024

A. Ukraine, 2024



B. Russia, 2024



Advantages over Existing Measures Our event-based approach offers three key advantages over existing measures of bilateral geopolitical relations: universal coverage across countries and time, precision in capturing the timing and intensity of bilateral dynamics, and comprehensive measurement from maximum conflict to maximum cooperation.

Existing literature predominantly relies on UN voting similarity to achieve broad coverage (Signorino and Ritter 1999; Bailey, Strezhnev, and Voeten 2017). However, as shown in Section 2.5, UNGA voting captures countries' global geopolitical stance but misses approximately three-quarters of the variation in bilateral relations.

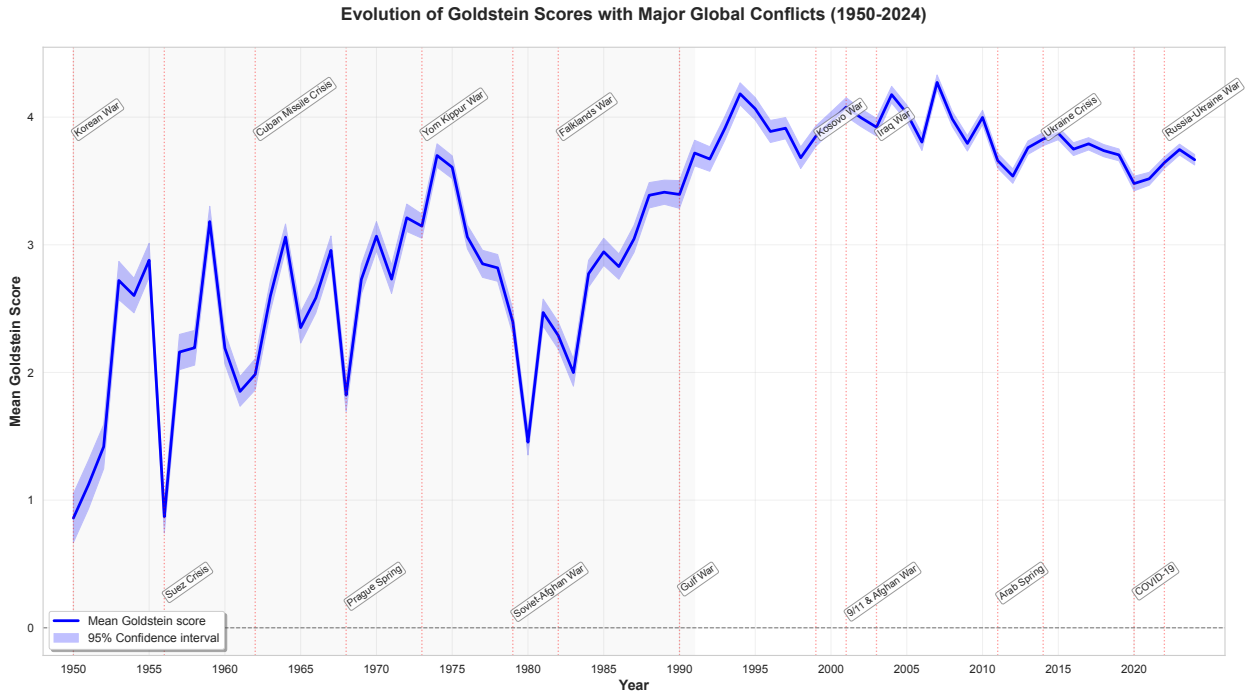
Our measure also complements categorical approaches that classify relationships using discrete indicators such as *Strategic Rivalry* (Thompson 2001; Aghion et al. 2019), *Sanctions* (Ahn and Ludema

2020; Felbermayr et al. 2021), *Formal Alliance* (Gibler 2008), and *Treaties* (Broner et al. 2025b). While these binary classifications capture important institutional milestones, they necessarily focus on specific relationship thresholds rather than continuous evolution. Our framework incorporates these landmark events—military rivalries, alliance formations, treaty signings—while situating them within a broader spectrum of bilateral interactions.

B.5. Evolution of Global Geopolitical Events

This section documents the evolution of geopolitical event scores globally and across UN geographical regions.

FIGURE B11. Global Mean Goldstein Scores with Major Conflicts, 1950–2024



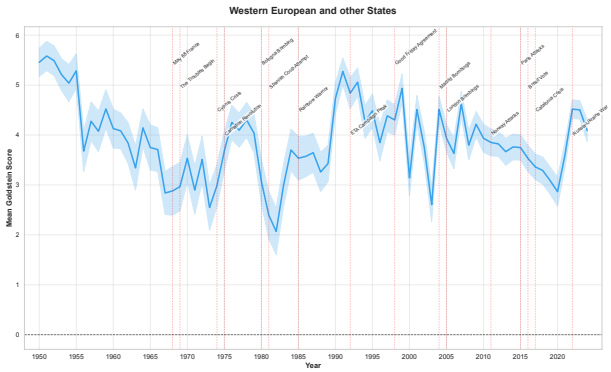
Notes: Mean Goldstein scores across all bilateral country pairs with 95% confidence intervals. Vertical lines indicate major international conflicts. Scores range from −10 (maximum conflict) to +10 (maximum cooperation). Shaded region denotes the Cold War period (1950–1991).

Figure B11 reveals the secular evolution of global geopolitical relations over seven decades. The Cold War period (1950–1991) exhibits persistently low cooperation levels, with mean scores oscillating between 1 and 3, punctuated by sharp deteriorations during major crises—the Korean War (1950), Suez Crisis (1956), Cuban Missile Crisis (1962), and Soviet-Afghan War (1979). The end of the Cold War marks a structural break: mean scores surge from 2.5 in 1989 to above 3.5 by 1993, subsequently stabilizing at this elevated level through the 2000s. This period of hyper-globalization coincides with historically high cooperation scores and reduced variance, reflecting expanded multilateral institutions and deepening economic integration. Since 2010, however, scores have

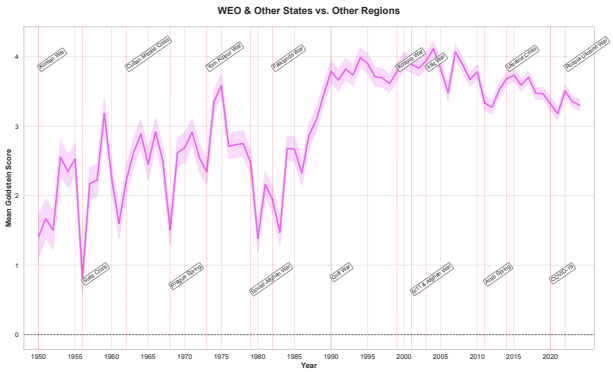
plateaued and begun declining, with the Arab Spring (2011), Ukraine Crisis (2014), and COVID-19 pandemic (2020) marking inflection points toward renewed fragmentation. The Russia-Ukraine War (2022) drives scores to their lowest level since the 1980s, suggesting the end of the post-Cold War cooperative equilibrium.

FIGURE B12. Geopolitical Scores for Western European and Other States

A. Western European and Other States



B. WEO States vs. Other Regions



Notes: Panel A shows intra-regional scores among Western European and Other States. Panel B shows inter-regional scores between WEO states and all other regions. Shaded areas represent 95% confidence intervals.

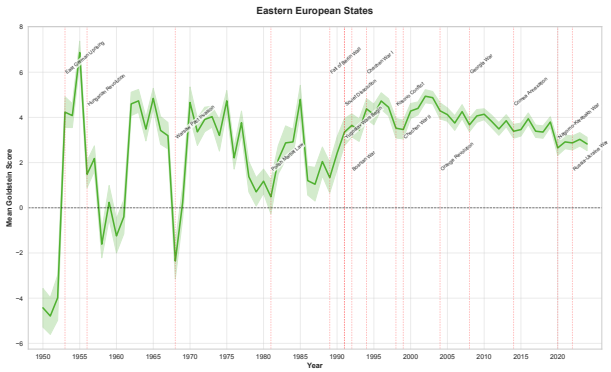
Figure B12 examines Western European and Other States (WEO), the core of the postwar liberal order. Panel A demonstrates stable intra-regional cooperation, with scores consistently above 3 and reaching peaks near 5 during periods of institutional deepening—the Single European Act (1986), Maastricht Treaty (1992), and Eastern enlargement (2004). Notable disruptions include the Cyprus Crisis (1974), which temporarily depressed scores to 2.5, and the dual shocks of Brexit (2016) and the Russia-Ukraine War (2022), which have driven scores below 3 for the first time since the 1980s. Panel B reveals that WEO states' relationships with other regions broadly track global patterns while maintaining systematically higher baseline cooperation—typically 0.5–1.0 points above the global mean. The divergence since 2015 between stable intra-WEO cooperation and deteriorating WEO-other relations provides clear evidence of selective decoupling: Western states maintain deep integration among themselves while political relationships with the Global South and non-aligned states deteriorate.

Figure B13 contrasts two regions with divergent trajectories. Eastern European states (Panel a) exhibit the highest volatility in our sample, with scores swinging from −5 during the Hungarian Revolution (1956) to above 7 immediately following German reunification (1990). The Soviet collapse initiates a decade of negative scores as Yugoslavia disintegrates and post-Soviet conflicts erupt. EU accession drives steady improvement from 2000 to 2014, with scores stabilizing around 4. The Crimean annexation (2014) triggers renewed deterioration, while the 2022 invasion produces the sharpest decline in any region, with scores plummeting near zero—effectively marking the end of post-Cold War European integration. Asia-Pacific states (Panel b) display a contrasting pattern of steady improvement from hostile relations in 1950 (Chinese Civil War, Korean War) to consistent

cooperation above 4 by 2000. This trajectory reflects sequential conflict resolution—the Vietnam War's end (1975), Sino-Vietnamese normalization (1991), and ASEAN expansion—combined with deepening economic integration. Unlike other regions, Asia-Pacific scores remain stable post-2010 despite U.S.-China tensions, suggesting that economic interdependence continues to moderate political conflicts.

FIGURE B13. Regional Geopolitical Scores: Eastern Europe and Asia-Pacific

A. Eastern European States



B. Asia-Pacific States

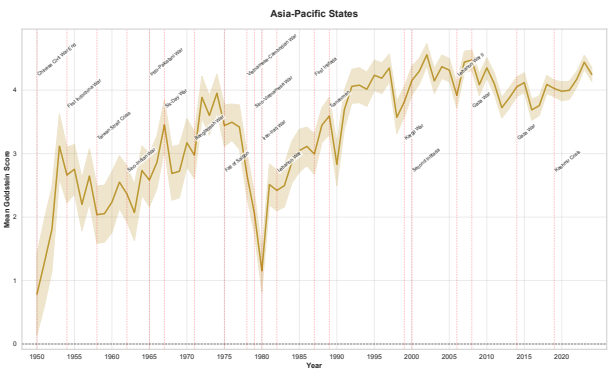
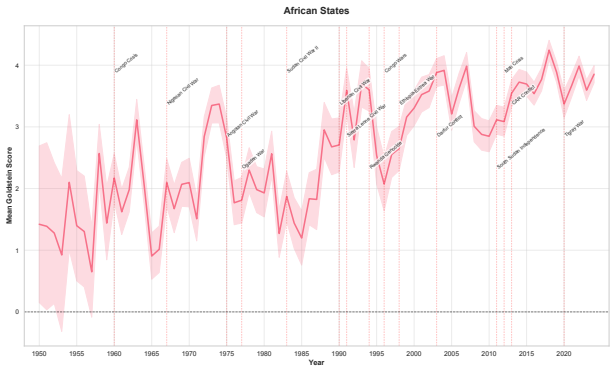


FIGURE B14. Regional Geopolitical Scores: Africa and Latin America

A. African States



B. Latin American States

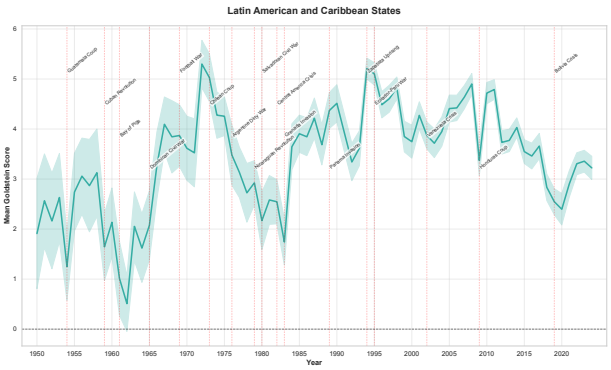


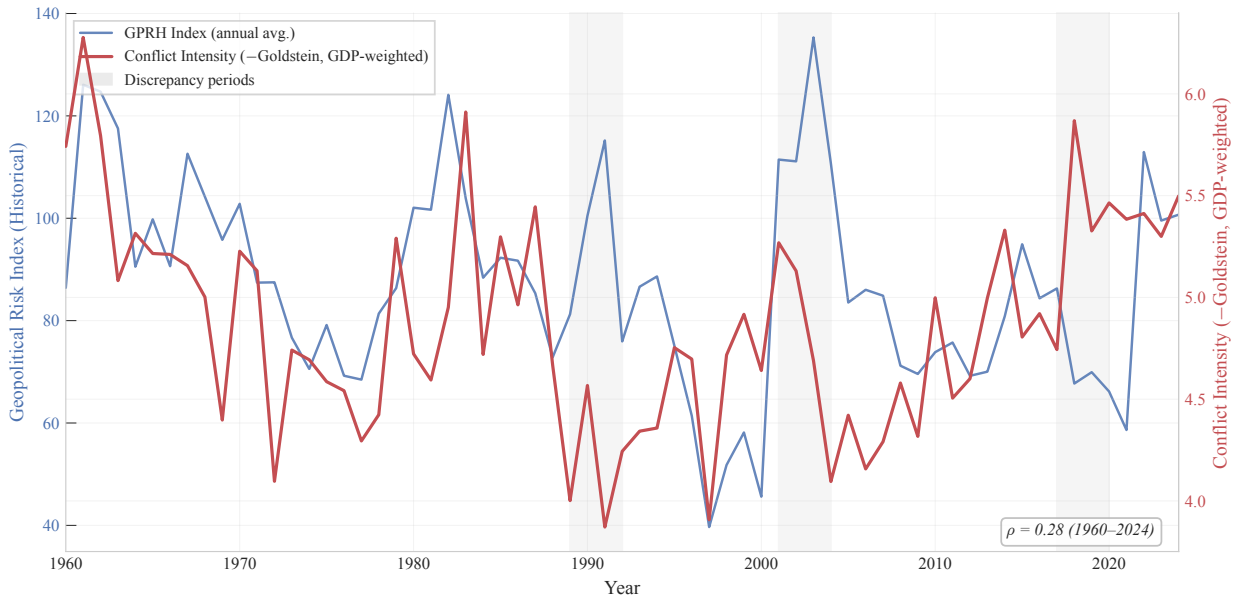
Figure B14 documents geopolitical evolution in the Global South. African states (Panel a) show persistent improvement from below 1 during the decolonization conflicts of the 1950s–1960s to above 4 by 2020. The upward trend is punctuated by severe regional crises—the Nigerian Civil War (1967), Angolan Civil War (1975), Rwandan Genocide (1994), and Congo Wars (1996–2003)—each causing temporary score collapses. The post-2000 acceleration reflects both conflict resolution (the conclusion of Sierra Leone and Liberian civil wars) and expanding South-South cooperation, particularly with China. The Tigray War (2020) marks the first major reversal in two decades. Latin American states (Panel b) display a distinct pattern of high volatility around a stable mean of 3–4. Major disruptions correspond to ideological conflicts—the Cuban Revolution (1959), Chilean coup (1973), Central American crises (1980s)—and economic shocks, particularly the debt crisis (1982)

that produces the sharpest decline. The post-2000 period shows unusual stability despite political polarization, suggesting that regional economic integration through Mercosur and the Pacific Alliance provides resilience against bilateral political tensions. The decline since 2019 reflects both Venezuela crisis spillovers and COVID-19's disproportionate impact on the region.

B.6. Comparison with the Geopolitical Risk Index

Our event-based bilateral measure complements but differs fundamentally from the Geopolitical Risk (GPR) index developed by Caldara and Iacoviello (2022). The GPR index quantifies media attention to geopolitical threats by counting newspaper articles mentioning war, terrorism, and military tensions. It captures aggregate risk perceptions rather than bilateral diplomatic dynamics.

FIGURE B15. Geopolitical Risk Index vs. GDP-Weighted Conflict Intensity, 1960–2024



Notes: The solid line plots the historical GPR index (GPRH) from Caldara and Iacoviello (2022). The dashed line plots GDP-weighted average conflict intensity from our event-based measure. Both series are standardized to facilitate comparison. The correlation between the two series is ρ = 0.28.

Figure B15 compares the GPR index with our GDP-weighted conflict intensity measure from 1960 to 2024. The correlation is modest (ρ = 0.28), and three episodes illustrate systematic discrepancies. First, in 1989–1992, the GPR spikes on Gulf War media coverage while our measure declines, reflecting the end of the Cold War and Soviet dissolution—events that improved the vast majority of bilateral relationships despite a regional military conflict. Second, in 2001–2004, the September 11 attacks and Iraq War produce the largest post-Cold War GPR spike, yet our measure shows only a modest increase: Iraq's GDP constituted less than 0.1% of world output, and the conflicts among major economic powers that drive trade patterns were limited. Third, in 2017–2020, our measure rises substantially—capturing the U.S.-China trade war, COVID-19 diplomacy, and geoeconomic

competition—while the GPR remains subdued because its keyword-based approach centered on military and terrorism language does not capture trade, technology, and pandemic disputes.

These discrepancies highlight a conceptual distinction. GPR shocks operate primarily through an uncertainty channel: heightened risk perceptions trigger precautionary behavior, flight to safety, and investment delays. Our conflict intensity measure captures a supply-side channel: trade disruptions, sanctions, and diplomatic deterioration that directly alter the cost and feasibility of cross-border economic exchange. For analyzing bilateral trade flows, the supply-side channel is the more relevant mechanism.

B.7. LLM Prompt Design and Implementation

This section documents the prompt structure used to instruct the large language model (Gemini 2.5 Pro with Google Search grounding) for compiling and classifying bilateral geopolitical events. For each country-pair-year observation, the LLM receives a structured prompt specifying two countries and a target year, then executes the procedure described below.

B.7.1. Prompt Evolution

The prompt design evolved through three versions, each addressing limitations identified in the preceding iteration:

- **Version 0 (Prototype):** A minimal prompt requesting bilateral events with basic Goldstein scoring. This version produced inconsistent event granularity and lacked systematic coverage of economic dimensions.
- **Version 1 (Topic Taxonomy):** Introduced the six-category event taxonomy (economic, diplomatic, security, legal, multilateral, other) with explicit subcategories. This structured the LLM's search process and substantially improved coverage of non-military dimensions. However, event descriptions remained variable in length and detail.
- **Version 2 (Current):** The production prompt used for the full database. It adds mechanism-first reasoning, requiring the LLM to identify the bilateral relationship context before searching for events. It enforces consistent output formatting and includes the complete CAMEO codebook with Goldstein score mappings as reference material.

  The remainder of this section documents the Version 2 prompt in full.

B.7.2. Overview and Relationship Assessment Framework

The prompt instructs the LLM to generate a single JSON object containing all significant political events that characterized the bilateral relationship between two specified countries during a given year. Each event is classified using the CAMEO framework (Section B.7.5) and scored on the Goldstein scale (Section B.7.6).

Relationship Assessment Framework. In addition to event-level classification, the LLM assigns an overall relationship assessment for each country-pair-year, selecting one category from a nine-point ordinal scale:

- **State of War / Active Conflict**: Open, large-scale armed conflict.
- **Crisis / Intense Confrontation**: Brink of war; high tension, major disputes, limited clashes.
- **Hostile / Antagonistic Relationship**: Deep animosity; sanctions, diplomatic friction, negative rhetoric.
- **Competitive / Rivalrous Relationship**: Strategic competition with limited cooperation.
- **Limited Contact / Cool Relationship**: Minimal, neutral interaction.
- **Selective Cooperation / Transactional Relationship**: Cooperation on specific mutual interests amid broader competition.
- **Broad Cooperation / Partnership**: Cooperation across many sectors; regular dialogue.
- **Strategic Partnership**: Deep cooperation on major strategic issues; high trust.
- **Alliance**: Formal mutual support treaty (especially military); highest integration.

B.7.3. Analytical Procedure

The LLM executes five sequential steps for each country-pair-year observation.

Step 0: Verify Political Entities. Before analyzing interactions, the LLM verifies whether the specified countries existed as political entities in the target year. If not, it identifies the primary political entity controlling the relevant territory—for example, the Soviet Union for Russia before December 26, 1991. The verified entity names are used throughout the analysis and reflected in the output.

Step 1: Search and Compile Events. The LLM systematically searches for all significant interactions between the verified entities during the target year, drawing on its knowledge base and internet sources. Source prioritization follows: (i) official government sources; (ii) international organizations (UN, WTO, IMF); (iii) major news archives (Reuters, AP, BBC); (iv) academic sources and diplomatic archives. Each event must be verified as occurring in the specified year.

Step 2: Identify Significant Political Events. The LLM identifies all significant political events involving direct interaction between the two entities that affect or indicate the state of the bilateral relationship. Each event is classified under one primary category based on its dominant mechanism; when economic tools are employed for political purposes, the event is classified under economic categories. The prompt instructs the LLM to search across six dimensions encompassing 22 subcategories (see Table B1 for the full taxonomy):

- *A. Economic Relations* (A1–A6): Trade policy, financial relations, economic coercion, strategic sectors, integration, and other economic events.
- *B. Diplomatic and Political Relations* (B1–B4): Formal diplomacy, high-level interactions, public diplomacy, and cultural exchanges.
- *C. Security and Defense* (C1–C3): Military cooperation, security incidents, and intelligence/cyber.

- *D. Legal, Territorial, and Movement* (D1–D3): Legal actions, territorial disputes, and movement of people.
- *E. Multilateral and Global Governance* (E1–E2): International organizations and global issues.
- *F. Other Significant Events* (F1–F7): Historical/symbolic, humanitarian, sports, technology, environment, communications, and other interactions.

Step 3: Analyze Each Event. For each identified event, the LLM extracts and records the following:

a. *Basic information*: Initiator/target country assignment, event name, and detailed event description.
b. *Temporal details*: The most precise temporal information available—exact date (`YYYY-MM-DD`), month (`YYYY-MM`), quarter (`YYYY-Q#`), and year—filled hierarchically from most to least precise.
c. *CAMEO classification*: Quadrant class, root code, and event code, following the codebook in Section B.7.5.
d. *Goldstein Scale score*: A numerical score from −10.0 to +10.0, following the guidelines in Section B.7.6.
e. *International organization involvement*: Whether any international organization played a substantive role (as venue, actor, or instrument), with identification of the specific organizations involved.
f. *Event category*: Primary category code (A1–F7) from Table B1.
g. *Evaluation summary*: A comprehensive justification explaining the CAMEO classification, Goldstein score, event category assignment, temporal details, and any entity verification issues.

Handling Third Parties. When events involve third parties or multilateral contexts, the CAMEO classification and Goldstein score focus on the bilateral relationship between the two focal countries. For example, if both countries jointly cooperate in a multilateral agreement, the event is classified based on their cooperative action toward each other, not the broader multilateral context.

Step 4: Overall Relationship Assessment. The LLM selects one overall relationship category for the target year, integrating the pattern, frequency, and intensity of all identified events with historical context. If no significant events are found, the assessment is based on the absence of interaction and historical trends.

B.7.4. JSON Output Structure

The output is a single JSON object with key `historical_political_events` containing a list of event objects. Each event object includes the following fields:

- `year`: Integer (the target year).
- `country1`, `country2`: Strings (verified entity names).
- `event_name`, `event_description`: Strings.
- `event_category`: String (A1–F7) or null.
- `event_exact_date`: String (`YYYY-MM-DD`) or null.

- `event_month`: String (`YYYY-MM`) or null.
- `event_quarter`: String (`YYYY-Q#`) or null.
- `event_year`: Integer.
- `CAMEO_quad_class`: String ("Verbal Cooperation," "Material Cooperation," "Verbal Conflict," or "Material Conflict") or null.
- `CAMEO_root_code`: String (two-digit) or null.
- `CAMEO_event_code`: String (three-digit) or null.
- `Goldstein_Scale`: Number (−10.0 to +10.0) or null.
- `international_org_involvement`: Object with subfields `involved` (Boolean) and `primary_organizations` (array of strings or null), or null.
- `relationship`: String (one of the nine relationship categories, uniform across all events in a given year).
- `evaluation_summary`: String.

When no significant events are found, the output contains a single placeholder object with `event_name` set to "No Significant Bilateral Events Found" and null values for classification fields, accompanied by a context-based relationship assessment.

B.7.5. CAMEO Classification

We employ the Conflict and Mediation Event Observations (CAMEO) framework (Schrodt and Yilmaz 2012) to classify each event along two dimensions: cooperation versus conflict, and verbal versus material. This produces four quadrant classes with hierarchical coding: root codes (two-digit) represent general action categories, and event codes (three-digit) specify precise actions. The LLM is instructed to: (i) identify the core bilateral action; (ii) determine the quadrant class; (iii) select the root code; and (iv) choose the most precise event code. We emphasize accurate classification of economic actions—distinguishing broad sanctions (code 163) from targeted administrative sanctions (code 172)—and mediation events (codes 028, 038, 039, 045, 108, 126, 135, 165). The complete CAMEO codebook with 20 root codes and 143 event codes is provided to the LLM as reference material; see Schrodt and Yilmaz (2012) for the full codebook.

B.7.6. Goldstein Scale Scoring Guidelines

Each event receives a Goldstein Scale score (Goldstein 1992) ranging from −10.0 (maximum conflict) to +10.0 (maximum cooperation). The LLM is instructed to assign scores using the CAMEO event code as the primary reference, with limited contextual adjustments. Table B4 presents the scoring guidelines.

The scoring instructions emphasize three principles. First, the score should primarily reflect the event type identified by the CAMEO event code, ensuring consistency across the database. Second, contextual adjustments are permitted but must remain logically consistent with the CAMEO code's general intensity level—a routine diplomatic meeting (CAMEO 040) should not be scored as highly

TABLE B4. Goldstein Scale Scoring Guidelines

Range	Description
+8 to +10	Major concessions, peace agreements, alliance formations
+6 to +8	Significant aid, material cooperation, major agreements
+2 to +5	Consultations, cooperative intent, routine diplomatic meetings
0 to +2	Initial positive gestures, expressions of interest
0	Neutral statements or actions
−2 to 0	Mild disagreements, tensions, negative rhetoric
−2 to −5	Diplomatic protests, rejections, criticism, minor sanctions
−5 to −8	Threats, coercion, severe sanctions, military mobilizations
−8 to −10	Military attacks, mass violence, war declarations

Notes: Guidelines provided to the LLM for Goldstein Scale assignment. The score primarily reflects the typical intensity associated with the CAMEO event code. Contextual adjustments are permitted when specific circumstances clearly indicate higher or lower intensity than typical for the event category—for example, a first meeting after years of hostility may score higher than a routine annual meeting. All adjustments must be justified in the evaluation summary. Source: Goldstein (1992).

as a major peace treaty (CAMEO 057). Third, when events involve third parties, the score reflects the impact on the bilateral relationship between the two focal countries, not the broader multilateral context.

B.7.7. International Organization Involvement

For each event, the LLM records whether international organizations played a substantive role—as a venue for the interaction, a party to the dispute, or an instrument of policy. The prompt specifies a comprehensive list of organizations spanning four tiers:

- *UN system*: United Nations (General Assembly, Security Council), ICJ, ICC, WTO, IMF, World Bank, WHO, IAEA, ILO, UNESCO, UNHCR, UNICEF, UNEP.
- *Regional organizations*: EU, NATO, OSCE, Council of Europe, African Union, ASEAN, OAS, MERCOSUR, Arab League, GCC, SAARC, CIS, SCO, APEC, Pacific Alliance, CARICOM, ECOWAS, SADC, EAC.
- *Economic and development bodies*: OECD, G7, G20, BRICS, OPEC, ADB, AfDB, IDB, EBRD, AIIB, NDB, BIS.
- *Specialized organizations*: INTERPOL, IOM, ICAO, IMO, ITU, WIPO, ISO, ICRC, Commonwealth, OIC, Non-Aligned Movement.

  Passing references to organizations are excluded; only substantive involvement is recorded.